MECHANISTIC STUDY ON THE ROLE OF ENDOCYTIC MACHINERY DURING NEURONAL PRUNING IN *DROSOPHILA MELANOGASTER*

ZHANG HENG

(*B. Sci., Sun Yat-sen University*)

A THESIS SUBMITTED

FOR THE DEGREE OF DOCTOR OF PHILOSOPHY

DEPARTMENT OF BIOLOGICAL SCIENCES

NATIONAL UNIVERSITY OF SINGAPORE

2015

To my family

Declaration

I hereby declare that this thesis is my original work and it has been written by me in its entirety. I have duly acknowledged all the sources of information which have been used in the thesis.

This thesis has also not been submitted for any degree in any university previously

Zhang Heng

30 March 2016

Acknowledgement

I am sincerely grateful to my supervisor Dr. Yu Fengwei. He is not only a supervisor in research but also a mentor in life. His passion, knowledge and discipline in science have set up a high-standard example of scientist for me. Without his patient guidance, it would not be possible for me to achieve anything in research during the past years.

I am thankful to my Thesis Advisory Committee members Assoc. Prof. Davis Nr and Dr Koh Tong-Wey for sharing experience and advice in research. I also express my gratitude to Assoc. Prof. Kah Leong Lim and Prof Gong Zhiyuan for their help when I first came to Singapore.

I would like to show my gratitude to members of Yu's lab. Thanks go to Dr. Daniel Kirilly and Dr. Gu Ying for teaching me from fly genetics when I joined the lab, to Dr Wong Jin Lin Jack, Edwin Lim, Zong Wenhui, Dr. Ng Kay Siong, Tang Quan and Wang Qiwei for their assistance in daily experiments. I thank all the friends, colleagues and others who provided help directly or indirectly in my research. Lastly, special thanks owe to Wang Yan for his collaboration in this work and friendship during my PhD journey.

I express gratitude to Temasek Life Sciences Laboratory and National University of Singapore for offering a nice environment which allows me to

focus on my research. I also thank the research community for the generosity in sharing reagents and ideas.

Finally, I would like to express deepest gratitude to my family, especially my parents for their understanding and support. You have to give up before you gain, which is extremely true for PhD students in biological research. The love from my family is fundamental to make me keep on going.

Table of Contents

Summary

Selective removal of exuberant neuronal projections without cell death, referred to as pruning, is critical for the maturation of the nervous system. However, the mechanisms underlying neuronal pruning remain elusive. Here, utilizing *Drosophila melanogaster* as a model organism, I identified Rab5/ESCRT-dependent endocytic degradation pathways as novel players for dendrite-specific pruning in sensory neurons, ddaCs. Loss of Rab5/ESCRT results in dendrite pruning defects and ubiquitinated protein aggregates on aberrant endosomes. Importantly, cell adhesion molecule (CAM) Neuroglian (Nrg) accumulates on aberrant endosomes. Moreover, Nrg is relocalized on endosomes and downregulated prior to dendrite pruning in wild-type ddaC neurons. Overexpression of Nrg leads to dendrite pruning defects while loss of Nrg induces precocious pruning, indicating an inhibitory function in pruning. Lastly, attenuation of Nrg suppresses pruning defects of Rab5/ESCRT mutants. Collectively, downregulation of Nrg via endocytic degradation pathways to facilitate dendrite pruning in *Drosophila* sensory neurons reveals a novel mechanism in regulating neuronal pruning.

List of Tables

List of Figures

List of Publications

Zhang H, and Yu F. (2015) Mechanisms of Dendrite-Specific Pruning in Drosophila Sensory Neurons. In*: **eLS. John Wiley & Sons Ltd, Chichester***. http://www.els.net [doi: 10.1002/9780470015902.a0025982]

Zhang H*, Wang Y*, Wong JJ, Lim KL, Liou YC, Wang H, Yu F. (2014) Endocytic pathways downregulate the L1-type cell adhesion molecule neuroglian to promote dendrite pruning in *Drosophila*. ***Dev Cell***. *30(4):463-478.* (*co-first authors)

Wong JJ, Li S, Lim EK, Wang Y, Wang C, **Zhang H**, Kirilly D, Wu C Liou YC, Wang H, Yu F. (2013) A Cullin1-based SCF E3 ubiquitin ligase targets the InR/PI3K/TOR pathway to regulate neuronal pruning. ***PLoS Biol*** *11(9): e1001657.*

Kirilly D, Wong JJ, Lim EK, Wang Y, **Zhang H**, Wang C, Liao Q, Wang H, Liou YC, Wang H, Yu F. (2011) Intrinsic epigenetic factors cooperate with the steroid hormone ecdysone to govern dendrite pruning in *Drosophila*. ***Neuron.*** *72(1):86-100.*

Abbreviations

AEL	After egg laying
APF	After puparium formation
BAX	BCL2-Associated X Protein
BDNF	brain-derived neurotrophic factor
Brm	brahma containing remodeler
CAM	Cell adhesion molecule
CBP	CREB binding protein
CCV	clathrin-coated vesicle
Ci	cubitus interruptus
CIE	clathrin-independent endocytosis
CME	clathrin-mediated endocytosis
CNS	central nervous system
Cul1	Cullin1
da	dendritic arborization
dda	dorsal dendritic arborization
DG	dentate granule
DIAP1	*Drosophila* inhibitor of apoptosis protein 1
DN	dominant negative
DR6	death receptor 6
Dronc	*Drosophila* Nedd2-like caspase
EB3	ephrinB3
ECD	extracellular domain
ECM	cell-extracellular matrix
EcR	ecdysone receptor
EGFR	epithelial growth factor receptor
eL3	early 3rd instar larva
ESCRT	the endosomal sorting complexes required for transport
FNIII	fibronectin type III
GAP	GTPase activating protein

GEF	Guanine nucleotide exchange factor
Hh	hedgehog
Hdc	Headcase
HRP	horseradish peroxidase
ICD	intracellular domain
IgSF	Immunoglobulin superfamily
IHC	inner hari cells
ILV	intraluminal vesicle
InR	insulin receptor
IPB	infra-pyramidal bundles
Kat-60L	Katanin p60-like 1
L1-CAM	L1 type CAM
MB	mushroom body
mical	molecule interacting with CasL
Mmp	matrix metalloprotease
MVB	multi-vesicular body
NGF	Nerve growth factor
NMJ	neuromuscular junction
Nrp2	Neuropilin-2
p75NTR	p75 neurotrophin receptor
PI3K	Phosphotidylinositol 3 kinase
lx	Plaxin
PNS	peripheral nervous system
PTEN	phosphatase and tensin homolog
PVR	PDGF/VEGF Receptor
RGC	retinal ganglion cells
RING	really interesting new gene
SCF	skp- cullin - F-box
Sema	Semaphorin
Sgg	shaggy
shi	shibire
Slimb	supernumerary limb

SMC	structural maintenance of chromosome
SPB	supra-pyramidal bundles
TGF-β	transforming growth factor-β
TH	thyroid hormone
Tkv	thickvein
TNF	tumor necrosis factor
TOR	target of rapamycin
Trk	Tyrosine receptor kinase
ts	temperature sensitive
Uba1	ubiquitin activation enzyme 1
UPS	ubiquitin-proteasome system
Usp	ultraspiracle
VCP	valosin containing protein
VGCC	voltage gated calcium channel
VNC	ventral nerve cord
Wg	Wingless
wL3	wandering 3rd instar larva
WP	white pupa (0 hr APF)
XIAP	X-linked inhibitor of apoptosis protein
β-gal	β-galactosidase
β2Chn	β2-Chimaerin

Chapter 1 Introduction

1.1 Development of the nervous system

The nervous system is a highly specialized and complicated system that responds to signal transductions in many organisms. It is composed of two major cell types called neuron and glia. Neuron is a specialized cell type with distinct subcellular compartments consisting of a long axon, branchy dendrites and a soma. Axons and dendrites from different neurons can form connections named synapses, which are important for signal transmissions. Glia are supporting cells that crucial for the normal functions of neurons by providing proper environment. The precise networks of neurons and glia form functional nervous systems.

Neural development can be divided into three phases. First, neurons are generated via neurogensis. During neurogensis, neurons are generated by series of symmetric and asymmetric divisions of neural progenitor cells, which give rise to diverse neuronal cell types to form the complicated nervous systems. Signaling pathways and mechanisms underlying the neurogensis are highly conserved between vertebrates and invertebrates, such as Notch, Wnt, Hedgehog signalings (Paridaen and Huttner, 2014). Second, after the birth of neurons, the neurite morphogenesis including outgrowth, pathfinding, synapse formation starts. Conserved pathways and molecules, for example, the growth cone components, guidance molecules, cell adhesion molecules, orchestrate to achieve the proper neural projections and

connections (Waites et al., 2005). Finally, the premature projections and connections undergo remodeling to form the precise and functional wirings, which involves apoptosis, pruning and regrowth (Buss et al., 2006; Hashimoto and Kano, 2013; Schuldiner and Yaron, 2015);.

1.2 Neuronal pruning

During neural remodeling, there are two main strategies to remove the unwanted projections and connections, namely, apoptosis and pruning. Neuronal pruning is a regressive process that neurons selectively remove the exuberant projections without causing cell death during development. It is a strategy widely utilized during neural development of both vertebrates and invertebrates. During the early developmental stages, neurons usually generate excessive projections and connections. Later on, via the temporal-spatial controlled pruning mechanisms, neurons remove the unwanted projections and connections to form the precise and functional circuits. Thus, pruning is an important of neuronal remodeling to achieve the maturation of nervous system.

1.2.1 Neuronal pruning in vertebrates

Neuronal pruning is widely observed in vertebrates during development. For instance, the layer 5 cortical neurons in rodents, one of first studied neuronal pruning models, project two axons to both visual areas and spinal cord, respectively. Subsequently, one of the axons is selectively removed to form the proper connection in either visual areas or spinal cord (Luo and O'Leary, 2005; Schuldiner and Yaron, 2015). Another extensively studied model is the

axon pruning of mossy fiber neurons in hippocampal dentate granule (DG). At postnatal day 4 (P4), mossy fiber neurons project two axon bundles, the supra-(SPB) and infra-pyramidal bundle (IPB) to the CA3 pyramidal neurons. From P10 onwards, the IPB undergoes specific pruning resulting in the adult short IPB by P45 (Bagri et al., 2003).

In the development of human and other primates, neuronal pruning occurs in almost every stage and is important for the normal maturation and function of the nervous system. For example, during adolescence, a critical stage for nervous system maturation, massive pruning of excitatory synapses is required for the normal cognitive function. Excessive synapses pruning in prefrontal cortex during adolescence is correlated with psychiatric illnesses, such as schizophrenia (Selemon and Zecevic, 2015). In addition, deficiency of supplementary motor area that resulted from the abnormal pruning in infancy correlates with the Infantile autism (Saugstad, 2011). Thus, studies on the mechanisms of neuronal pruning may contribute to identification of a novel therapeutic target for treatment of relevant neurological disorders.

1.2.1.1 Hormone and trophic factor

Hormones are critical cues to regulate the various developmental and physiological events. Recently, it is reported that the thyroid hormone (TH) is required for synaptic pruning during perinatal development(Sundaresan et al., 2015). In hypothyroid mouse model, the inner hair cells (IHC) show afferent synapse pruning defects. More interestingly, the supplement of TH during

postnatal day 3 to day 8 can rescue the IHC synapse pruning defect, suggesting that TH regulates pruning in a temporal manner. Interestingly, androgen secreted by gonads has been shown to trigger the male-specific axon pruning in mouse mammary gland (Liu et al., 2012).

Trophic factors are secreted proteins that regulate developmental events, such as proliferation, differentiation and survival. In mammals, cultured neuron systems implicate the importance of trophic factors in regulated neuronal pruning. Nerve growth factor (NGF) is one of the most studied trophic factors for neural survival. Interestingly, compartmentalized deprivation of NGF in axons leads to pruning instead of cell death, suggesting a relationship between the pruning and dying mechanisms. (Campenot, 1982). Another trophic factor Brain-derived neurotrophic factor (BNDF) is involved neuronal pruning with opposite functions. Via cell death receptor p75NTR, BNDF activates the axon pruning in both cultured neurons and sympathetic neurons in mouse model (Singh et al., 2008). On the contrary, BNDF via receptor Tyrosine receptor kinase B (TrkB) serves as a growing signal. Deprivation of BNDF-TrkB signal promotes axon pruning in mouse mammary gland. (Liu et al., 2012)

1.2.1.2 Cell death receptor and caspase

Apoptotic machinery is widely used during the nervous system development to remove the unnecessary neurons (Buss et al., 2006). In vertebrates, a growing body of studies have revealed the involvement of apoptotic system in neuronal pruning. Two cell death receptors from tumor necrosis factor (TNF)

receptor superfamily, DR6 with ligand APP (Nikolaev et al., 2009) and p75 with ligand BNDF/myelin (Singh et al., 2008) have been shown to promote axon pruning both *in vivo* and *in vitro*. Downstream of these receptors, proapoptotic protein BCL2-Associated X Protein (BAX) mediated release of cytochrome-C is required for axon pruning. In addition, Caspases as important proteases to execute apoptosis are also required for neuronal pruning. In mammals, both cultured neurons and *in vivo* systems have shown that the initiator caspase Caspase-9 and executer caspases Caspase-3 and Caspase-6 are required for local axon pruning (Cusack et al., 2013; Nikolaev et al., 2009; Schoenmann et al., 2010; Simon et al., 2012; Vohra et al., 2010). Moreover, anti-apoptotic gene *bcwl* is locally translated in axons to inhibit BAX mediated axon degeneration (Cosker et al., 2013) In addition, X-linked inhibitor of apoptosis protein (XIAP) that antagonizes Caspase3 also negatively regulate neuronal pruning (Unsain et al., 2013). Therefore, it is likely that apoptotic machinery function locally to induce neuronal pruning.

1.2.1.3 Guidance molecule

Guidance molecules regulate diverse aspects of nervous system development including path finding, neurite growth, cell death, etc (Van Battum et al., 2015; Vanderhaeghen and Cheng, 2010). Two families of canonical guidance molecules, semaphorins and ephrins have been shown to regulate the axon pruning in mammalian. In 2003, Bagri and colleagues found that the IPB axon pruning of DG cells are defective in semaphorin receptors Plexin-A3 (PlxA3)

and Neuropilin-2 (Nrp2) or Semaphorin3F (Sema3F) mutant mice (Bagri et al., 2003). Based on the *In situ* hybridization data, PlxA3 and Nrp2 are expressed in DG cells (Chen et al., 2000), whereas Seme3F is expressed along the IPB tract from P20 onwards, indicating a temporal-spatial regulation of semaphorin signaling in regulating IPB azon pruning. Later, Riccomagno and colleagues uncovered the Nrp2/β2-Chimaerin (β2Chn)/Rac1 pathway downstream of Semaphorin signaling in IPB axon pruning (Riccomagno et al., 2012). β2Chn is a Rac GTPase-activating protein (GAP) that binds to Nrp2 and weakly to Plx3A. Upon Seme3F binding, β2Chn is released by Npr2 and activated to restrain Rac1 activity, which subsequently promotes IPB axon pruning. Beside Semaphorin signaling, the ephrin reverse signaling is also involved in IPB axon pruning (Xu and Henkemeyer, 2009). Ephrin-B3 (EB3) functions as a receptor in mossy fiber neurons while EphB receptors as ligands that might express in CA3 neurons to activate EB3 tyrosine phosphorylation of intracellular domain. The second SH3 domain of adaptor protein Grb4 which is necessary and sufficient to transduce EB3 reverse signaling in IPB axon pruning can bridge EB3 to Rac Guanine nucleotide exchange factors (GEF) Dock180 and Rac downstream effector Pak. Consistently, activation of Rac signaling is required for the EB3 induced IPB pruning in mossy fiber neurons. However, the relationship between semaphorins and ephrins remains elusive. It is controversial that Rac signaling is downregulated in semaphorins signaling while upregulated in ephrins signaling to promote IPB axon pruning.

This might be explained by a difference in spatial-temporal requirement for two signaling pathways, which awaits further study.

1.2.2 Neuronal pruning in invertebrates

1.2.2.1 Neuronal pruning in C. *elegans*

In 2005, Eriko Kage and colleagues first discovered that neuronal pruning occurs in *C. elegans* during development (Kage et al., 2005). Majority of the two AIM interneurons show excessive axonal connection in L1 stage but only around 10% of the AIM neurons remain connected in adult stage, suggesting an conserved axonal pruning process in *C. elegans* during nervous system maturation. In the same study, a transcriptional cascade UNC-86/mbr-1 was identified to be important for the AIM axonal pruning. UNC-86 is a POU-domain transcription factor while mbr-1 is a highly conserved transcription factor consisting RHF2 and NR-box motif. Later on, a Wnt-Ror kinase signaling was reported to regulate AIM axonal pruning through an inhibitory function (Hayashi et al., 2009). Cam-1, a Frizzle domain consisting transmembrane tyrosine kinase inhibits pruning in Wnt-dependent manner. Genetic data suggested that Wnt is secreted by nearby neurons that activate the cell autonomous signaling in AIM, for the first time demonstrating that a non-cell-autonomous cue can regulate local pruning in *C. elegans*. The Wnt-Ror signaling acts in parallel with UNC-86/mbr-1 pathway. Moreover, in this study these signalings are also required for behavioral response to odor by regulating the pruning in another subclass of interneurons RIF, showing that

the precise neuronal pruning is indeed crucial for normal nervous system function. In 2010, a worm study showed the Fusogen EFF-1 is important for dendrite pruning in PVD neurons (Oren-Suissa et al., 2010). The EFF-1 mutants showed excessive and abnormal dendrite arbor while the gain-of-function displayed reduced branching. Through live imaging, authors demonstrated that EFE-1 controls dendrite branching pattern by dendrite autofusion and fission. The study provides evidence for the concept that neurite retraction is an important cellular mechanism for neuronal pruning.

1.2.2.2 Neuronal pruning in *Drosophila melanogaster*

Neuronal pruning process is highly conserved in *Drosophila melanogaster*. As a powerful model organism, extensive studies on the cellular and molecular mechanisms of neuronal pruning have been conducted in *Drosophila*. Various types of neurons in *Drosophila* undergo pruning during metamorphosis, a critical transition stage between larval and adult stages, such as the mushroom body (MB) γ neurons in the central nervous system, subsets of dendritic arborization (da) neurons, and neuromuscular junctions in the peripheral nervous system (Schuldiner and Yaron, 2015; Yu and Schuldiner, 2014). MBs are important neuropils in CNS that are required for learning and memory in Drosophila. MB γ neurons undergo stereotype pruning during early metamorphosis, making it an attractive model system to study the molecular mechanisms of neuronal pruning. During larval stage, γ neurons axons project bifurcating branches into the medial and dorsal lobes of the MB. At around 4

hr after puparium formation (APF), the dendrites of γ neurons start to undergo fragmentation at 4 hr APF followed by the medial and dorsal axonal branches at around 8 hr APF. By 24 hr APF, the dorsal and medial axonal branches together with the dendrites are completely pruned. Later, γ neurons regrow and form adult-specific axonal branch into medial lobe (Lee et al., 1999; Watts et al., 2003).

da neurons are sensory neurons located between epidermis and muscle layer closed to the cuticle during larval stage. da neurons play important roles in sensing mechanical force and UV light (Tsubouchi et al., 2012; Xiang et al., 2010). Among different subtypes of da neurons, ddaC neurons exhibit the most complex dendrite arbor covering the dorsal larval body wall redundantly and project a single axon to form synapses in the central nerve cord (Fig 1E, E')(Grueber et al., 2002). da neurons are born by mid-embryogenesis (Bodmer et al., 1987). The dendrites of da neurons branch out at around 16 hr After Egg laying (AEL) and finally tile the body wall by around 48 hr AEL (Song et al., 2012). Subsequently, the dendrite arbors keep growing coordinated with the expansion of the animal size to until puparium formation (Fig 1A, A'). In contrast to the growing phase, dendrite pruning begins at around 3 hr after puparium formation (APF) marked by the blebs formation along the proximal dendrites (Williams and Truman, 2005). Subsequently, the dendrite thinning occurs at the blebs along the proximal dendrites which eventually result in severing at around 6 hr APF (Fig 1B, B') (Kirilly et al., 2009). Severed

dendrites undergo rapid fragmentation into small debris. By 16 hr APF, all the fragments and debris are cleared by phagocytes (Han et al., 2014; Williams and Truman, 2005). After pruning completion, the dendrite arbors of ddaC neurons regrow and form the adult specific pattern from 24 hr APF.

For more than a decade, studies on MB γ neurons and ddaC neurons have shed light on the cellular and molecular mechanisms of neuronal pruning.

1.2.2.2.1 Ecdysone signaling

The steroid hormone 20-hydroxyecdysone (ecdysone) is the trigger of various changes of the body plan during metamorphosis. Upon ligand binding, nuclear receptor ecdysone receptor (EcR) together with its co-receptor Ultraspiracle (Usp) forms a heterodimer to regulate transcription of their downstream targets (Thummel, 1996). In both MB γ neurons and ddaC neurons, expression of EcR B1 isoform (EcR-B1) is specifically upregulated during late larva/ early pupa stage, correlated with the ecdysone peak (Kirilly et al., 2009; Kuo et al., 2005; Lee et al., 2000). Disruption of *EcR* or *Usp* expression almost fully blocks the pruning events in both MB γ neurons and ddaC neurons, supporting that ecdysone signaling is the master regulator to initiate pruning. Interestingly, EcR/Usp with ecdysone activates EcR expression to form a self-activation loop for EcR (Karim and Thummel, 1992; Koelle et al., 1991), which is also demonstrated by Microarray data in MB (Hoopfer et al., 2008). Beside EcR/Usp itself, the expression of EcR requires TGF-β signaling (Yu et al., 2013; Zheng et al., 2003). Upon the binding of their ligand Myoglianin,

TGF-β type I receptor Baboon and type II receptor Punt or Wishful thinking together with Plum, TGF- β accessory receptor, lead to the phosphorylation of the effector dSmad2 to promote the EcR-B1 expression, although the direct mechanism is unknown. In addition, a nuclear receptor FTZ-f1 is found to be an upstream of EcR expression (Boulanger et al., 2011). FTZ-f1 binds to upstream of EcR-B1 transcription starting site and activates the expression of EcR-B1 by inhibiting Hr39, a homologue of FTZ-f1 that represses EcR-B1 expression. Moreover, the cohesin complex is also required for EcR-B1 expression, which is likely through the binding to the EcR locus (Schuldiner et al., 2008). Activated by ecdysone, EcR/Usp heterodimer nuclear receptor binds to the specific DNA sequence called ecdysone response element to regulate gene expression (Boulanger and Dura, 2015). However, for a long time, little was known about the EcR downstream targets during neuronal pruning. In a large-scale RNAi screen of potential ecdysone early-response targets, *Sox14*, an HMG domain transcription factor, was first identified as a downstream target of EcR/Usp during dendrite pruning in ddaC neurons (Kirilly et al., 2009). Loss of *Sox14* function results in severe pruning defects in both ddaC neurons and MB γ neurons whereas overexpression of Sox14 leads to precocious dendrite pruning in ddaC neurons, suggesting that Sox14 is necessary and sufficient to induce neuronal pruning. Moreover, overexpression of Sox14 rescues the majority of pruning defect in EcR dominant negative expressing background, supporting that Sox14 is a key

downstream target of EcR during dendrite pruning in ddaC neurons. Later on, subsequent study showed that EcR forms a complex with the histone acetyltransferase CREB-binding protein (CBP) with the presence of ecdysone and a chromatin remodeler Brahma to promote the H3K27 acetylation at the *sox14* locus to facilitate its expression, further suggesting Sox14 is a direct target of EcR (Kirilly et al., 2011). Furthermore, through a pupa lethal collection screen, a cytoskeleton regulator Mical was identified as a downstream factor of Sox14 in ddaC neurons. Sox14 can bind to Mical promoter region to activate Mical expression during early metamorphosis, revealing the EcR/Sox14/Mical pathway in regulating ddaC dendrite pruning. Another genetic interaction screen in heterozygous EcR mutant sensitized background identified *headcase* (hdc) as another EcR downstream target during ddaC dendrite pruning (Loncle and Williams, 2012). Hdc is cytoplasmic protein that required for dendrite pruning cell-autonomously. The upregulation of hdc during late larva/ early pupa requires EcR, CBP and Brm but not Sox14, indicating that hdc might be parallel to Sox14. However, the exact regulation of *hdc* expression by EcR and function of Hdc during pruning remain to be uncovered.

1.2.2.2.2 Ubiquitin-proteasome system

The Ubiquitin-proteasome system (UPS) is important for the proteins turnover in different cell types. The UPS consists of ubiquitin-activating enzyme E1, ubiquitin-conjugating enzyme E2, ubiquitin ligase E3 and proteasome. E1, E2

and E3 are required for poly-ubiquitination of target proteins that serve as a signal for proteasome-mediated protein degradation. So far, UPS is found to be involved in neuronal pruning in different organisms. In *Drosophila*, the only E1 ubiquitin activation enzyme 1 (Uba1) and the proteasome 19S particle subunit Mov34 were first identified to regulate both axon pruning in MB γ neurons and dendrite pruning in ddaC neurons (Kuo et al., 2005; Watts et al., 2003). After that, uncovered by a candidate mutant screen, E2 UbcD1 is required for dendrite pruning in ddaC neurons. Acting downstream of UbcD1, E3 ligase Drosophila inhibitor of apoptosis protein 1 (Diap1) undergoes auto-ubiquitination and degradation to release the inhibition of initiator caspase DRONC (Kuo et al., 2006). Consistently, gain-of-function Diap1 or loss of Dronc caused pruning defect in ddaC neuron, suggesting a Ubcd1/Diap1/Dronc pathway during dendrite pruning in ddaC neurons but not axon pruning in MB γ neurons. Another study shows that Loss of Valosin containing protein (VCP), a ubiquitin-selective AAA chaperone, leads to pruning defect that associated with high Diap1 level (Rumpf et al., 2011). However, on the basis of relatively weak phenotype and no requirement for MB γ neuron pruning of this pathway, compared with E1 Uba1, there exist other E2/E3 required for the UPS function during pruning process.

Recently, a RING-domain E3 ligase complex composed of Cullin1 (Cul1), Roc1a, SkpA, and Slimb has been found to be important for pruning in both MB γ neurons and ddaC neurons (Wong et al., 2013). A candidate screen in

ddaC neurons suggests that attenuation of the InR/PI3k/Tor pathway specifically recues the pruning defect in Cul1 complex mutants. Consistently, hyperactivation of InR/PI3k/Tor pathway is sufficient to causes pruning defect in ddaC neurons. Biochemical data shows that Cul1 complex attenuates InR/PI3k/Tor pathway through the ubiquitination and degradation of Akt, a positive regulator of Insulin pathway. And the substrate recognition of Akt is mediated via the WD40 domains of Slimb, the F box-containing protein important for target specificity in Cul1 complex. Given that the InR/PI3k/Tor pathway is a growth pathway, this finding suggests that UPS can antagonize the growth signaling to facilitate the regressive pruning events.

Several lines of evidence indicate that UPS acts as downstream of EcR signaling. First, the UPS is not required for the expression of EcR and its downstream targets (Watts et al., 2003; Wong et al., 2013). Second, overexpression of EcR cannot rescue the UPS mutants, different from the EcR upstream mutants. Third, the microarray and qPCR data indicate that the expression of some UPS components depend on EcR (Hoopfer et al., 2008) and its downstream target Sox14 (Wong et al., 2013).

1.2.2.2.3 Caspase activation

Consistent with the studies in vertebrates, caspase activity is not only required for apoptosis but also neuronal pruning. It has been demonstrated that the local activation of caspase in certain compartment promotes pruning, but not cell death, in ddaC neurons (Kuo et al., 2006; Williams et al., 2006). The

involvement of caspases in pruning is first demonstrated by initiator caspase Dronc, homolog of mammalian Caspase-9 (Kuo et al., 2006). *dronc* mutant showed dendrite fragmentation and clearance defects in ddaC neurons. During apoptosis, Diap1 is a caspase inhibitor that, generally, high Diap1 level attenuates Dronc activity. In ddaC neuron, Diap1 gain-of-function mutant or overexpression of Diap1 results in dendrite pruning defects, which is associated with loss of caspase activity (Kuo et al., 2006). Interestingly, Dronc activity can also be suppressed by hyperactivated insulin pathway during dendrite pruning, although direct mechanism is unknown (Wong et al., 2013). Besides initiator caspase, pruning defects result from overexpression of p35, an inhibitor of effector caspases, suggesting that effectors caspases are also required for dendrite pruning. However, the caspases seem to be required for clearance of the dendrite fragments and debris but dispensable for dendrite severing step, raising a possibility that caspases only function in the late stages of dendrite pruning. A genetically coded reporter of Dronc activity revealed that caspase activity is restricted mainly in severed dendrites after 5h APF, supporting the notion that caspases function locally after dendrite detachment (Williams et al., 2006).However, the downstream targets of activated caspases during dendrite pruning remain unknown.

1.2.2.2.4 Cytoskeleton disassembly

Cytoskeletal breakdown is a hallmark of pruning before neurites severing in both MB γ neuron and ddaC neurons (Watts et al., 2003; Williams and

Truman, 2005). In ddaC neurons, both actin and microtubule cytoskeletons are eliminated in the proximal dendrite region prior to the membrane fission at 4 hr APF. A candidate-based screen searching for microtubule destabilizing molecules identified Katanin p60-like 1 (Kat-60L1) which is required for cytoskeletal breakdown and dendrite pruning (Lee et al., 2009). However, the exact function and regulation of Kat-60L1 in dendrite pruning is still elusive. Another cytoskeletal regulator Mical is also required for dendrite pruning. As a downstream effector of ecdysone signaling, *mical* transcription is directly activated by Sox14 and another study has shown that VCP is required for proper *mical* mRNA splicing (Kirilly et al., 2009). Interestingly, Mical can oxidize and disassemble actin filaments (Hung et al., 2011), but the downstream events of Mical in regulating cytoskeleton stability and pruning remain unclear.

1.2.2.2.5 Calcium signaling

Recently, it has been reported that compartmentalized calcium transients serve as temporal-spatial cues to induce dendrite pruning (Kanamori et al., 2013) et al., 2013). Calcium influxes occur in certain dendrite branches starting from 2 hr APF in succession, which predicts the occurrence of dendrite pruning. The voltage-gated calcium channel (VGCC) was identified to be responsible for generation of the calcium transients in the dendrites of ddaC. Loss of VGCC function largely eliminates calcium transients and leads to dendrite pruning defects in ddaC neurons. The excitability of dendritic branches increases

locally at 2 to 3 hr APF, which facilities robust calcium influx in dendritic compartments. Furthermore, a candidate-based screen of Ca^{2+}-activated molecules identified Ca^{2+}-activated protease calpains that appear to function downstream of calcium transients to promote dendrite pruning. It is of great interest to investigate downstream events of calcium signaling during dendrite pruning.

1.2.2.2.6 Phagocytosis

Phagocytosis is required for pruning in both MB γ neurons and ddaC neurons. In MB γ neurons, glial cells, especially the astrocytes, infiltrate the axon branches and engulf the axon fragments (Awasaki and Ito, 2004; Watts et al., 2004; Williams and Truman, 2005). In ddaC neurons, the epithermal cells are the major phagocytes responsible for the engulfment of the dendrite debris, while the hemocytes partially contribute to the fragmentation of severed dendrites (Han et al., 2014). Disruption of endocytosis via overexpression of temperature sensitive *shibire* (*shi*^{ts}), encoding *Drosophila* homolog of *dynamin*, in the glial cells or epithermal cells results in fragmentation and clearance defects in MB γ neurons or ddaC neurons, respectively (Awasaki and Ito, 2004; Han et al., 2014; Watts et al., 2004). Moreover, the engulfment receptor Draper in phagocytes is required for the phagocytosis of the debris (Williams et al., 2006). Another study in ddaC neurons suggests that the matrix metalloproteases Mmp1 and Mmp2, presumably secreted by epithermal

cells, are also required for dendrite fragmentation and clearance but not severing during dendrite pruning (Kuo et al., 2005).

In addition, glial cells also take part in ddaC dendrite pruning. Glia cells wrap the axon, soma and proximal dendrites of ddaC neurons. The initiation of dendrite severing occurs in the glia cell wrapped regions and the severed dendrites undergo rapid degradation in the glia. Blocking endocytosis by overexpression shi^{ts} in glial cells, the dendrite severing was delayed. Similarly, overexpression of EcR^{DN} in glial cells resulted in delay of the dendrite degradation and retraction. However, the glial cells seem to have little effect on overall dendrite pruning (Han et al., 2011).

1.3 Endocytic pathways and neural development

Endocytosis is a process that the cells internalize the plasma membrane and extracellular contents into cytoplasm to form vesicles named endosomes, which is highly conserved in eukaryotic cells (Cosker and Segal, 2014).

1.3.1 endocytic machinery

Endocytosis can be mainly classified as two types which are clathrin-mediated endocytosis (CME) and clathrin-independent endocytosis (CIE) pathways. In CME pathway, membrane invagination is coated by clathrin monomers to assemble a cage structure, which is facilitated by adaptor proteins like AP2 as a linker between membrane proteins and clathrins. Driven by the dynamin GTPase, the clathrin-coated pit is abscised from plasma membrane to form the

clathrin-caoted vesicles (CCV). Then, CCVs undergo uncoated process which involves the chaperones, for example, Hsc70, to remove the clathrin cage structure (Sousa and Lafer, 2015). On the other hand, the CIE pathway is less understood and more complicated. Based on the involvement of different molecules and lipids, clathrin-independent pathway can be further divided into several distinct subtypes, such as caveolar endocytosis, macropinocytosis, phagocytosis, etc (Doherty and McMahon, 2009). The caveolae is the one of the most studied non-clathrin coated plasma membrane invaginations that regulated by Caveolins and flotillins in many mammalian cell types(Fischer et al., 2006; Hansen and Nichols, 2009). Different from CME and caveolar endocytosis, macropinocytosis is a large-scale internalization of plasma membrane without obvious coating structure. It has been reported that macropinocytosis is regulated by actin remodeling, cholesterol-rich membrane raffles and Na^+/H^+ exchanger (Lim and Gleeson, 2011; Mulcahy et al., 2014). Phagocytosis is required for internalization of extracellular particles, such as bacteria and apoptotic debris. It is regulated by membrane receptors and actin cytoskeleton remodeling signaling (Mulcahy et al., 2014).

Endocytosed vesicles undergo homotypic fusion and fuse with early endosomes/sorting endosomes, a process regulated by small GTPase Rab5. GTP-bound Rab5 recruits various effectors on early endosomes, such as Vps34, snares, EEA1, Rabex-5, which regulate phosphoinositide conversion, membrane fusion, effectors recruitment, etc (Huotari and Helenius, 2011).

After that, the contents in endocytosed vesicles can be mainly targeted to two distinct routes, the recycling pathway and the degradation pathway. Guided by Rab4 and Rab11, the cargos in early endosomes can be transported back to the plasma membrane via the endosomal recycling pathway (Scott et al., 2014). Alternatively, early endosomes undergo endosomal maturation to form multi-vesicular bodies (MVBs) /late endosomes. During the endosomal maturation, endosomal cargos undergo sorting into intraluminal vesicles (ILVs) on MVBs, which is regulated the endosomal sorting complexes required for transport (ESCRT) machinery (Hurley, 2010). ESCRT machinery includes 4 sub-complexes, namely ESCRT 0, I, II and III, and several accessory components. ESCRT 0 component Hrs target on early endosomes via FYVE domain binding to phosphatidylinositol 3-phosphate and interact with ubiquitinated cargo via ubiquitin-binding motif. Subsequently, ESCRT I, II and III are assembled on endosomes. ESCRT I and II are important for ILV membrane budding while ESCRT III is responsible for membrane fission. Later on, the late endosomes/MVBs can fuse with the lysosomes to degrade the contents.

1.3.2 endocytosis in neural development

Endocytosis is involved in many aspects of neural development, including cell fate determination, axon outgrowth and pathfinding, neuronal migration, synaptic plasticity, etc (Schwarz and Patrick, 2012; Villarroel-Campos et al., 2014; Yap and Winckler, 2012). Endocytosis regulates neurite outgrowth in

both vertebrates and invertebrates. Knockdown of Rab5 or Rab5 GEF Rabex-5 in cultured mouse hippocampal neurons leads to neurite outgrowth defects (Mori et al., 2013). Similarly, Rab5 and ESCRT component Vps32 have been reported to regulate dendrite morphology in Drosophila ddaC neurons (Satoh et al., 2008; Sweeney et al., 2006). In addition, endocytosis also mediates growth cone collapse which is important for outgrowth and pathfinding in response to various repulsion cues including Sema3A, Slit and Ephrin (Tojima and Kamiguchi, 2015). Moreover, cell migration is also controlled by endocytic pathways. In mouse cerebral cortex, Rab5 and Rab11-dependent endocytic recycling pathways mediate the proper level of N-Cadherin to facilitate neural migration (Kawauchi et al., 2010). Interestingly, a similar mechanism is used during Drosophila border cell migration to maintain the Receptor tyrosine kinases in the leading edge (Assaker et al., 2010). In summary, functions of the endocytic machinery in neural development are highly conserved between vertebrates and invertebrates.

1.4 Cell adhesion molecules in neural development

Cell adhesions are important for the physical tissue integrity, materials exchange, signaling transductions, etc. CAMs are membrane-bound proteins that are required for the formation of cell-cell or cell-extracellular matrix (ECM) adhesions. Based on the structure similarity, CAMs are classified into various families, such as cadherins, integrins, neurexins, selectins,

Immunoglobulin superfamily (IgSF), etc (Benson et al., 2000; Hortsch, 2000). CAMs usually consist of extracellular domain (ECD) for homophilic or heterophilic binding, a transmembrane domain for membrane anchoring, and an intracellular domain (ICD) for cytoskeletal interaction or signaling transduction. With diverse structures and functions, CAMs regulate almost every aspect during development including proliferation, differentiation, survival, etc (Aplin, 2003). During neural development, CAMs are involved in neuron differentiation, neural migration, synapse formation, neurite growth, axon pathfinding, which are conserved between vertebrates and invertebrates. (Schafer and Frotscher, 2012; Sheng et al., 2013; Sun and Xie, 2012; Zhang et al., 2008).

1.4.1 L1 type CAM

L1 type CAM (L1CAM) is a highly conserved subgroup of IgSF CAMs. Vertebrate genomes contain multiple L1 type CAMs. For example, there are four L1 type CAMs, namely L1-CAM, CHL1, neurofascin and NrCAM in mammals. However, invertebrate genomes usually encode one L1 CAM, such as *Neuroglian* in *Drosophila* or *Sax-7* in *C. elegan* (Hortsch, 2000). L1 type CAMs are single transmembrane proteins that typically consist of a large ECD with six Immunoglobulin (Ig) domains followed by five fibronectin type III (FNIII) domains and a small ICD with conserved Ankyrin-binding motif and FERM domain-bind motif. ECD of L1 CAMs mediated interactions with various ligands and receptors. It has been reported that the Ig domains mediate

the homophilic binding of L1 CAMs (Wei and Ryu, 2012). Moreover, ECD of L1 CAMs exhibits heterophilic interactions with other molecules, such as neuropilin/semaphoring (Castellani et al., 2002), integrins (Silletti et al., 2000; Thelen et al., 2002), EGFR (Nagaraj et al., 2009), etc. The short ICD of L1 CAMs is important for the intracellular binding partners and cytoskeletons. The ankyrin-binding motif (FIGQY) is highly conserved between vertebrates and invertebrates. Via ankyrins, L1 CAMs is linked to the spectrin/actin cytoskeleton, which is critical for the adhesion functions (Wei and Ryu, 2012). In addition, FERM domain binding motif binds to ezrin which also subsequently links to actin cytoskeleton (Schafer and Frotscher, 2012).

1.4.2 L1 type CAM in neural development

In mammals, L1 CAMs are involved in different developmental processes, such as neurite outgrowth, axon pathfinding, neuron migration, synapse formation, etc (Kenwrick and Doherty, 1998; Schafer and Frotscher, 2012). In human, mutations of L1 CAM have been linked to various neurological diseases, such as corpus callosum hypoplasia, mental Retardation, spasticity, multiple sclerosis, low-IQ syndrome, developmental delay, and schizophrenia (Kenwrick et al., 2000).

In *Drosophila*, Nrg also has been shown to regulate outgrowth (Forni et al., 2004; Martin et al., 2008; Yamamoto et al., 2006; Yang et al., 2011), synapse formation (Godenschwege et al., 2006; Godenschwege and Murphey, 2009; Kudumala et al., 2013), pathfinding (Garcia-Alonso et al., 2000; Hall and

Bieber, 1997; Kristiansen et al., 2005; Kudumala et al., 2013) and fasciculation (Goossens et al., 2011; Siegenthaler et al., 2015). Thus, the functions of L1-CAM are highly conserved between mammals and *Drosophila.* Taking the advantage of single L1-CAM in *Drosophila* genome, we can further study the cellular and molecular mechanisms of L1-CAM in regulating various aspects of neural development.

1.5 Aim of this study

With years' studies, we have gained more and more knowledge on the regulation of neuronal pruning. Particularly in *Drosophila melanogaster*, with powerful genetics, numerous elegant studies for more than a decade have shed light on the cellular and molecular mechanisms of pruning. However, the in-depth understanding of neuronal pruning is still far away from us, especially for the downstream executive steps. In order to further explore the cellular and molecular control of neuronal pruning, in our lab, a genome-wide unbiased forward genetic RNA interference (RNAi) screen has been conduct in ddaC neurons to isolate novel regulators in neuronal pruning. In addition, in order to understand of the biological function of these novel players during neuronal pruning, various approaches including genetics, biochemistry, imaging have been taken, which aiming to provide better understanding in ddaC dendrite pruning in *Drosophila* and hopefully hints in neuronal pruning in human as well.

Chapter 2 Material and methods

2.1 Fly Strains

2.1.1 Fly stocks requested from research labs

Rab5^{2} (M. Gonzalez-Gaitan), *Vps28*^{B9} (D. Bilder), *Vps32*^{G5} (D. Bilder), *avl*^{1} (D. Bilder), *fab1*^{21}(H. Stenmark), *UAS-GFP-Rab5* (M. Gonzalez-Gaitan), *UAS-Rab5*^{DN} (M. Gonzalez-Gaitan), *UAS-Vps4*^{DN} (H. Stenmark), *elav-GeneSwitch-Gal4* (H. Keshishian), *UAS-Mical*$^{N\text{-}ter}$ (A. Kolodkin), UAS-*UAS-Ci*^{Cell} (K. Basler), *UAS-Notch*^{DN} (d.n.N) (S. Artavanis-Tsakonas), *UAS-PVR*^{DN} (P. Rorth), *UAS-Tkv*^{DN} (M. O'Connor), *E(spl)m8-lacZ* (S. Bray), *UAS-LAMP1-GFP* (H. Kramer), *UAS-GFP-2xFYVE* (M. Gonzalez-Gaitan), *dpp-lacZ* (S. Cohen), *ppk-Gal4* on II and III (Y. Jan), *UAS-Myc-Vps32* (T. Klein), *UAS-Vps28* (H. Kramer), *UAS-Robo* (B. Dickson), *UAS-N-Cad*, *SOP-flp (#42)* (T. Uemura), *UAS-Nrg-EGFP* (J. Pielage), *UAS-Nrg*$^{\Delta ABD}$ (J.Pielage), *UAS-Nrg*$^{\Delta ICD}$ (This study), *Nrg*$^{\Delta ABD+PBD}$ (This study), *nrg*^{14} *FRT19A* (J. Pielage), *P[nrg_wt]* (J. Pielage), *P[nrgΔIg3+4]* (J. Pielage), *P[nrgΔABD+PBD]* (J. Pielage), *P[nrgΔABD]* (J. Pielage), *P[nrgΔPBD]* (J. Pielage), *UAS-Brm*^{DN} *(K804R)* (J.W. Tamkun).

2.1.2 Stocks obtained from Bloomington stock center (BSC)

UAS-Vps32-GFP (BL#32559), *UAS-Sgg*^{S9A} (BL#5255), *UAS-Mito-GFP* (BL#8443), *UAS-Arm*^{S10} (BL#4782), *UAS-EGFR*^{DN} (BL#5364), *Gal4*$^{2\text{-}21}$, *elav-Gal4, 201Y-Gal4* (BL#*4440*) *UAS-YFP-Rab5* (BL#24616). UAS-*Nrg*

(BL#24169), *nrg* RNAi #1 (BL#38215), *nrg* RNAi #2 (BL#37496), *robo* RNAi (BL#35768), *N-Cad* RNAi (BL#41982), *ppk-CD4-tdGFP* (BL#35843), GSG2295-*Gal4* (BL#40266), *UAS-EcR^{DN} (EcR.B1-DeltaC655.W650A TP1-9)* (BL#6872). *UAS-GCaMP3* (BL#32116), *Rab7^{EY10675}* (BL#20630), *FRTG13 spinster^{11F5}* (BL#5862), *Df(spinster)* (BL#8915).

2.1.3 Stocks purchased from Vienna *Drosophila* RNAi Centre (VDRC)

Rab5 RNAi #1 (v103945) and #2 (v34096), *CBP* RNAi (v3787).

2.1.4 Generation of Rab7 mutant

I crossed *y^{1} w^{67c23}*; P{EPgy2}Rab7^{EY10675} flies with a fly strain carrying the 2-3 transposase to obtain the founders to induce imprecise excision. The founders were crossed to *w*;;TM3, Sb/Tm6B, Tb to set up individual excised lines. About 300 independent lines were established on the basis of the absence of the *w^{+}* marker. Two pupal lethal lines were recovered and subjected to genomic PCR and DNA sequencing analysis. The line with a 1,012-bp deletion was named *Rab7^{EX1}*.

2.1.5 Generation of *UAS-Nrg$^{\Delta ICD}$* and *Nrg$^{\Delta ABD+PBD}$* Transgenes

The truncation *nrg$^{\Delta ICD}$* (encoding aa 1–1157 aa) and *nrg$^{\Delta ABD+PRD}$* (encoding aa 1-1223aa) were PCR form *nrg* cDNA with corresponding primers as follows.

nrg$^{\Delta ICD}$ and *nrg$^{\Delta ABD+PRD}$* Forward:

5’ CACCATGTGGCGGCAGTCAACGATA 3’

nrg$^{\Delta ICD}$ Reverse: 5’ ATTGCGTCGGATAATGCAGAT 3’

nrg$^{\Delta ABD+PRD}$ Reverse: 5’ TCCTGTATCGCCATCACCGTA 3’

Using the The Gateway® recombination cloning technology (Invitrogen) fragments were cloned into pENTR/D-Topo vector (Invitrogen), according to manufacturer’s protocol. The vectors carrying insertions were purified with Qiagen Mini Extraction Kit and sequenced. Next, by using Gateway® LR Clonase® II Enzyme mix (Invitrogen) and pTWF/pTW destination vector, plasmids for transgenic flies were obtained. After that, plasmids were shipped to Bestgene Inc for injections. A few independent transgenic lines were generated and balanced.

2.2 Immunohistochemistry and staining

2.2.1 The primary antibodies for immunohistochemistry and dilution

rabbit and chicken anti-Avl (1:500; a gift from D. Bilder), guinea pig anti-Hrs (1:300; a gift from H. Bellen), mouse anti-Ubiquitin (1:500; FK2, Enzo Life Sciences), rabbit anti-GM130 (1:200; Abcam), mouse anti-KDEL (1:200; 10C3, Abcam), mouse anti-Nrg (1:20, BP104, DSHB), mouse anti-Robo (1:50, 13C9, DSHB), mouse anti-α-PS1-integrin (1:10, DK.1A4, DSHB), rat anti-N-Cad (1:50, DN-EX #8, DSHB), rat anti-Tkv (1:200, a gift from S. Cohen), rat anti-EGFR (1:200, a gift from P. Rorth), rat anti-PVR (1:200, a gift from P. Rorth), mouse anti-Smoothened (1:50, 20C6, DSHB), mouse anti-Patched(1:50, Apa 1, DSHB), mouse anti-Notch Intercellular (1:50, C17.9C6, DSHB), mouse anti-Notch Extracellular (1:50, C458.2H, DSHB),

mouse anti-Delta (1:50, C594.9B, DSHB), mouse anti-p-ERK (1:200, Sigma-Aldrich), rabbit anti-Ci (1:50, a gift from T. Kornberg), mouse anti-Armadillo (1:50, N2 7A1,DSHB), guinea pig anti-Senseless (1:200, a gift from H. Bellen), rabbit anti-GFP (1:500, Invitrogen), mouse anti-Wingless (1:50, 4D4, DSHB), mouse anti-EcR-B1 (1:50; AD4.4, DSHB), rabbit anti-Vps28 (1:200; H. Krämer), mouse anti-integrin–□-PS (1:10, CF.6G11, DSHB), mouse anti-α-PS2-integrin (1:10, CF.2C7, DSHB), rabbit anti-Rab5 (1:200, Yu Lab), mouse anti-□-Gal (1:1000; Promega), goat Cy5-conjugated anti-HRP (1:200, Jackson Laboratorie).

2.2.2 The secondary antibodies (Jackson Laboratories) and dilution

Cy3- conjugated secondary antibodies (1:500), Cy5- conjugated secondary antibodies (1:200), and fluorescein isothiocyanate (FITC) conjugated secondary antibodies (1:100).

2.2.3 Imunostaining preparation

For immunostaining, pupae or larvae were dissected in cold PBS and fixed with 4% formaldehyde for 15 min. After fixation, samples were washed with wash buffer (PBS+1%Triton X) for 3 times for 10 min each. Then, samples were incubated in block buffer (5% NGS in wash buffer) for 30 min. Samples were incubated in primary antibodies with proper dilution overnight. After that, samples were washed with wash buffer 3 times for 10 min each. After that, samples were incubated with secondary antibodies with proper dilution in

wash buffer for 3 hr. Finally, samples were washed in wash buffer for 3 times for 10 min each. Mounting was performed in VectaShield mounting medium.

2.2.4 LysoTracker staining

For LysoTracker staining, fillets from w3L larvae were dissected in cold PBS and incubated with LysoTracker Red DND-99 (Molecular Probes) with the dilution of 1:1000 in M3 buffer for 2 min. Samples were briefly washed in PBS for 3 times. Mounting was performed in PBS.

2.3 Microscopy imaging

2.3.1 Live imaging of da neurons

For live imaging of da neurons at e3L, WP or 6 hr APF, larvae or pupae were mounted with 70% glycerol. For imaging of 12.5 hr or 16 hr APF, pupal cases were moved, then pupae were mounted with 70% glycerol. Images of da neurons were acquired on Leica SPE laser confocal microscope.

2.3.2 Imaging of fixed samples

Fixed samples were mounted on slide with VectaShield mounting medium. Images were acquired on Leica SPE laser confocal microscope.

2.3.2 Time-lapse Calcium imaging

Calcium imaging was performed with microLAMBDA spinning disk using a microscope (Plan Apo oil objective, x40 NA=1.4, Nikon), equipped with a

spinning-disk confocal unit Yokogawa CSU-X1 (Yokogawa, Tokyo, Japan) and a sCMOS digital camera (ORCA-Flash4.0, Hamamatsu Photonics, Japan). GCaMP3 fluorescence was collected from 8-10 optical sections at 1.5-μm thickness (exposure time 150-180 msec) without interval. Obtained images were analyzed using Metamorph (Molecular Devices, USA) and Fiji software (Schindelin et al., 2012).

2.3 MARCM clonal and Gene-Switch system analysis

2.3.1 MARCM analysis of da neurons

For MARCM clonal analysis study of da neurons, clones of da neurons were induced by *sop-Flippase*. The clones of ddaC neurons were visualized *by ppk-Gal4* at different stages. The ddaD/E/F clones were visualized by *ealv-Gal4.*

2.3.2 MARCM analysis of MB γ neurons

For the MARCM clonal analysis study of MB γ neurons, embryos were collected at 6 hr intervals and aged for 24 hr. The clones were induced by *hs-Flipase* at the 1st instar larval stage with 1 h heat shock at 38°C. *201Y-Gal4* labels postmitotic MB γ neurons.

2.3.3 RU486/mifepristone treatment for the Gene-Switch system

Embryos were collected at 3 hr intervals and were reared on standard food to the late 3rd instar larval stage. Then, the larvae were transferred to the standard

culture medium containing 240 µg/ml mifepristone (Sigma Aldrich M8046) until proper stages for analysis. The overall development of animal was not affected by RU486 treatment.

2.4 Quantification and Statistics

2.4.1 Quantification of immunolabeling

To quantify the immunolabeling intensities of Nrg at wL3/WP/6h (Figure 16D), soma/dendrite/axon regions were drawn on the appropriate fluorescent channel according to the GFP channel in ImageJ. After the background subtraction (Rolling Ball Radius=50), we measured the mean grey value of Nrg in the marked areas and normalized to that at wL3 stage. To quantify the ddaC/ddaE relative immunolabeling intensities ratio of Nrg (Figure 17D), soma/dendrite/axon regions were drawn on the appropriate fluorescent channel according to the GFP channel in ImageJ. After subtracting the background (Rolling Ball Radius=50) on the entire image of that channel, we measured the mean grey value in the marked areas in ddaC or ddaE on the same images and calculated their ratios. The ratios were normalized to corresponding average control values and subjected to statistical t-test for comparison between different conditions (*$p<0.05$, **$p<0.01$, ***$p<0.001$, n.s., not significant). Graphs display the average values of ddaC/ddaE ratios and the standard error of means (S.E.M). The number of samples (n) in each group is shown on the bars.

2.4.2 Quantification of ddaC dendrites

Live confocal images of ddaC neurons expressing *UAS-mCD8-GFP* driven by *ppk-GAL4* were shown at WP, 6h APF and 16h APF. The average number of primary and secondary dendrites attached to soma was counted from wild type or mutant ddaC neurons. The total length of unpruned dendrites was measured by lines aligned with wild type or mutant ddaC neuron dendrites in Image J. The number of samples (n) in each group is shown on the bars. Error represent S.E.M. Dorsal is up in all images.

Chapter 3 Results

3.1 Dendrite remodeling of ddaC neurons during metamorphosis

At larval stage, ddaC neurons in PNS exhibit complex dendrite arbors (Fig 1A, A') and project long single axon to VNC in CNS (1E, E'). During early metamorphosis, class IV ddaC neurons in PNS undergo rapid extensive dendrite-specific pruning (Fig 1A-D'). At 0 hr APF (WP), the transition between larval and pupal stages, ddaC neurons display elaborate dendrite arbors (Fig 1A, A'). As metamorphosis progresses, the proximal dendrites of ddaC neurons form blebs at the proximal regions (Fig 1B, B'), the initial signs of dendritic instability. Subsequently, the dendrites thinning occur at the blebs along the dendrites which result in detachment, a process known as dendrite severing, at around 6 hr APF (Fig 1B, B'). The detached dendrites undergo rapid fragmentation (Fig 1C, C'). By 16 hr APF (Fig 1 D, D'), all the fragments and debris are cleared up, leaving the soma and intact axon. Taking the advantages of genetic manipulations and live imaging feasibility, we can explore the cellular and molecular mechanisms underlying neuronal pruning.

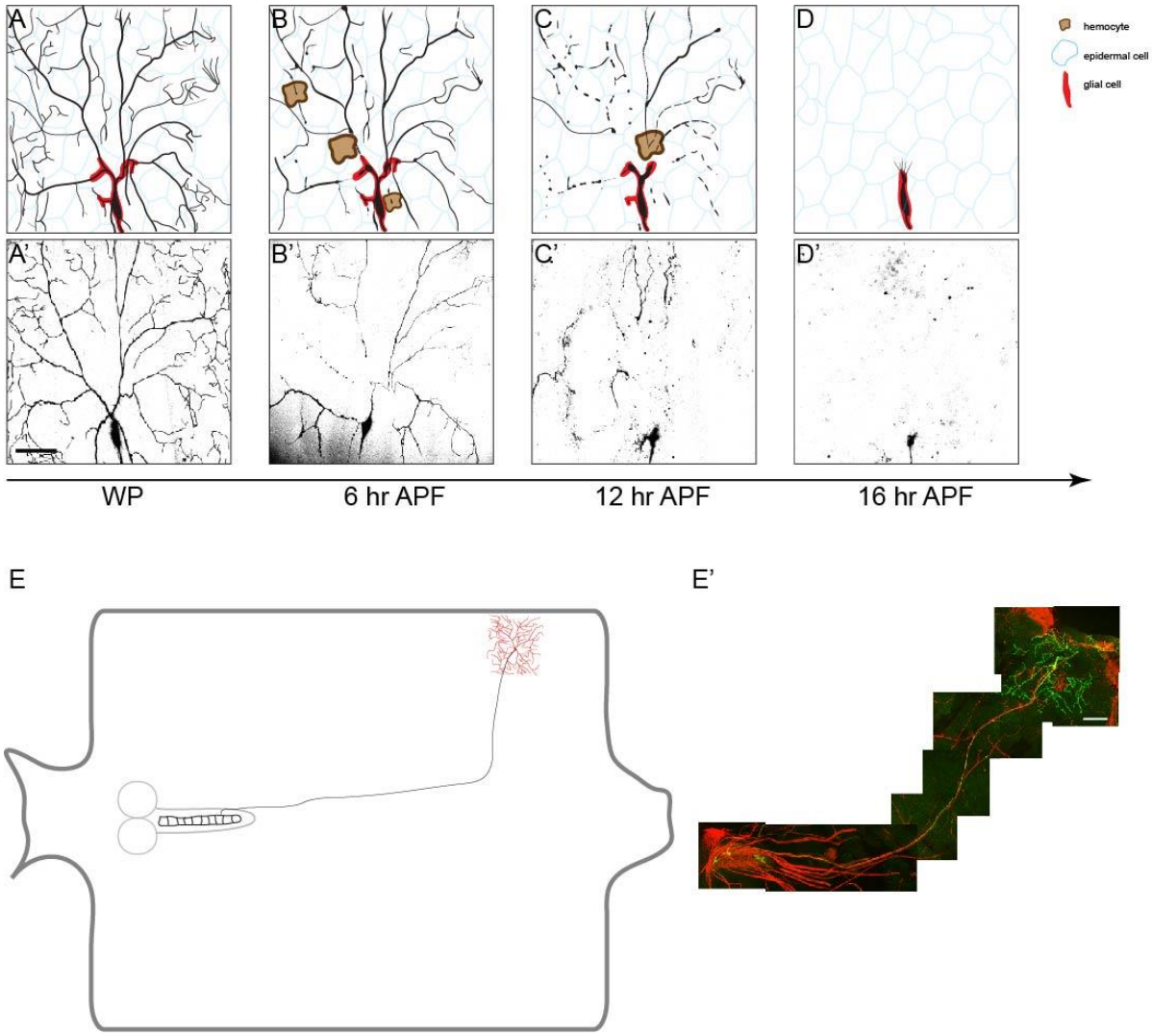

Figure 1. ddaC neurons undergo dendrite specific pruning during early metamorphosis.
(A-D) A scheme of dendrite pruning in ddaC neuron at different stages during early metamorphosis. (A'-D') Live confocal images of ddaC neurons expressing *UAS-mCD8-GFP* driven by *ppk-Gal4* at different stages during early metamorphosis. (E) A scheme of axon, dendrites and soma of ddaC neuron. (E') Live confocal images of f axon, dendrites and soma of ddaC neuron expressing *UAS-mCD8-GFP* (in green) driven by *ppk-Gal4* and neurite labelled by Futch staining (in red). Scale bars are 50 µm.

3.2 Genome-wide RNAi screen identifies novel players in dendrite pruning in ddaC neurons

In order to isolate novel players involved in dendrite pruning, my colleagues and I have conducted genome-wide RNA interference (RNAi) screen in ddaC

neurons. We took advantage of Gal4/UAS expression system (Brand and Perrimon, 1993) and ddaC-specific driver *Pickpocket-Gal4* (*ppk-Gal4*) (Grueber et al., 2003) to knockdown individual gene in ddaC neuron by expressing the corresponding inverted repeats RNAi construct (Dietzl et al., 2007). We built up a drive line that contains *ppk-Gal4* for ddaC-specific expression, *UAS-mCD8GFP* for live labelling, and *UAS-Dicer2* for efficient cleavage of double-strain RNA. The screen was highly efficient. After crossing the VDRC RNAi library with the drivers, we picked up the white pupae of offspring, aged them for 16 h and processed live confocal imaging for phenotypes (Fig2A).

Among 303 RNAi lines I screened, 14 lines corresponding to 13 genes were isolated with various pruning defects in the ddaC neurons at 16 hr APF (Table 1). These genes are potential candidates involved in ddaC dendrite pruning that require further studies.

A

♂♂ *UAS-RNAi* × *ppk-Gal4, UAS-mCD8-GFP; UAS-Dicer2* ♀♀

$$\frac{\textit{ppk-Gal4, UAS-mCD8-GFP}}{+};\frac{\textit{UAS-RNAi}}{\textit{UAS-Dicer2}}$$

1) Pick up pupae at 0 h APF
2) Age them for 16 h
3) Conduct live confocal imaging for pruning phenotype

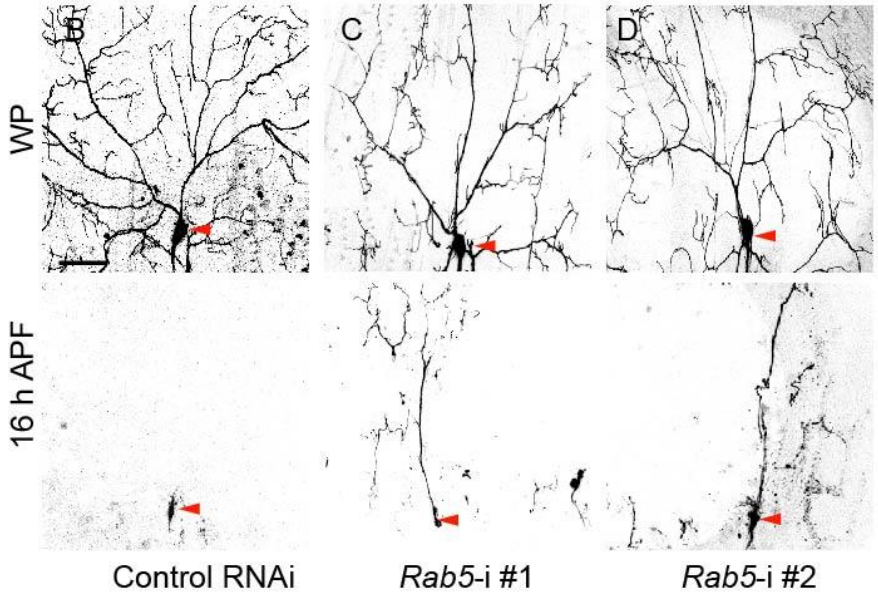

E

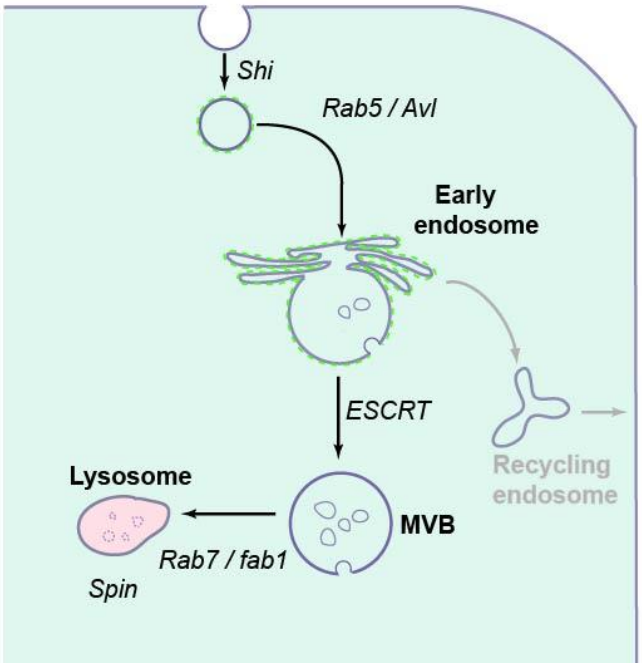

Figure 2. Genome-wide RNAi screen identifies Rab5 as a novel player in ddaC dendrite pruning. (A) A scheme of RNAi screen in ddaC dendrite pruning. (B-D) Live confocal images of ddaC neurons expressing *UAS-mCD8-GFP* driven by *ppk-Gal4* at WP stage and 16 hr APF. While the wild-type ddaC neurons pruned all the larval dendrites at 16 hr APF. Red arrowheads point to the ddaC somas. (B), knockdown Rab5 via v103945 (C) and v34096 (D) resulted in consistent dendrite pruning defects at 16 hr APF. (E) A scheme of endocytic pathways including endosomal formation, MVB maturation, endosomal recycling and lysosomal degradation. Scale bar is 50 μm.

3.3 Endocytic pathways are required for dendrite pruning in ddaC neurons

3.3.1 Rab5-denpednt early endocytic pathway is required for dendrite pruning in ddaC neurons

3.3.1.1 Rab5 is cell-autonomously required for dendrite pruning in ddaC neurons

Interestingly, my colleagues and I uncovered two independent RNAi lines v103945 and v34096 targeting the same gene Rab5 that resulted in dendrite pruning defects at 16 hr APF. Compared to control RNAi expressing ddaC neurons that completely pruned the larval dendrites at 16 hr APF (n=20, Fig 3A), knockdown *Rab5* by v103945 and v34096 in ddaC neurons caused mild but consistent dendrite pruning defects (n=16 and 15, respectively; Fig 2C, D). Rab5, a member of Rab protein family, is highly conserved between vertebrates and invertebrates to regulate many aspects of cellular vesicle trafficking (Fig 2E). Rab proteins are small GTPases that can convert between guanosine-triphosphate (GTP)-bound active state and guanosine diphosphate (GDP)-bound inactive state (Huotari and Helenius, 2011). In order to verify

the RNAi knockdown phenotype, a dominant-negative GDP-bound mutated form *Rab5*^{S43N} (*Rab5*^{DN}) (Entchev et al., 2000) was expressed via *ppk-Gal4* in ddaC neurons. Importantly, overexpression two copies of *Rab5*^{DN} with two copies of *ppk-Gal4* induced strong dendrite pruning defects with 5.2±0.6 primary and secondary dendrites attached to soma and 963±47 μm unpruned dendrites remained in ddaC neurons at 16 hr APF (n=19, 100%; Fig 3B). Moreover, the pruning defects caused by *Rab5*^{DN} overexpression could be rescued by co-overexpression of functional GFP-Rab5 (n=20, 0%, Fig 3C), suggesting the specificity of *Rab5*^{DN}. To further support the involvement of Rab5 in dendrite pruning, homozygous ddaC clones for *Rab5*^{2} null allele were generated by mosaic analysis with a repressible cell marker (MARCM) technique (Lee et al., 1999). Consistently, null allele *Rab5*^{2} mutant ddaC clones showed severe dendrite pruning defects with 8.3±0.9 primary and secondary dendrites attached to soma and 1,286±74 μm unpruned dendrites remained (n=15, 100%; Fig 3D) at 16 hr APF. Similarly, overexpression of functional YFP-Rab5 almost fully recued the dendrite pruning defects in *Rab5*^{2} ddaC clones (n=6, 0%; Fig3E).

Taken together, Rab5 is required for dendrite pruning in ddaC neurons during early metamorphosis.

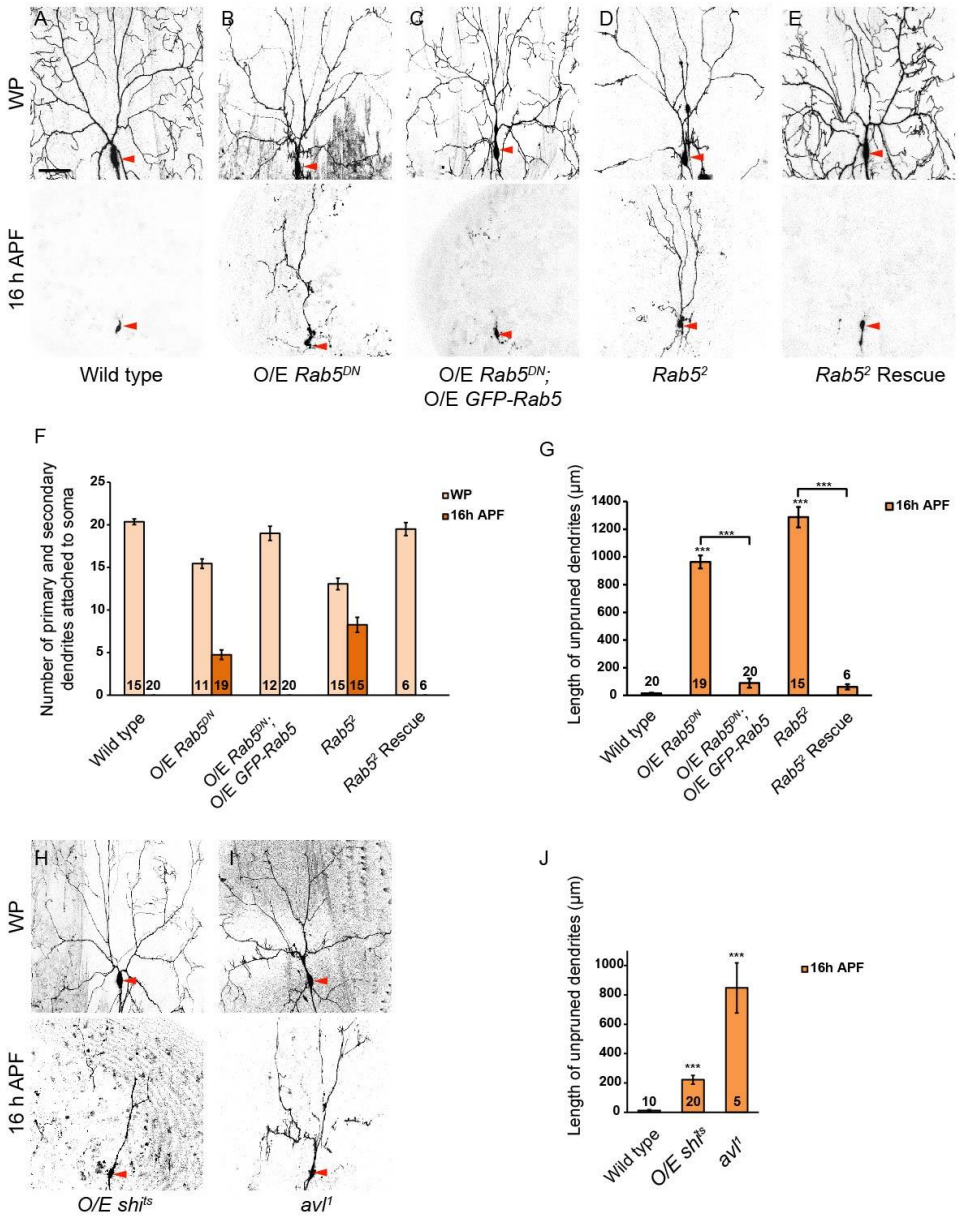

Figure 3. Early endocytic pathway is required for dendrite pruning in ddaC neurons. (A-E, .H, J) Live confocal images of ddaC neurons expressing *UAS-mCD8-GFP* driven by *ppk-Gal4* at WP stage and 16 hr APF. Red arrowheads point to the ddaC somas. While the wild-type ddaC neurons pruned all the larval dendrites (A), ddaC neurons overexpressing $Rab5^{DN}$ exhibited obvious dendrite severing defects at 16 h APF (B). Co-overexpression of GFP-tagged full-length Rab5 fully rescued the severing defect in $Rab5^{DN}$ expressing ddaC neurons at 16 h APF (C). $Rab5^{2}$ MARCM ddaC clones exhibited more severe dendrite severing defects at 16 h APF (D). Overexpression of YFP-tagged full-length Rab5 fully rescued the dendrite pruning defects in $Rab5^{2}$ MARCM ddaC clones at 16 h APF (E). Shi^{TS}-expressing ddaC neurons (H) or Avl^{1} MARCM ddaC clones (J) exhibited consistent dendrite pruning defects at 16 h APF. (F) Quantification of the average number of primary and secondary dendrites attached to the somas of wild-type and mutant ddaC neurons at WP stage and 16 h APF. (G, I, K) Quantification of the average length of unpruned dendrites of

ddaC neurons at 16 hr APF. The number of samples (n) in each group is shown on the bars. Error bars represent S.E.M.. *** p<0.001. Dorsal is up in all images. Scale bar is 50 μm.

3.1.1.2 Early endocytic pathways components shibire and Avalanche are involved in dendrite pruning in ddaC neurons

Rab5 is a key regulator in early endocytic pathway that control early endosome formation which leads to a hypothesis that the early endosomal function is required for dendrite pruning in ddaC neurons. Therefore, I examined overexpression of temperature-sensitive shibire (shi^{ts}), a dominant-negative form of *Drosophila* Dynamin at restrictive temperature, which could block the membrane fission during budding of early endosomes (Waddell et al., 2000). Indeed, with culture at restrictive temperature 32℃ for 2 days before puparium formation, overexpression of shi^{ts} caused dendrite pruning defects at 16 hr APF (55%, n=20; Fig 3H, J). Moreover, I tested the potential function of Avalanche (Avl), a *Drosophila* homolog of early endosomal syntaxin7, that regulates early endosome fusion(Lu and Bilder, 2005). Importantly, null allele avl^{1} mutant ddaC clones exhibited consistent dendrite pruning defects (100%, n=5; Fig 3I, J).

Collectively, the early endocytic pathway is crucial for dendrite pruning in ddaC neurons during early metamorphosis.

3.1.1.3 Rab5 regulates dendrite pruning in ddaC neurons independently of dendrite outgrowth defects

As reported previously, the dendrite outgrowth was strongly disrupted in Rab5 mutant ddaC neurons, reflected by simplified dendrite arbor at WP stage (Fig

3B, D)(Satoh et al., 2008). In order to rule out the possibility that the dendrite pruning defect are side effects of initial morphology defects, I used inducible gene-switch system (Osterwalder et al., 2001) to express *Rab5*^{DN} at 3rd instar larval stage, which did not affect the initial ddaC dendrite branching. Importantly, with wild-type dendrite arbors at WP stage, dendrite pruning defects were still observed in ddaC neurons of the RU486-fed animals at 16 h APF (50%, n=32; Fig 4A-C), suggesting that pruning defects derived from Rab5 mutant are not side effects of abnormal dendrite outgrowth.

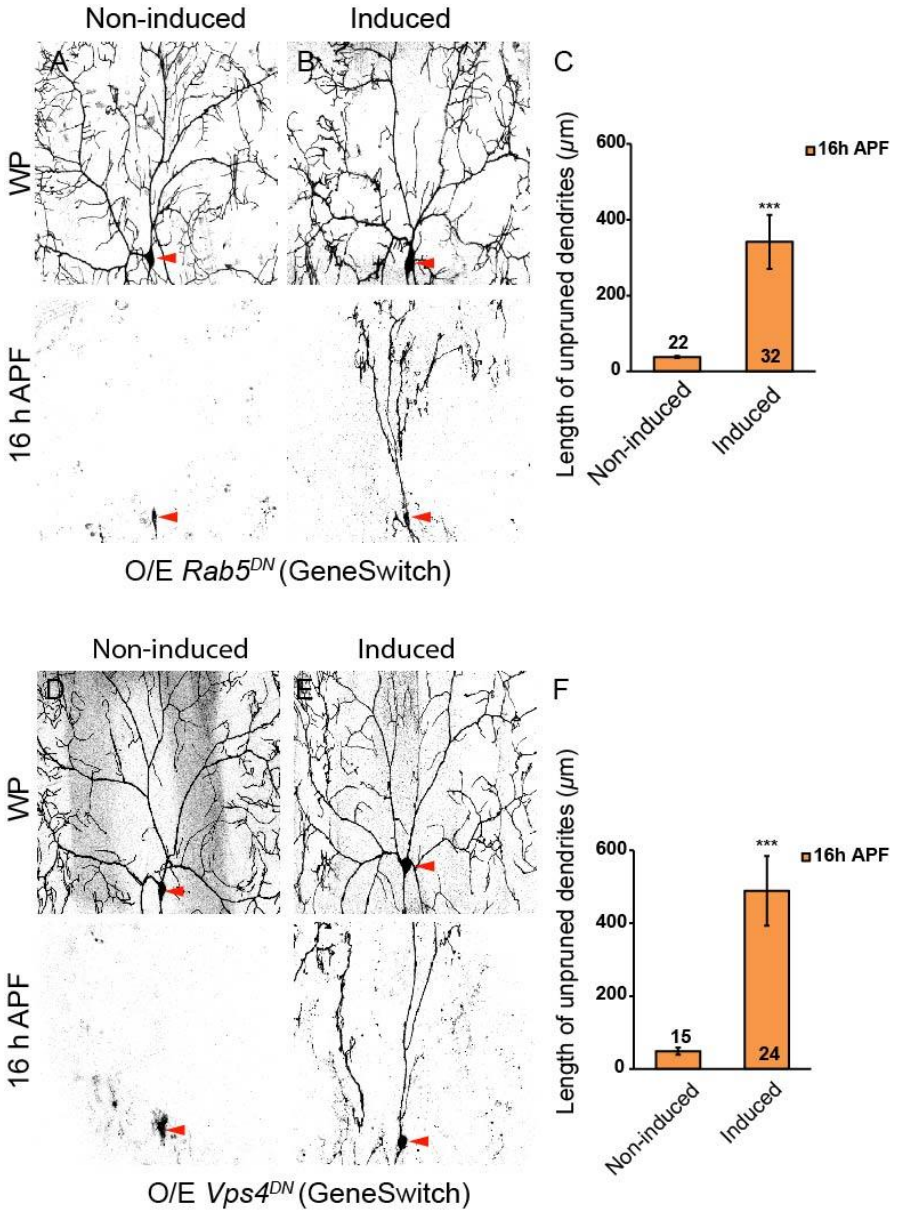

Figure 4. Endocytic pathways function in dendrite pruning independently of dendrite outgrowth defects in ddaC neurons. (A, B, D, E) Live confocal images of ddaC neurons expressing *ppk-mCD4-tdGFP* at WP stage and 16 h APF. Red arrowheads point to the ddaC somas. Using the RU486-inducible Gene-Switch system, inducible expression of $Rab5^{DN}$ (B) or $Vps4^{DN}$ (C) at the 3rd instar stage resulted in dendrite severing defects in ddaC neurons at 16 h APF without morphology defects at WP stage (A, D). (C, F) Quantification of the average length of unpruned dendrites of ddaC neurons at 16 hr APF. The number of samples (n) in each group is shown on the bars. Error bars represent S.E.M.. *** $p<0.001$. Dorsal is up in all images. Scale bar in A is 50 μm.

3.1.1.4 Rab5 is required for dendrite pruning in ddaD/E neurons but not apoptosis in ddaF neurons

During early metamorphosis, ddaD/E neurons also undergo dendrite pruning. In contrast to wild-type ddeD/E neurons that pruned their dendrite by 19 hr APF (n=20; Fig 5A), *Rab5*^{2} mutant ddaD/E clones showed strong pruning defect (100%, n=3; Fig 5B). Next, I examined ddaF neurons which undergo apoptosis during early metamorphosis. Interestingly, similar to wild-type ddaF neurons (n=5; Fig 5F), *Rab5*^{2} mutant ddaF clones died by 16 hr APF (n=3; Fig 5G), suggesting that Rab5 is dispensable for apoptotic neurons during early metamorphosis.

Taken together, Rab5 is specifically required for dendrite pruning in sensory neurons during early metamorphosis.

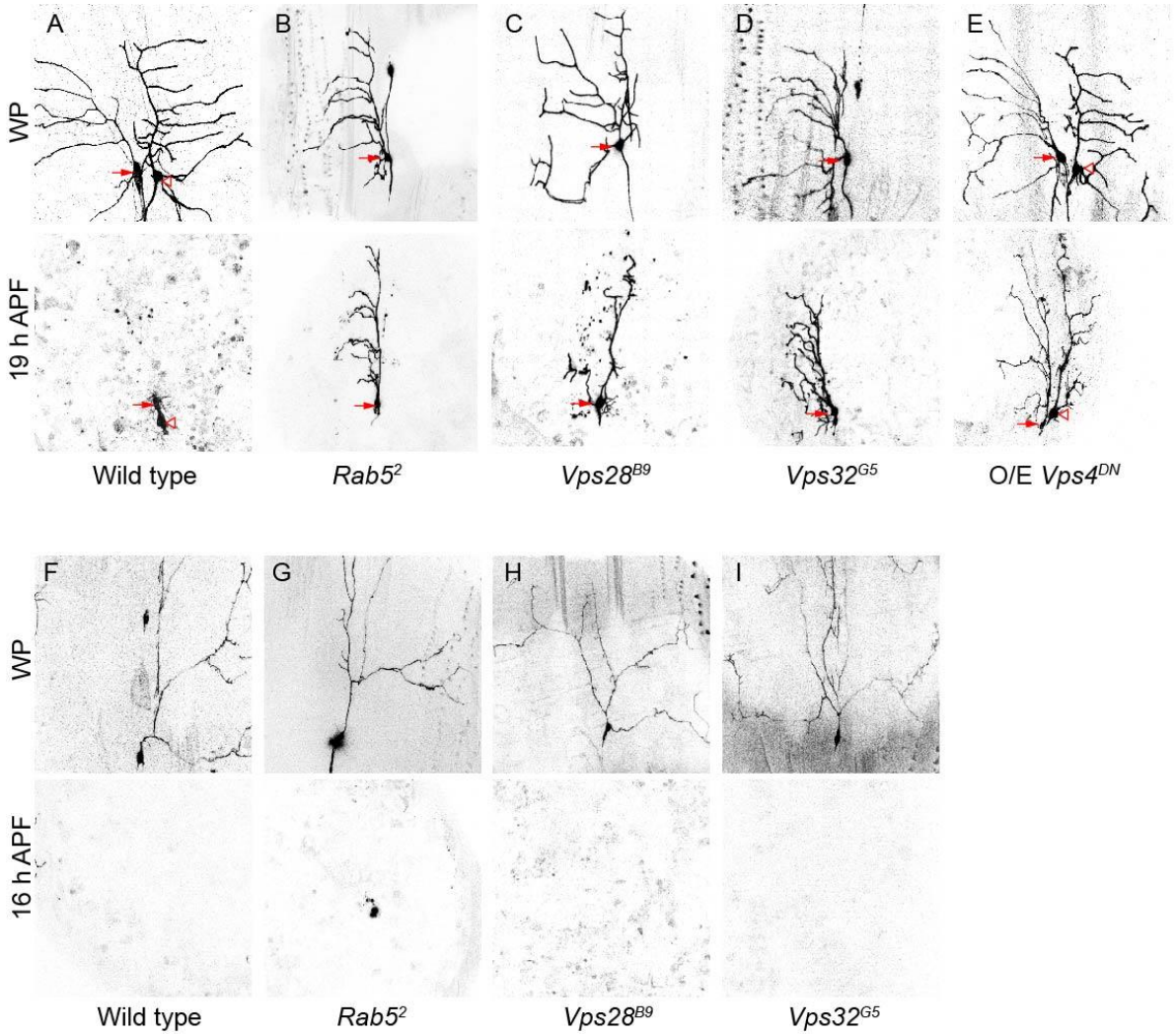

Figure 5. Endocytic pathways are important for dendrite pruning in ddaD/E neurons but dispensable for apoptosis in ddaF neurons. (A-I) Live confocal images of ddaD/E (A-E) or ddaF (F-I) neurons expressing mCD8-GFP at WP stage, 16 h or 19 h APF. Red arrowheads point to the ddaC somas. Red arrows point to the ddaD somas and open arrowheads to the ddaE somas. (A-E) While wild-type class I ddaD/ddaE neurons pruned their larval dendrites at 19 h APF (A), *Rab5*^{2} (B), *Vps28*^{B9} (C), *Vps32*^{G5} (D) or *Vps4*^{DN}-expressing (E) ddaD neurons failed to prune their larval dendrites at 19 h APF. (F-I) Similar to wild-type ddaF (F), *Rab5*^{2} (B), *Vps28*^{B9} (C), *Vps32*^{G5} (D) MARCM ddaF clones died at 16 hr APF. Scale bar is 50μm.

3.1.1.5 Rab5 is required for dendrite pruning rather than a general effect on cell survival

Since early endocytic pathway is critical for homeostasis in almost all cell types, it is possible that the dendrite pruning defects are side-effects of the unhealthy state in endocytic pathway mutant neurons. To rule out this

possibility, first, I examined two ddaC neuron specific markers Cut and Knot (Jinushi-Nakao et al., 2007). Interestingly, in *Rab5*^{DN}-expressing ddaC neurons (n=5, 5; Fig 6B, E), Cut and Knot staining were indistinguishable with wild-type neurons (n=5, 5; Fig 6A, D), suggesting that early endocytic pathway mutants do not affect the cell fate and identity of ddaC neurons. Second, I tested the upregulation of EcR-B1, a key upstream target of ecdysone signaling, during early metamorphosis in ddaC neurons (Kirilly et al., 2009). Similarly, EcR-B1 expression was also unaffected in *Rab5*^{DN}-expressing ddaC neurons (n=10; Fig 6H) compared to wild type (n=20 Fig 6G), indicating that the general response to metamorphosis is normal.

Taken together, early endocytic pathway appears to be required for dendrite pruning rather than maintenance of general cellular homeostasis.

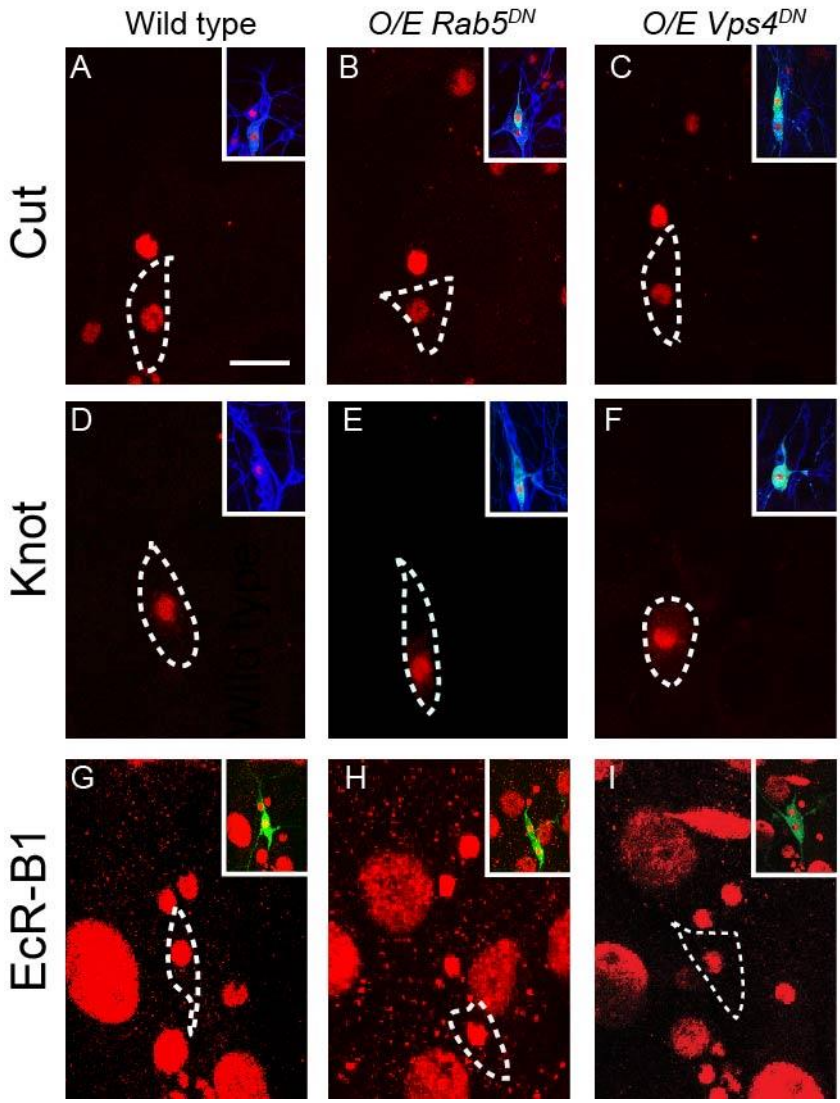

Figure 6. Loss of Rab5/ESCRT function does not lead to changes in general cell fate or identity of ddaC neurons. (A-I) Confocal images of wild-type and mutant ddaC neurons at WP stage immunostained with anti-Cut (A-C), anti-Knot (D-F), or anti- EcR-B1 (G-I). *Rab5^{DN}* (B, E, H) or *Vps4^{DN}*-expressing (C, F, I) ddaC neurons showed normal Cut, Knot and EcR-B1 staining at WP stage as wild-type control (A, D, G). Dorsal is up in all images. Scale bar is 20μm.

3.2.2 ESCRT-dependent endosomal maturation pathway is required for dendrite pruning

3.2.2.1 ESCRT is required for dendrite pruning in ddaC neurons

ESCRT-dependent endosomal maturation pathway is one of downstream routes after early endosome formation (Huotari and Helenius, 2011). Thus, I

examined the potential involvement of ESCRT during dendrite pruning by testing several core components of ESCRT complexes. First, I tested the Vps32, a component of ESCRT-III complex. null allele *Vps32*^{G5} (Vaccari et al., 2009) mutant ddaC clones for showed strong dendrite pruning defects with 4.4±0.7 primary and secondary dendrites attached to soma and 796±97 μm unpruned dendrites remained at 16 hr APF (87%, n=23; Fig 7B, G, H). The pruning defects of *Vps32*^{G5} mutant clones could be rescued by reintroduction of functional Myc-Vps32 (n=6; Fig 7E, G, H). Second, for Vps28, a component of ESCRT-I complex, null allele *Vps28*^{B9} (Vaccari et al., 2009) mutant ddaC clones exhibited similar dendrite pruning defects at 16 hr APF (62%, n=13; Fig 7D, G, H), which could be rescued by overexpression of wild-type Vps28 (n=3; Fig 7E, G, H). Lastly, disruption of Vps4, an AAA ATPase to disassembly ESCRT-III complex, by overexpression of dominant-negative form of Vps4 (*Vps4*^{DN}) that lacking the AAA ATPase activity (Rusten et al., 2007) resulted in consistent dendrite pruning defects (n=25, 72%; Fig 7F, G, H).

Collectively, ESCRT is required for dendrite pruning in ddaC neurons during metamorphosis.

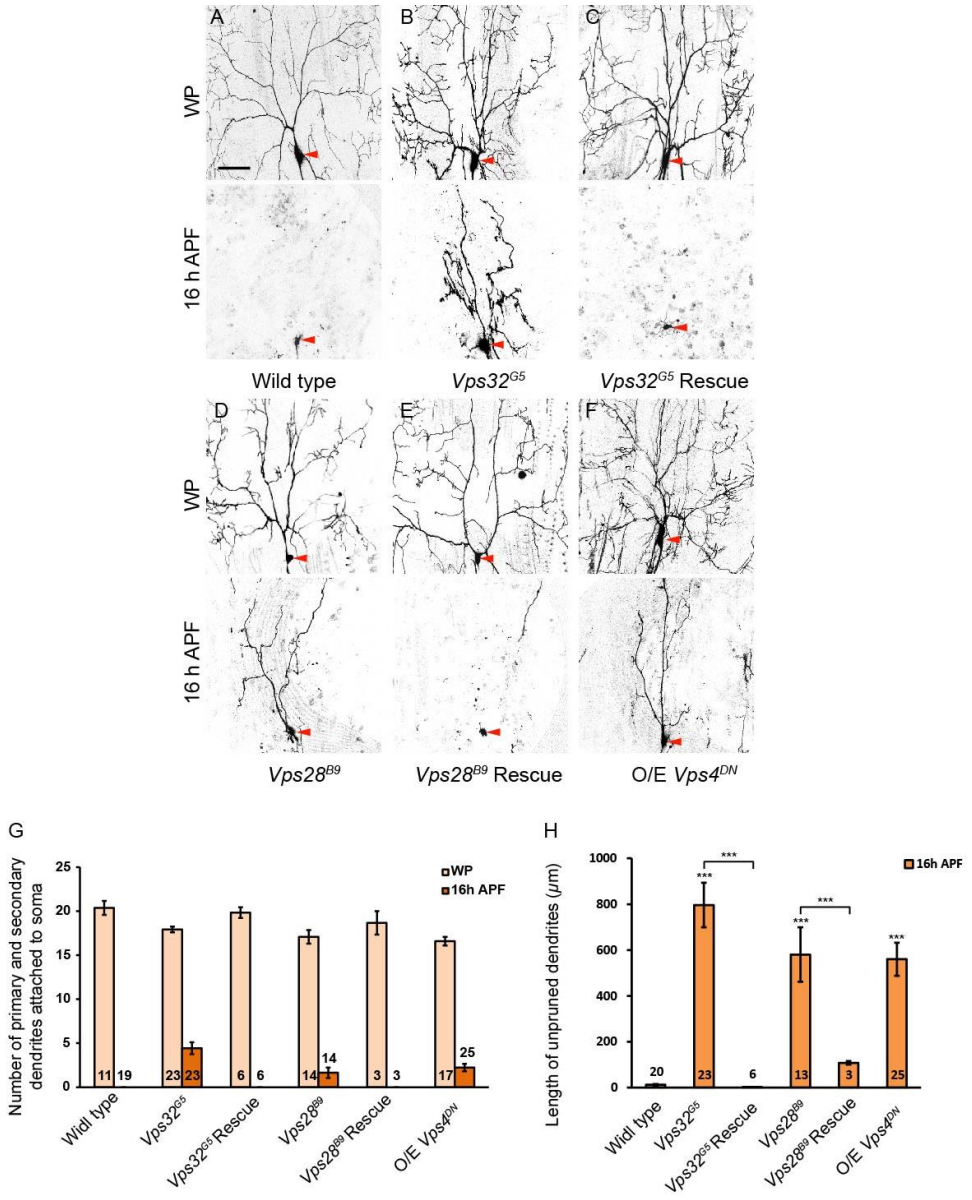

Figure 7. Endosomal maturation pathway is critical for dendrite pruning in ddaC neurons. (A-F) Live confocal images of ddaC neurons expressing *UAS-mCD8-GFP* at WP stage and 16 h APF. Red arrowheads point to the ddaC somas. While wild-type (A) ddaC neurons removed all their larval dendrites at 16 h APF, $Vps32^{G5}$ (B) or $Vp28^{B9}$ MARCM ddaC clones exhibited dendrite severing defects at 16 h APF. Overexpression of Myc-tagged full-length Vps32 fully or full-length Vps28 rescued the dendrite severing defects in $Vps32^{G5}$ (C) or ddaC $Vp28^{B9}$ MARCM clones at 16 h APF, respectively. Moreover, ddaC neurons overexpressing $Vps4^{DN}$ (D) also exhibited dendrite severing defects at 16 h APF. (G) Quantification of the average number of primary and secondary dendrites attached to the somas of wild-type and mutant ddaC neurons at WP stage and 16 h APF. (H) Quantification of the average length of unpruned dendrites of ddaC neurons at 16 hr APF. The number of samples (n) in each group is shown on the bars. Error bars represent S.E.M.. *** p<0.001. Dorsal is up in all images. Scale bar in A is 50 µm.

3.3.2.2 ESCRT function in dendrite pruning independently of dendrite outgrowth defects in ddaC neurons

Consistent with the previous study, Vps32 mutant (Sweeney et al., 2006) and other ESCRT components mutant showed over-branching at proximal dendrite region (Fig 7B, D, F). Thus, I used Gene-switch system to overexpress $Vps4^{DN}$ at late 3rd instar larval stage to avoid the outgrowth defects. Compared to the non-fed control (Fig 4D), $Vps4^{DN}$-expressing ddaC neurons from RU486-fed animals exhibited consistent dendrite pruning defects (75%, n=24; Fig 7E) without affecting the initial dendrite morphology, suggesting that ESCRT regulates dendrite pruning independently of dendrite branching.

3.3.2.3 ESCRT-dependent endosomal maturation pathway phenocopies Rab5-dendepdent early endocytic pathway during dendrite pruning in ddaC neurons

Resembling $Rab5^{2}$ mutant, $Vps28^{B9}$ (100%, n=3; Fig 5C), $Vps32^{G5}$ (100%, n=4, Fig 5D) and $Vps4^{DN}$-expressing ddaD/E neurons (100%, n=28; Fig 5E) showed pruning defect at 19 hr APF. Moreover, apoptosis of $Vps28^{B9}$ (n=3; Fig 5H), $Vps32^{G5}$ (n=3; Fig 5I) mutant ddaF neurons remained normal as wild type, indicating ESCRT-dependent endosomal maturation pathway is specifically required for dendrite pruning instead of apoptosis. In addition, consistent with $Rab5^{DN}$-expressing ddaC neurons, Cut (n=5; Fig 6C), Knot (n=5; Fig 6F) and EcR-B1 (n=10; Fig 6I) staining in $Vps4^{DN}$-expresssing ddaC neurons remained the same as wild-type ddaC neurons (n=5, 5, 20; Fig 6A, D, G), further suggesting ESCRT is specifically required for dendrite pruning instead of overall cellular homeostasis.

Collectively, ESCRT-dependent endosomal maturation pathway, resembling early endocytic pathway, is required for dendrite pruning in sensory neurons.

3.3.3 Lysosomal function regulator Rab7/Fab1/Spinster is dispensable for dendrite pruning

After endosomal maturation, one major route for MVB is to fuse with lysosomes for contents degradation (Huotari and Helenius, 2011). Thus, I investigated the potential involvement of the lysosomal function in ddaC dendrite pruning. First, I focused on Rab7, another highly conserved Rab family small GTPase which is important for lysosomal fusion and regeneration in mammalian studies (Bucci et al., 2000; Jordens et al., 2001). In order to test the potential function during ddaC dendrite pruning, I generated Rab7 null allele $Rab7^{EX1}$ which deletes the translation starting site by imprecise P-element excision technique (Fig 8A). Interestingly, like wild-type neurons, homozygous $Rab7^{EX1}$ mutant ddaC neurons pruned the larval dendrites by 16 hr APF (n=6; Fig 8B). Second, I examined *fab1* which has been reported to regulate MVB/lysosome fusion (Rusten et al., 2007). Consistently, $fab1^{21}$ mutant ddaC clones pruned the dendrite as wild-type neurons by 16 hr APF (n=6; Fig 8C). Thirdly, my colleague and I tested Spinster, a predicted lysosomal sugar transporter that regulates lysosome acidification (Dermaut et al., 2005; Sweeney and Davis, 2002). Similarly, Spinster mutants did not show obvious pruning defects (n=16; Fig 8D). Collectively, functions of the Rab7,

fab1 or Spinster appear to be dispensable in dendrite pruning during early metamorphosis.

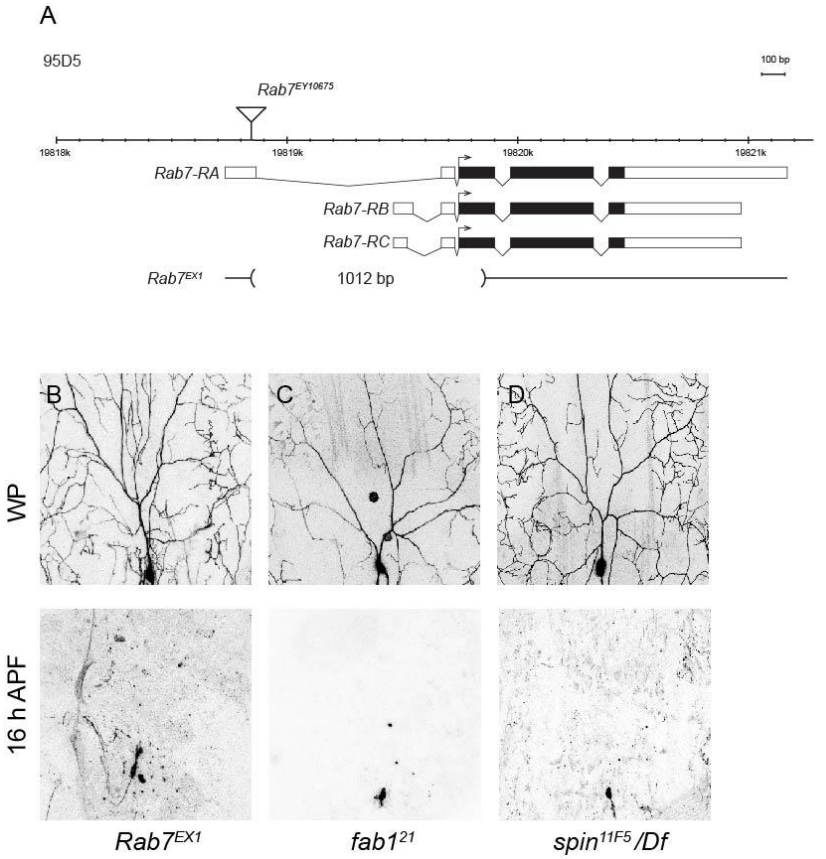

Figure 8. Lysosomal pathway components Rab7, fab1, Spin are not required for dendrite pruning in ddaC neurons. (A) A scheme of *Rab7*^{EX1} mutant. (B-D) Live confocal images of ddaC neurons expressing *UAS-mCD8-GFP* at WP stage and 16 h APF. Red arrowheads point to the ddaC somas. *Rab7*^{EX1} (B), *fab1*^{21} (C) or *spin*^{11F5} (D) mutant ddaC neurons exhibited normal dendrite pruning at 16 hr APF. Dorsal is up in all images. Scale bar in A is 50 μm.

3.4 Endocytic pathways regulate the turnover of certain cell surface molecules in ddaC neurons

3.4.1 Disruption of Rab5/ESCRT endocytic pathways leads to abnormal endosome formation

3.4.1.1 Disruption of endocytic pathways lead to aberrant endomsomes and Ubiquitinated protein deposits in ddac neurons

Based on the well-defined functions of Rab5/ESCRT in regulating endocytic trafficking, I attempted to investigate the cellular mechanisms underlying the endocytic pathways in dendrite pruning. Making use of the early endosomal marker Avl (Lu and Bilder, 2005), I examined the pattern of endosomal compartments in ddaC neurons. In wild-type ddaC neurons, Avl labelled small and weak puncta which reflecting the distribution of early endosomes (n=8; Fig 9A). However, in $Rab5^{2}$ (100%, n=4; Fig 9B) and $Rab5^{DN}$-expressing (100%, n=12; Fig 10B) ddaC neurons, Avl staining strongly labelled several large punctate structures, consistent with the previous report that disruption of early endocytic pathway results in enlarged aberrant endosomes (Satoh et al., 2008). Moreover, these enlarged abnormal endosomes were colabelled by anti-ubiquitin antibody (100%, n=4, 100%, n=12; 12Fig 9B, 10B), indicating the failure of ubiquitinated contents degradation. Interestingly, mutants of ESCRT components $Vps32^{G5}$ (100%, n=4; Fig 9C), $Vps28^{B9}$ (100%, n=4; Fig 9D) and $Vps4^{DN}$-expressing (100%, n=10; Fig10C) ddaC neurons exhibited even more diffused and severe Avl/Ubi-positive aberrant endosomes. In addition, early endosome/MVB marker hrs (Lloyd et al., 2002) also accumulated on these aberrant endosomes in $Rab5^{2}$ (100%, n=5; Fig 9F),

Rab5^{DN}-expressing (100%, n=14; Fig 10F), *Vps32*^{G5} (100%, n=3; Fig 9G), *Vps28*^{B9} (100%, n=3; Fig 9H) and *Vps4*^{DN}-expressing (100%, n=10; Fig10G), further supporting the disruption of normal endocytic trafficking. In addition, using Gene-Swtich system to express *Rab5*^{DN} (52%, n=21, 60%, n=10; Fig 17K, L) or *Vps4*^{DN} (80%, n=10, 89%, n=9; Fig 17M, N) at late larval stage was sufficient to induce the formation of aberrant endosomes at WP stage or 6 hr APF, indicating the aberrant endosomes and ubiquitinated deposits at least partially formed during dendrite pruning. Taken together, Rab5 and ESCRT complexes-dependent endocytic pathways are required for proper endosomal trafficking and degradation of ubiquitinated proteins in ddaC neurons.

Given that the pattern of aberrant endosomes were different between Rab5 and ESCET mutants, I tried to co-express *Rab5*^{DN} and *Vps4*^{DN} in ddaC neurons. Ideally, Co-overexpression of *Rab5*^{DN} and *Vps4*^{DN} should mimic *Rab5*^{DN} phenotype because Rab5 is upstream of ESCRT. Indeed, disruption of Rab5 and Vps4 led to two to three enlarged endosomes (n=10, 10; Fig 10D, H), mimicking loss of Rab5 alone (n=12, 14; Fig 10B, F), indicating Rab5 is epistatic to ESCRT in aberrant endosome formation.

Next, I went on examining the late endosome/lysosome marker GFP tagged lysosome-associated membrane protein 1 (LAMP1-GFP) in ddaC neurons (Pulipparacharuvil et al., 2005). In wild-type neurons, LAMP1-GFP exhibited dispersive and small puncta (n=12; Fig 9I). However, in *Rab5*^{DN} (100%, n=20; Fig 9J) and *Vps4*^{DN}-expressing (100%, n=10; Fig 9J) ddaC neurons,

LAMP1-GFP showed two to three enlarged puncta that colocalized with ubiquitinated protein deposits, indicating that the aberrant endosomes might possess the nature of late endosomes and/or lysosomes.

Taken together, disruption of endocytic pathways results in formation of aberrant endosomes and ubiquitinated protein aggregations in ddaC neurons.

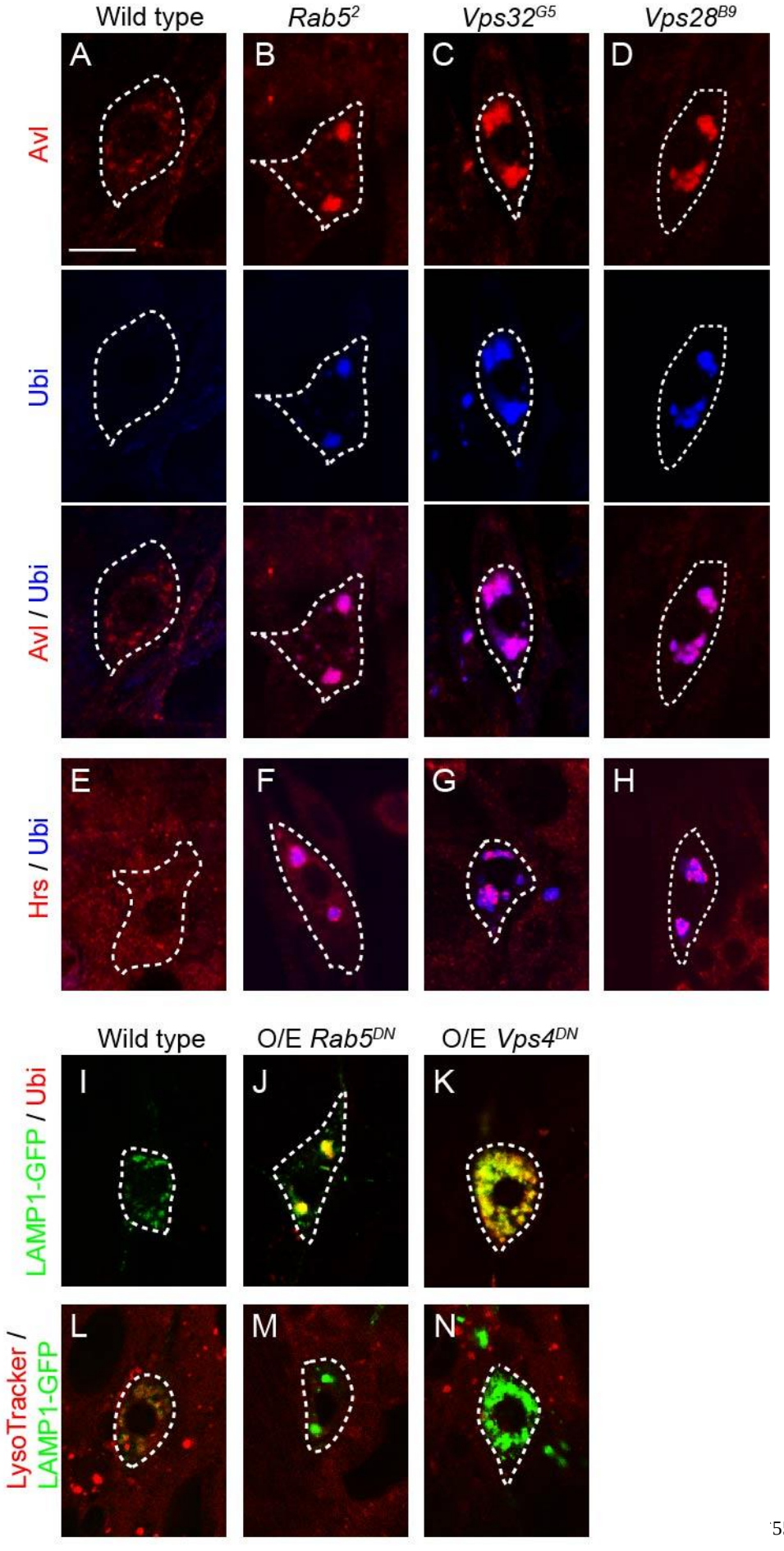
Wild type
Rab5²
Vps32G5
Vps28B9
A
B
C
D
Avl
Ubi
Avl / Ubi
E
F
G
H
Hrs / Ubi
Wild type
O/E Rab5DN
O/E Vps4DN
I
J
K
LAMP1-GFP / Ubi
L
M
N
LysoTracker / LAMP1-GFP

Figure 9. Loss of Rab5/ESCRT function leads to aberrant endosome formation and ubiquitinated protein deposits in ddaC neurons. (A-H) Confocal images of wild-type and mutant ddaC neurons at the late wL3 stage immunostained with anti-Avl (in red), anti-Ubiquitin (in blue), or anti- Hrs (in red). ddaC somas are marked by dashed lines. (A-D) Avl and ubiquitinated protein deposits were accumulated on enlarged endosomes in $Rab5^{2}$ (B), $Vp32^{G5}$ (C) or $Vps28^{B9}$ (D) MARCM ddaC clones, but not in the wild-type (A) ddaC neurons. (E-H) Hrs proteins were accumulated on aberrant endosomes in $Rab5^{2}$ (F), $Vp32^{G5}$ (G) or $Vps28^{B9}$ (H) MARCM ddaC clones but not in wild-type (E) ddaC neurons. (I-K) Confocal images of ddaC neurons expressing a late endosomal/lysosomal marker LAMP1-GFP (in green) driven by *ppk-Gal4* at the late wL3 stage immunostained with anti-Ubiquitin (in red). While LAMP1-GFP showed uniform distribution in wild-type ddaC neurons (I), LAMP1-GFP was enriched on the enlarged endosomes in $Rab5^{DN}$ (J) or $Vps4^{DN}$ (K) expressing ddaC neurons. (L-N) Confocal images of ddaC neurons expressing LAMP1-GFP driven by *ppk-Gal4* at the late wL3 stage were stained with LysoTracker (in red). While LysoTracker signals were partially colocalized with LAMP1-GFP in wild-type (L) ddaC neurons, LysoTracker staining did not colocalize with LAMP1-GFP-positive aberrant endosomes in ddaC neurons expressing $Rab5^{DN}$ (M) or $Vps4^{DN}$ (N). Dorsal is up in all images. Scale bar is 10μm.

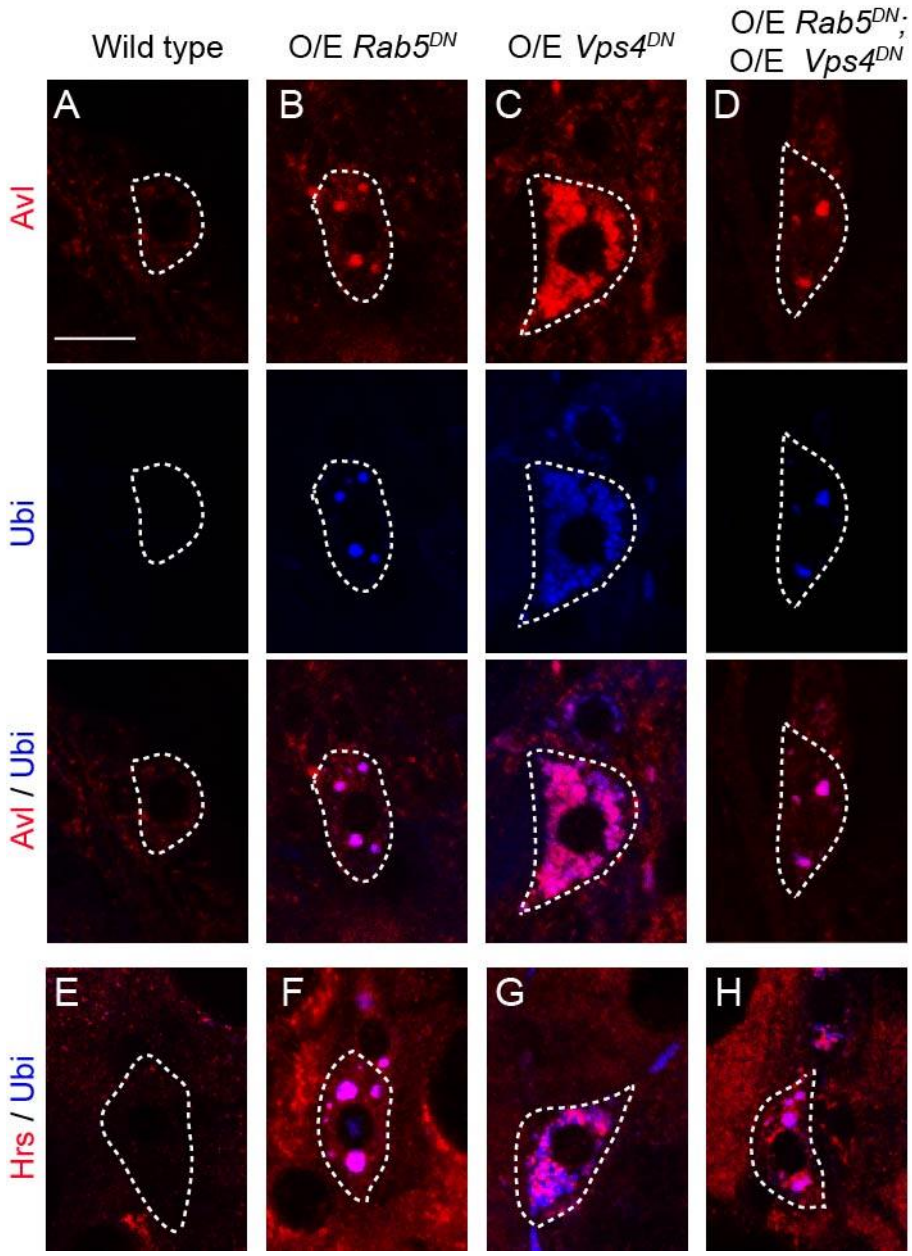

Figure 10. Early endocytic pathway is upstream of endosomal maturation pathway in ddaC neurons. (A-H) Confocal images of wild-type and mutant ddaC neurons expressing *UAS-mCD8-GFP* driven by *ppk-Gal4* at the late wL3 stage immunostained with anti- Avl (in red), anti-Ubiquitin (in blue), or anti-Hrs (in red). ddaC somas are marked by dashed lines. (A-D) Avl proteins and ubiquitinated proteins were accumulated on aberrant endosomes in $Rab5^{DN}$ (B) or $Vps4^{DN}$-expressing (C) ddaC neurons in distinct patterns, while $Rab5^{DN}$ and $Vps4^{DN}$ co-expressing (D) mimicked $Rab5^{DN}$-expressing ddaC neurons. (E-H) Consistently, Hrs proteins and ubiquitinated proteins were accumulated on aberrant endosomes in $Rab5^{DN}$ (F) or $Vps4^{DN}$-expressing (G) ddaC neurons in distinct patterns, while $Rab5^{DN}$ and $Vps4^{DN}$ co-expressing (H) mimicked $Rab5^{DN}$-expressing ddaC neurons. Dorsal is up in all images. Scale bar is 10μm.

3.4.1.2 Aberrant endosomes derived from endocytic pathways mutants fail to fuse with lysosomes to degrade the contents in ddaC neurons

To further clarify the feature of aberrant endosomes derived from Rab5/ESCRT mutant ddaC neurons, I utilized LysoTracker, a fluorescent dye labels highly acidified lysosomal compartments, to stain the aberrant endosomes. In wild-type neurons, LysoTracker staining partially colocalized with LAMP1-GFP, suggesting part of the LAMP-GFP-positive vesicles were acidified lysosomes (n=13; Fig 9L). On the contrary, LysoTracker failed to label the LAMP-GFP-positive aberrant endosomes derived from $Rab5^{DN}$ (n=8; Fig 9M) or $Vps4^{DN}$-expressing (n=10; Fig 9N) ddaC neurons, suggesting that aberrant endosomes are not capable to fuse with lysosomes to degrade the contents.

Thus, aberrant endosomes and ubiquitinated protein deposits in Rab5/ESCRT mutant ddaC neurons appear to result from disruption of normal endosomal maturation and failure of endosome/lysosome fusion.

3.4.1.3 Disruption of endocytic pathways do not affect other organelles in ddaC neurons

As control experiments, I tested the patterns of other organelles in endocytic mutant ddaC neurons via various markers, such as the mitochondria marker Mito-GFP (n=10, respectively; Fig A-C), the *cis*-Golgi marker GM130 (n=10, respectively; Fig D-F) and ER marker KDEL (n=10, respectively; Fig G-I). Importantly, all these markers showed normal patterns in $Rab5^{DN}$ or $Vps4^{DN}$-expressing ddaC neurons and did not colocalized with the

ubiquitinated deposits, indicating that endocytic pathways mutant specifically affect endosomal compartments in ddaC neurons.

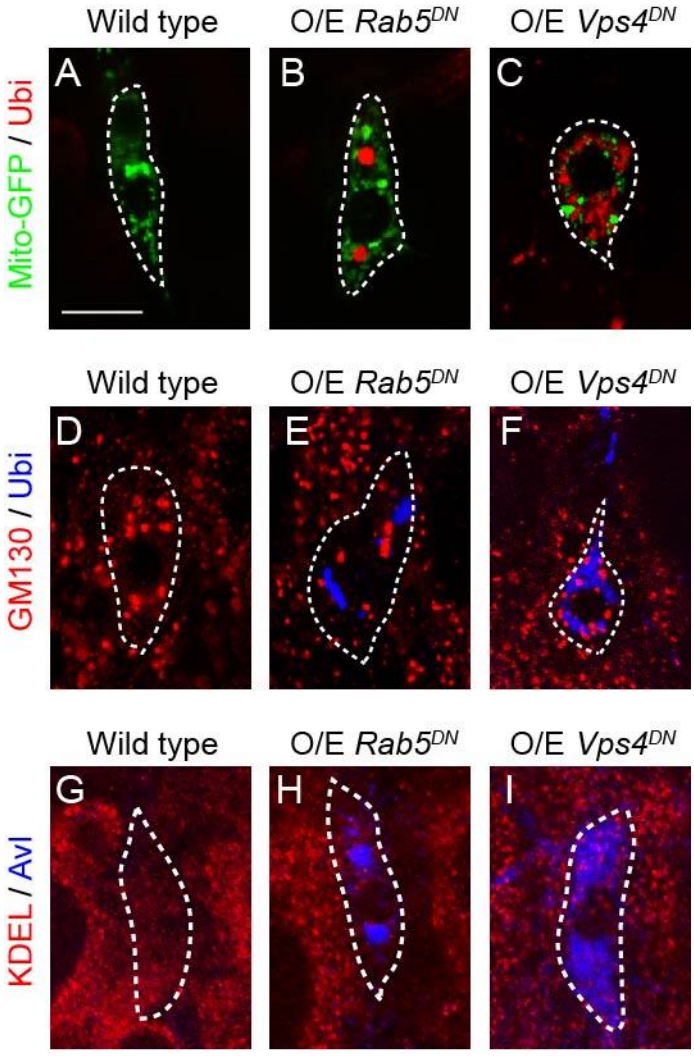

Figure 11. Loss of *Rab5*/*ESCRT* functions does not affect other organelles in ddaC neurons. (A-E) Confocal images of wild-type and mutant ddaC neurons expressing *UAS-mCD8-GFP* or *UAS- Mito-GFP* (in green) driven by *ppk-Gal4* at the late wL3 stage immunostained with anti-Ubiquitin (in blue), anti-*cis*-Golgi marker GM130 (in red) or anti-endoplasmic reticulum maker KDEL (in red). ddaC somas are marked by dashed lines. (A-C) Mito-GFP in $Rab5^{DN}$ (B) or $Vps4^{DN}$ (C) ddaC neurons was distributed similar to that in wild-type ddaC neurons (A) and absent from the aberrant endosomes. (D-F) GM130 in ddaC neurons expressing $Rab5^{DN}$ (E) or $Vps4^{DN}$ (F) was similar to wild-type ddaC neurons (D) and absent from the aberrant endosomes. (G-I) KDEL staining in ddaC neurons expressing $Rab5^{DN}$ (H) or $Vps4^{DNv}$ (I) remained indistinguishable to wild-type ddaC neurons (G) and absent from the aberrant endosomes. Dorsal is up in all images. Scale bar in A is 10 µm.

3.4.2 Cell-surface molecules accumulate on aberrant endosomes in Rab5/ESCRT mutant ddaC neurons

3.4.2.1 Endocytic pathways do not regulate canonical targets turnover in ddaC neurons

Endocytic pathways are crucial for internalizing cell-surface molecules to attenuate various signaling pathways to achieve proper homeostasis in different cell types (Ceresa and Schmid, 2000). In order to uncover the potential endocytosed membrane molecules involved in ddaC dendrite pruning, I tested the some known signaling pathways undergo endocytosis in Drosophila during development, including Notch, Wingless, Dpp, EGFR, TKR, PVR and Hegehog (Dubois et al., 2001; Jekely and Rorth, 2003; Lloyd et al., 2002; Thompson et al., 2005; Vaccari and Bilder, 2005). However, none of these signaling pathways seem to be involved in ddaC dendrite pruning. First, via antibody immunostaining, none of the ligands/receptors in these pathways accumulated on aberrant endosomes in $Rab5^{DN}$ or $Vps4^{DN}$-expressing ddaC neurons (Table 2). Second, reporters and effectors of these pathways showed no difference in $Rab5^{DN}$ or $Vps4^{DN}$-expressing ddaC neurons when compared to wild-type neurons (Table 3). Lastly, suppression of these pathways via overexpression of dominant negative components did not alter the dendrite pruning defects caused by overexpression of $Rab5^{DN}$ in ddaC neurons (Table 4).

Collectively, these known targets of endocytic pathways are not required for dendrite pruning in ddaC neurons.

3.4.2.2 Antibody-based screen uncovers cell-surface molecules Nrg, Robo and N-Cad as cargoes of endocytic pathways in ddaC neurons

In order to search for the potential targets of endocytic pathways in ddaC neurons, I made use of a monoclonal antibody collection from Developmental Studies Hybridoma Bank (DSHB) against cell-surface molecules. In this antibody-based candidate screen, Nrg, Roundabout (Robo) and N-Cadherin (N-Cad) were identified to accumulate on the aberrant endosomes among 45 antibodies tested (Table 5).

Nrg is a highly conserved L1-CAM cell adhesion molecule that regulates axon targeting, neurites legation, synapse formations in both vertebrates and invertebrates (Hortsch, 2000). BP104 specifically recognized the neuron isoform Nrg180 (Hortsch et al., 1990). At wandering 3rd instar larval stage (w3L), Nrg located on plasma membrane in ddaC neurons (n=12; Fig 12A). Interestingly, in contrast to wild-type ddaC neurons, Nrg strongly accumulated on aberrant endosomes labelled by Avl in *Rab5*^{2} mutant (100%, n=12; Fig 12B) and *Rab5*^{DN}-expressing (100%, n=12; Fig 12C) ddaC neurons. In addition, Nrg level also increased by 1.5 folds on soma cortex in *Rab5*^{2} (Fig 12B) and *Rab5*^{DN}-expressing (Fig 12C) mutant ddaC neurons compared to wild-type ddaC neurons (Fig 12A), which might due to the disruption of Nrg internalization from plasma membrane. Knockdown of Nrg via RNAi in *Rab5*^{DN}-expressing ddaC neuron almost fully eliminated Nrg staining (n=5; Fig 12D), suggesting that the Nrg staining was specific. In *Vps32*^{G5} mutant (100%, n=8; Fig 12E) or *Vps4*^{DN}-expressing (100%, n=10; Fig 12F) ddaC

neurons, Nrg showed even stronger aggregations on the aberrant endosomes, which could be removed by Nrg RNAi knockdown (n=10; Fig 12G). Taken together, Nrg turnover requires Rab5/ESCRT-dependent endocytic pathways.

Similarly, Robo, a transmembrane receptor of Slit that is important for axon guidance (Kidd et al., 1999), and N-Cad, a cell adhesion molecule regulate various neuronal development including outgrowth, fasciculation, differentiation (Kurusu et al., 2012), exhibited accumulations on aberrant endosomes in Rab5/ESCRT mutant ddaC neurons. By using 13C9 that recognized Robo, accumulations were detected on aberrant endosomes in $Rab5^{2}$ (100%, n=3; Fig 13B), $Rab5^{DN}$-expressing (100%, n=3; Fig 13I), $Vps32^{G5}$ (100%, n=3; Fig 13C), $Vps28^{B9}$ (100%, n=3; Fig 13D) or $Vps4^{DN}$-expressing (100%, n=10; Fig 13K), although endogenous Robo staining was undetectable in wild-type ddaC neurons (n=10; Fig 13A). Likewise, the Robo accumulations were eliminated by RNAi knockdown (n=6; Fig 13J), indicating the specificity of antibody staining. Displaying similar pattern as Robo, N-Cad Strongly accumulated on aberrant endosomes by DN-Ex #8 staining (100%, n=3, 5, 4, 10, 10, respectively; Fig 13F-H, J, K) and showed no obvious staining in wild-type ddaC neurons (n=10; Fig 13E). N-Cad staining was specific which was demonstrated by removal of accumulations by RNAi knockdown (n=6; Fig 13L). These data suggest that Robo and N-Cad also undergo endocytosis in ddaC neurons.

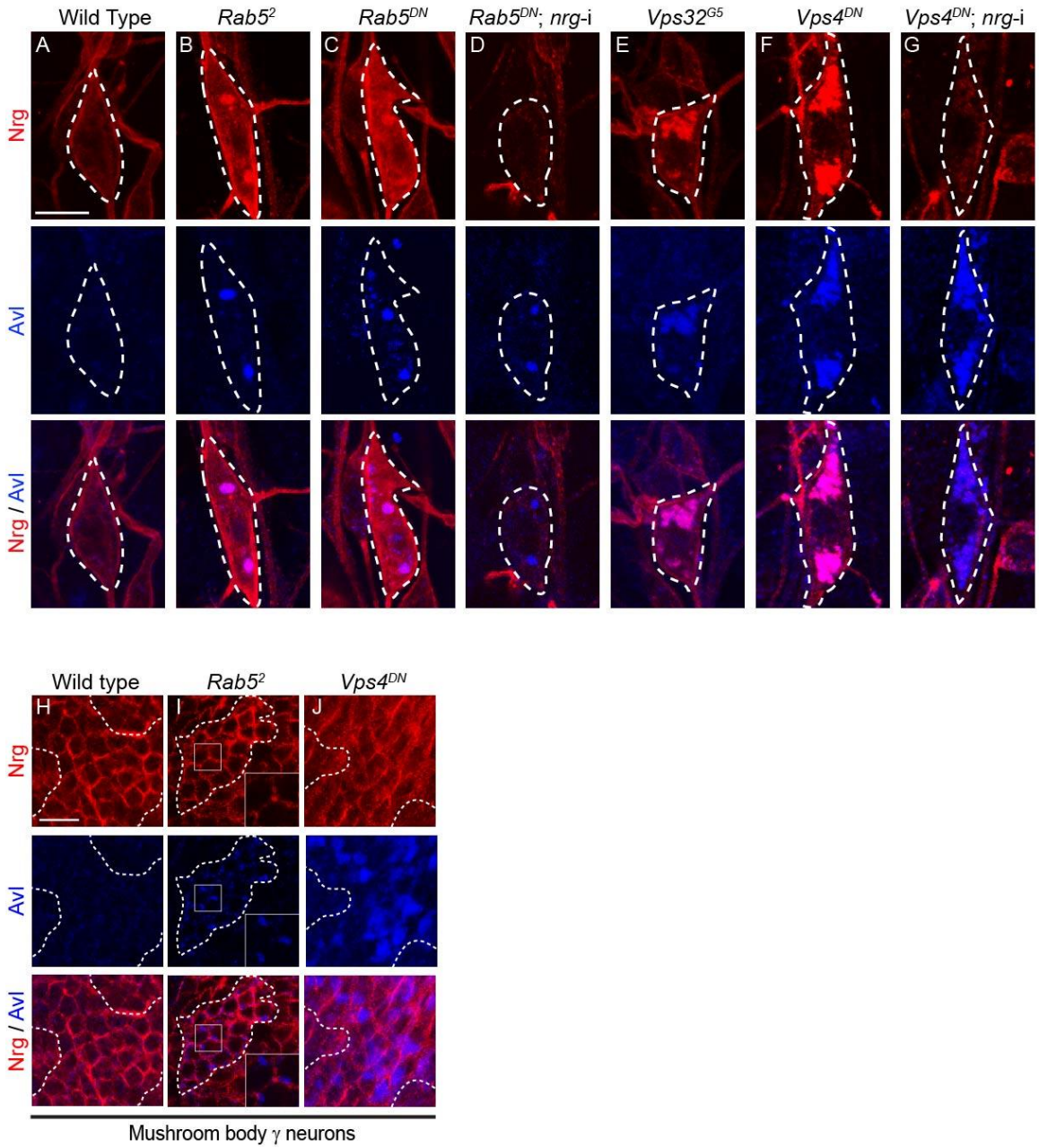

Figure 12. Cell adhesion molecule Nrg accumulates on the aberrant endosomes in *Rab5*/*ESCRT* mutant ddaC neurons. (A-G) Confocal images of ddaC neurons expressing *UAS-mCD8-GFP* driven by *ppk-Gal4* at late wL3 stage immunostained for Nrg (in red) and Avl (in blue). ddaC somas are marked by dashed lines. In wild-type (A) ddaC neurons, cortically localized Nrg and weak Avl puncta were detected at late wL3 stage in ddaC neurons, whereas Nrg proteins were robustly accumulated on Avl-positive aberrant endosomes in $Rab5^{DN}$ (B) or $Vps4^{DN}$ (F) expressing ddaC neurons, $Rab5^{2}$ (C), $Vp32^{G5}$(E) MARCM ddaC clones. The Nrg levels in $Rab5^{DN}$ (D) or $Vps4^{DN}$ (G) expressing ddaC neurons were greatly diminished by Nrg RNAi knockdown. (H-J) Confocal images of wild-type and mutant MB γ neurons expressing *UAS-mCD8-GFP* driven by *201Y-Gal4* at the late wL3 stage immunostained for Nrg (in red) and the early endosomal marker Avl (in blue). Somas of MB γ neuron are marked by dashed lines. Wild-type γ neurons (H) exhibited cortical Nrg staining and weak Avl staining. $Rab5^{2}$ MARCM (I) and $Vps4^{DN}$-expressing γ neurons (J) exhibited

enlarged Avl-positive endosomes with no Nrg aggregates. Dorsal is up in all images. The scale bar in A is 10 μm, and scale bar in H is 20 μm.

3.4.2.3 Endocytosis of Nrg is cell type-specific

Furthermore, I examined if endocytosis of Nrg was a common event in different types of neurons. I generated *Rab5*^{2} mutant clones for mushroom body γ neurons, CNS neurons that also undergo pruning. Interestingly, these *Rab5*^{2} mutant clones showed obvious aberrant endosomes labelled by Avl (n=10; Fig 12I). However, Nrg was still localized on plasma membrane instead of aberrant endosomes (n=5; Fig 12I), similar to wild type (n=10; Fig 12 H). Consistently, Nrg was not enriched on aberrant endosomes in *Vps4*^{DN}-expressing mushroom body γ neurons (n=10; Fig 12J).

Thus, active redistribution and downregulation of Nrg via endocytic pathways appears to be a specific event during dendrite pruning in ddaC neurons.

3.4.2.4 Endocyitc pathways are selectively required for the turnover of certain cell-surface protein

Nrg, Robo and N-Cad are specifically mediated by endocytic pathways rather than generally endocytosed together with all the membrane-associated proteins. First, the majority of the antibody-based screen candidates did not accumulate on aberrant endosomes (Table 5). Second, the membrane-bond mCD8-GFP did not colocalize with aberrant endosomes. Third, CAMs intergrins that function in ddaC neuron during dendrite branching (Han et al., 2012) did not show enrichment on aberrant endosomes (n=5, 5; Fig 13N, O).

Taken together, turnovers of Nrg, Robo and N-Cad appear to be regulated by endocytic pathways in ddaC neurons specifically.

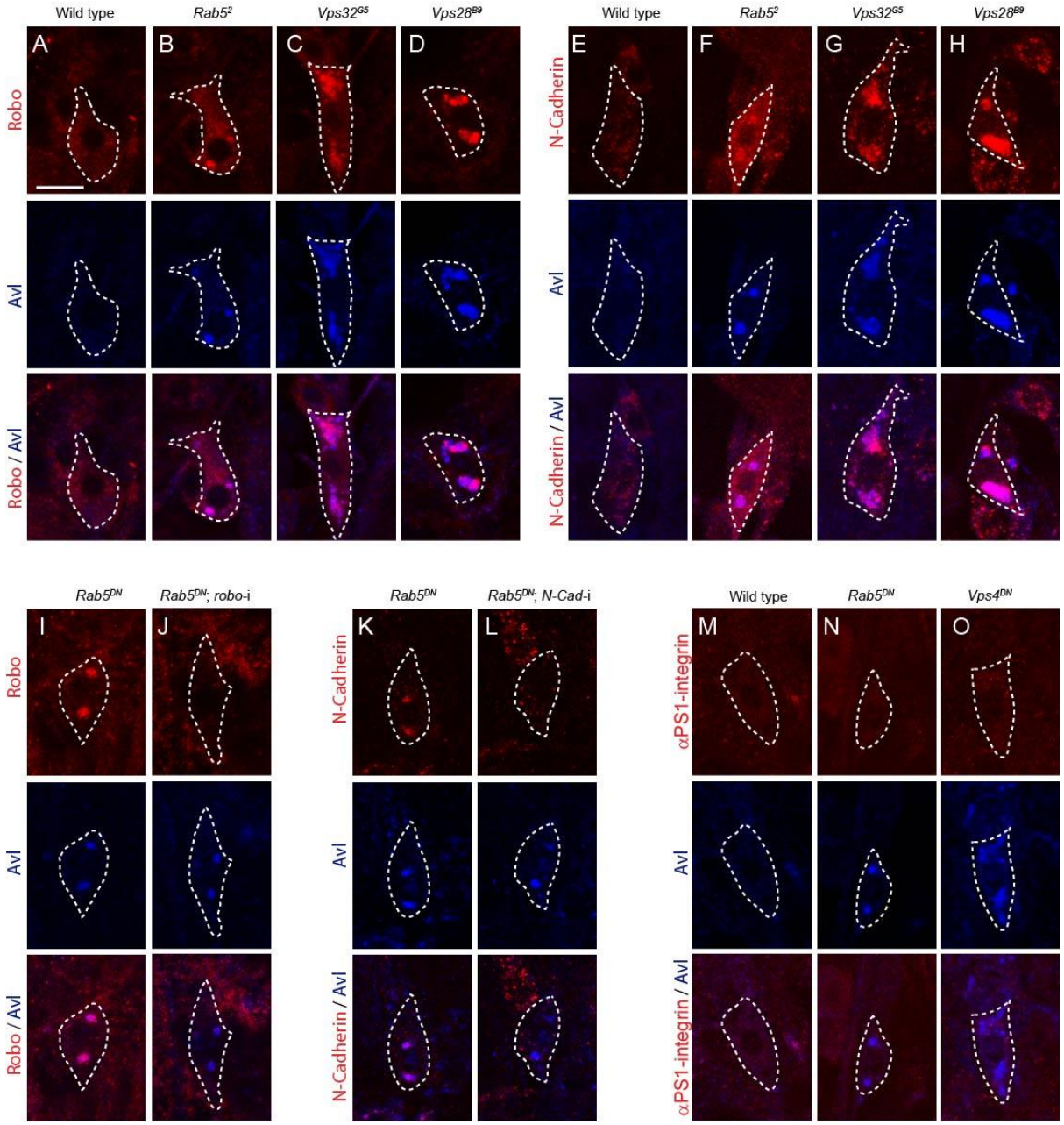

Figure 13. The cell-surface molecules Robo and N-Cad enrich on aberrant endosomes in *Rab5*/*ESCRT* mutant ddaC neurons but not integrin. (A-E) Confocal images of wild-type and mutant ddaC neurons expressing *UAS-mCD8-GFP* at the late wL3 stage immunostained with anti-Robo (in red), anti-Avl (in blue), anti-N-Cad (in red) or anti-α-PS1-integrin (in red).

ddaC somas are marked by dashed lines. (A) Compared to weak staining in wild-type ddaC neurons, Robo protein was accumulated on aberrant Avl-positive endosomes in *Rab5*^{2}, *Vp32*^{G5} or *Vps28*^{B9} MARCM ddaC clones. (B) Compared to weak staining in wild-type ddaC neurons, N-Cad was accumulated on aberrant Avl-positive endosomes in *Rab5*^{2}, *Vp32*^{G5} or *Vps28*^{B9} MARCM ddaC clones. (C) Accumulation of Robo protein on aberrant Avl-positive endosomes in *Rab5*^{DN}-expressing ddaC neurons was greatly diminished by *robo* RNAi knockdown. (D) Accumulation of N-Cad protein on aberrant Avl-positive endosomes in *Rab5*^{DN}-expressing ddaC neurons was greatly diminished by *N-Cad* RNAi knockdown. (E) Similar to wild-type ddaC neurons, α-PS1-integrin was not accumulated on the aberrant Avl-positive endosomes in ddaC neurons expressing *Rab5*^{DN} or *Vps4*^{DN}. Scale bar is 10 μm in A.

3.5 Nrg plays an inhibitory role during dendrite pruning in ddaC neurons

3.5.1 Overexpression of Nrg is sufficient to inhibit dendrite pruning ddaC neurons

3.5.1.1 Overexpression of Nrg results in dendrite pruning defects in ddaC neurons

Based on the strong accumulations of Nrg in endocytic pathways mutant ddaC neurons, I suspected that upregualtion of Nrg might play an inhibitory role during dendrite pruning. To justify this hypothesis, Nrg was overexpressed in ddaC neurons by two independent transgenes UAS-Nrg (Islam et al., 2003) and UAS-Nrg-EGFP (Enneking et al., 2013). Interestingly, overexpression of Nrg via two copies of UAS-Nrg and two copies of *ppk-Gal4* in ddaC neurons exhibited strong pruning defects with 4.0±0.4 primary and secondary dendrites attached to soma and 556±37 μm unpruned dendrites remained at 16 hr APF (87%, n=23; Fig 13B, G, H). Similarly, overexpression of Nrg via two copies

of UAS-Nrg-EGFP and two copies of *ppk-Gal4* led to strong pruning defects with 3.9±0.4 primary and secondary dendrites attached to soma and 637±40 μm unpruned dendrites remained at 16 hr APF (90%, n=24; Fig 13C, G, H). Importantly, overexpressed Nrg was strongly localized on plasma membrane of soma cortex, dendrites and axons that persisted throughout dendrite pruning process from late larval stage to 16 hr APF.

In summary, overexpression of Nrg is sufficient to cause dendrite pruning defects in ddaC neurons.

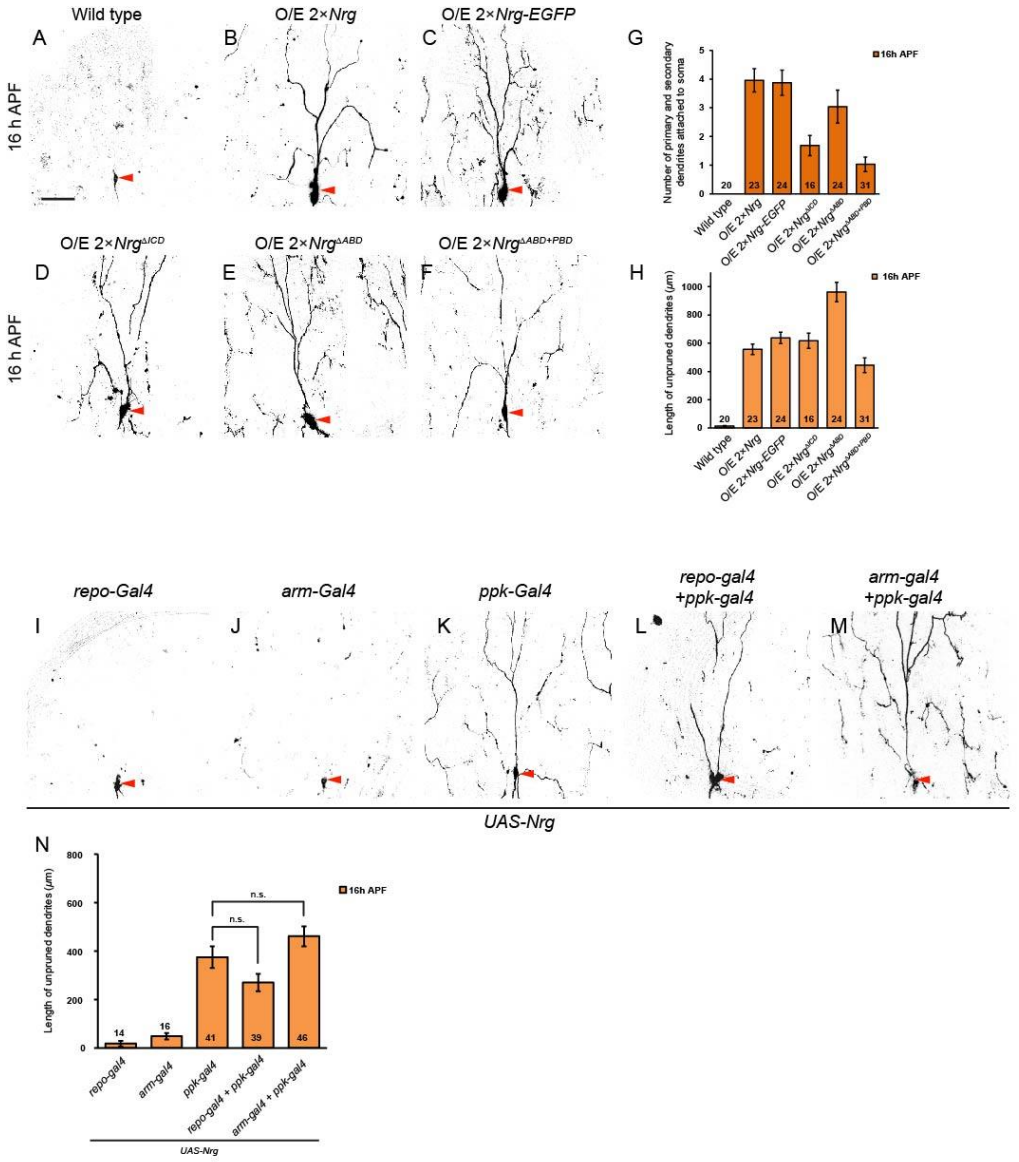

Figure 14. Overexpression of Nrg is sufficient to inhibit dendrite pruning in ddaC neurons. (A-D) Live confocal images of ddaC neurons expressing *UAS-mCD8-GFP* driven by *ppk-Gal4* at 16 h APF. Red arrowheads point to the ddaC somas. (A-F) While wild-type neurons removed all their larval dendrites at 16 h APF, the ddaC neurons expressing higher levels of Nrg (B), Nrg-EGFP (C), $Nrg^{\Delta ICD}$ (D), $Nrg^{\Delta ABD}$ or $Nrg^{\Delta ABD+PBD}$ exhibited notable severing defects at 16 h APF. (G) Quantification of the average number of primary and secondary dendrites attached to the somas of wild-type and mutant ddaC neurons at 16 h APF. (H) Quantification of the average length of unpruned dendrites of ddaC neurons at 16 hr APF. The number of samples (n) in each group is shown on the bars. Error bars represent S.E.M.. Dorsal is up in all images. Scale bar is 50 μm.

3.5.1.2 Nrg extracellular domain is sufficient to inhibit dendrite pruning in ddaC neurons

Nrg is a conserved single-transmembrane CAM consists of large extracellular domain (ECD) and small intracellular domain (ICD) (Fig 22A). The extracellular region contains six immunoglobulin (Ig) and five FnIII domains, which is known to be important for homotypic interaction with Nrg itself or heterotypic binding to other molecules. The intracellular region of Nrg contains FERM-binding domain, ankyrin-binding domain (ABD), and PDZ-binding domain (PBD). It has been reported that ABD is required for Ankyrin and actin cytoskeletons attachment (Enneking et al., 2013). In order to investigate the Nrg function in dendrite pruning, various truncations of Nrg were overexpressed in ddaC neurons. Interestingly, overexpression of Nrg truncation lacking the whole ICD ($Nrg^{\Delta ICD}$) caused dendrite pruning defects (n=16; Fig 13D), suggesting that the ECD is sufficient to inhibit dendrite pruning. Moreover, Nrg truncations lacking ABD alone ($Nrg^{\Delta ABD}$) (n=24; Fig14E) or both ABD and PBD ($Nrg^{\Delta ABD+PBD}$) (n=31; Fig 14F) had consistent inhibitory function during dendrite pruning in ddaC neurons.

Thus, the ECD of Nrg appears to be important for the inhibitory function in ddaC dendrite pruning during early metamorphosis.

3.5.1.3 Nrg homophilic binding between ddaC and neighboring cells are not required for inhibiting dendrite pruning

Homophilic interaction via Nrg ECD between da neurons and glial cells is important for da neuron branching (Yamamoto et al., 2006). Therefore, I

investigated that whether Nrg ECD interaction between ddaC and neighboring cells are important for its inhibitory role in dendrite pruning. To this end, I overexpressed Nrg glial cells by using *repo-Gal4* or in epithelial cells by *arm-Gal4*. Interestingly, overexpression of Nrg via *repo-Gal4* (n=14; Fig 14I) or *arm-Gal4* (n=16; Fig 14J) did not resulted in dendrite pruning defects in ddaC neurons. Moreover, neither overexpression of Nrg in glial cells (n=39; Fig 14L, L) or epidermal cells (n=46; Fig 14M) enhanced the dendrite pruning defects of Nrg-overexpressing ddaC neurons.

Thus, homotypic interaction of Nrg between ddaC neurons and glia/epidermal cells appears to be dispensable for the inhibitory function of Nrg in regulating dendrite pruning in ddaC neurons.

3.5.1.4 Overexpression of Robo or N-Cad do not induce dendrite pruning defects in ddaC neurons

Next, I also attempted to assess if overexpression of Robo or N-Cad was able to cause dendrite pruning defects in ddaC neurons. In contrast to Nrg, overexpression of Robo (n=20; Fig 19B) or N-Cad (n=10; Fig 19C) did not lead to obvious dendrite pruning defects, suggesting the specificity of Nrg in regulating dendrite pruning among these cell-surface molecules.

Taken together, overexpression of Nrg alone is sufficient to induce dendrite pruning process but not Robo or N-Cad.

3.5.2 Loss of Nrg induces precocious dendrite pruning in ddaC neurons

3.5.2.1 Nrg mutant ddaC neurons exhibit precocious dendrite pruning

Given that overexpression of Nrg is sufficient to inhibit dendrite pruning in ddaC neurons, I further examine whether there is opposite phenotype, precocious dendrite pruning, in loss of Nrg background. In wild type ddaC neurons, the majority of dendrite arbor remained connected to the soma with an average of 10.1±1.0 primary and secondary dendrites attached (n=29; Fig 15A, G). Surprisingly, in null allele nrg^{14} mutant ddaC clones which eliminated Nrg proteins (n=5; Fig 15K), the dendrites were severed form soma and underwent fragmentation at 6 hr APF with average of 1.6±0.4 primary and secondary dendrites attached to soma only (n=47; Fig 15B, G). In addition, the progressive precocious pruning phenotypes could be observed at different time points such as 4 or 5 hr APF. To further verify the precocious pruning phenotype in nrg^{14} ddaC clones, by using the genetically encoded calcium indicator GCaMP3, I examined the compartmentalized calcium transients in the dendrites of ddaC neurons from 4 to 4.5 hr APF, which is reported to be temporal-spatial cue to trigger dendrite pruning (Kanamori et al., 2013). Interestingly, compartmentalized calcium transients in the dendrites were observed in all nrg^{14} mutant ddaC clones (100%, n= 9), whereas only 25% in wild-type neurons during in the same period (25%, n=12), indicating the early onset of dendrite pruning.

Collectively, loss of Nrg cause precocious dendrite pruning, supporting the inhibitory function of Nrg during dendrite pruning in ddaC neurons.

3.5.2.2 Nrg extracellular domain is sufficient to rescue the precocious dendrite pruning phenotype

To verify specificity of precocious pruning phenotypes in *nrg^{14}* mutant ddaC clones, I performed rescue experiments by using Pacman-based genomic rescue transgenes. Wild-type Nrg genomic transgene *P[nrg_wt]* (Enneking et al., 2013) restored the Nrg endogenous protein level in *nrg^{14}* mutant ddaC clones (n=5; Fig 15L). Importantly, *P[nrg_wt]* also fully rescued the precocious dendrite pruning phenotype (n=10; Fig 15C). Next, I conduct rescue experiment by utilizing the genomic rescue transgene *P[nrgΔIg3+4]* deleting the extracellular Ig domains 3 and 4 that disrupts the Nrg homotypic interaction (Enneking et al., 2013). Interestingly, *P[nrgΔIg3+4]* transgene fully rescued the precocious pruning phenotypes in *nrg^{14}* mutant ddaC clones (n=8; Fig 15D), further supporting that the homophilic interaction of Nrg is not required for the inhibitory function in dendrite pruning. Moreover, the genomic transgenes *P[nrgΔABD+PBD]* deleting both ABD and PBD domains (n=14; Fig 15E) fully rescued precocious pruning phenotypes in *nrg^{14}* ddaC clones, suggesting the ABD and PBD domains are disposable for Nrg functions in dendrite pruning. In addition, overexpression of Nrg$^{\Delta ICD}$ partially but significantly rescued the precocious pruning phenotypes in *nrg^{14}* mutant ddaC clones (n=12; Fig 15F). Taken together, the stabilization function of Nrg against dendrite pruning is likely to depend on ECD, presumably via the adhesive property.

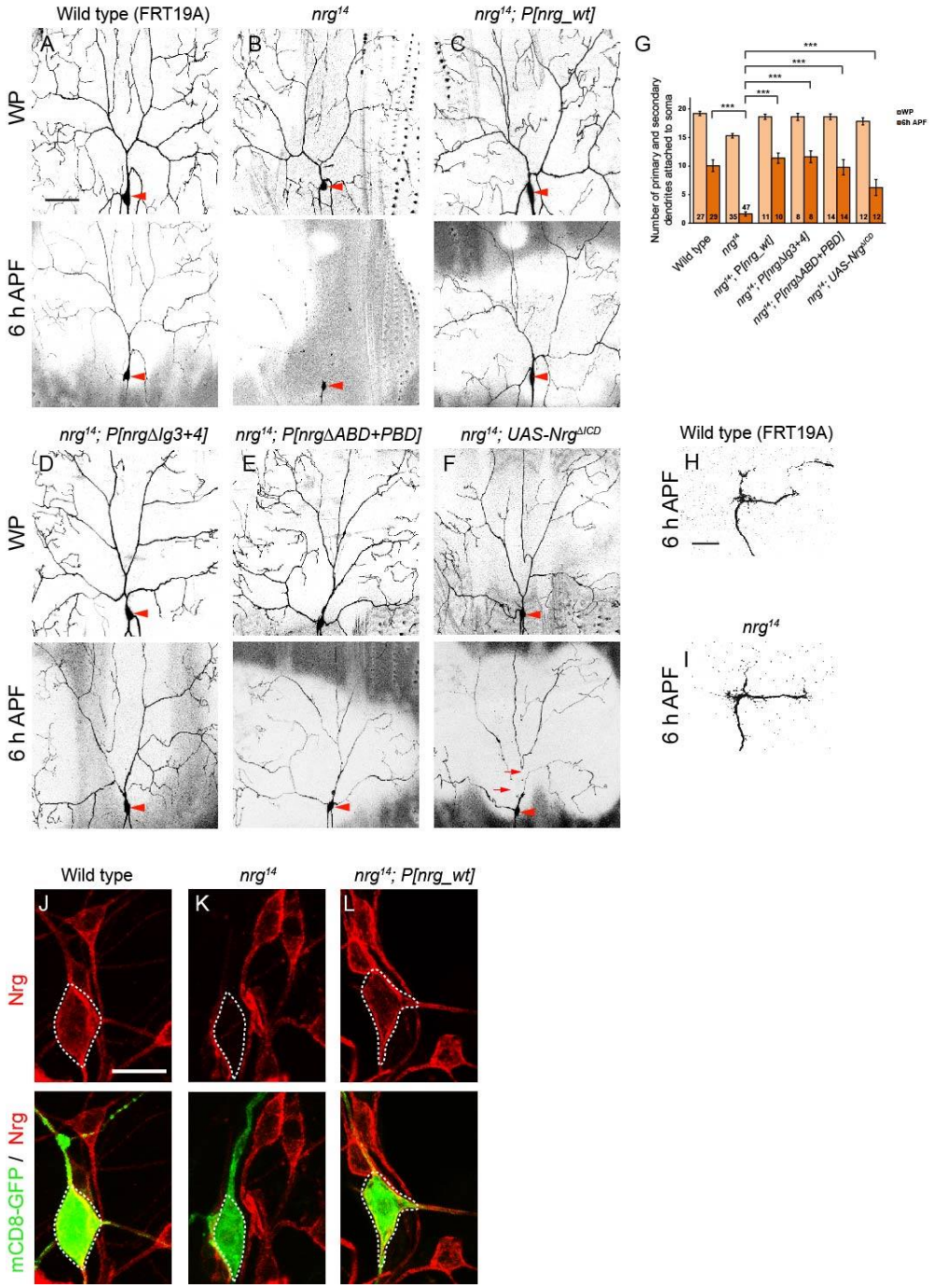

Figure 15. Loss of *nrg* leads to precocious dendrite pruning in ddaC neurons. (A-G, I, J) Live confocal images of ddaC neurons expressing *UAS-mCD8-GFP* at WP stage and 6 h APF. Red arrowheads point to the ddaC somas. (A-G) Wild-type (FRT 19A) MARCM (A) ddaC clones kept the majority of main dendrites attached to their somas at 6 h APF, whereas nrg^{14} MARCM (B) clones pruned majority of their dendrites at 6 h APF. The precocious dendrite pruning defects in nrg^{14} MARCM ddaC clones were fully rescued by genomic rescue transgenes *P[nrg_wt]*(C) , *P[nrgΔIg3+4]* (E) or P[nrgΔABD+PBD], and partially rescued by $Nrg^{\Delta ICD}$ expression (G) at 6 h APF. (I, J) Confocal images of axonal termini of ddaC neuron expressing *UAS-mCD8-GFP* at 6 h APF immunostained for GFP. The axonal termini in nrg^{14} (J) MARCM ddaC clones exhibited normal morphology and proper connection with the VNC

at 6 h APF, similar to those in the wild-type (FRT19A) MARCM clones (I) at 6 h APF. (H) Quantification of the average number of primary and secondary dendrites attached to the soma of ddaC neurons at WP stage and 6 h APF. Error bars represent S.E.M. *** p<0.001. n is shown on the bars. (K-M) Confocal images of ddaC neurons expressing *UAS-mCD8-GFP* driven by *ppk-Gal4* at wL3 stage immunostained for Nrg (in red). Compared to wild-type ddaC neurons (K), Nrg staining were abolished in nrg^{14} MARCM ddaC clones (L) and recovered by genomic rescue transgenes *P[nrg_wt]* (M). Dorsal is up in all images. Scale bar in A is 50 μm, and in K is 10 μm.

3.5.2.3 Loss of Nrg does not affect general stability of neuronal projections

Consistent with previous studies (Yang et al., 2011), loss of Nrg resulted in obvious reduction of high order dendrite branches but little in primary and secondary dendrites (Fig B). In order to rule out the possibility that Nrg is required for general stabilization of neuronal projections, I tested the axon terminals of ddaC neuron that form synapses in the VNC. Importantly, in nrg^{14} mutant ddaC clones (n=14; Fig 14I), the axon terminals were comparable with the wild-type controls at 6 hr APF (n=11; Fig 14H), indicating that Nrg is specifically required for stabilizing dendrites against dendrite pruning but not the axons.

3.5.3Nrg is downregulated via endocytic pathways prior to dendrite severing in ddaC neurons

3.5.3.1Nrg is relocalized on endosomes and downregulated prior to dendrite pruning in ddaC neurons

Given the inhibitory function of Nrg in ddaC dendrite pruning, I further examined the dynamics of Nrg during different stages in ddaC neurons. At

w3L stage, wild-type ddaC neurons exhibited membrane-bond Nrg staining (n=17; Fig 16A). High level of Nrg was detected on cortex, dendrites and axons. At WP stage, Nrg remained localized on plasma membrane although there was a subtle reduction of Nrg level and a slight increase of cytoplasmic punctate structures (n=10; Fig 16B). Surprisingly, at 6 hr APF, a critical time point that the main dendrites severing begins, Nrg exhibited dramatic redistribution from plasma membrane to cytoplasm as small vesicle-like puncta and downregulation in intensity in somas, dendrites and axons (n=15; Fig 16C, D). In order to investigate if the Nrg punctate structures were endosomes at 6 hr APF, I made use of the early endosomal marker GFP-2xFYVE (Wucherpfennig et al., 2003) to label the endosomes in ddaC neurons at different stages. Interestingly, at w3L stage or WP stage, Nrg showed little overlap with intracellular GFP-2xFYVE positive early endosomes (n=32, 27; Fig 16E, F). In contrast, Nrg punctate structures exhibited striking colocalizaiton with GFP-2xFYVE at 6 hr APF (n=30; Fig 16G), suggesting that Nrg indeed undergoes dramatic redistribution on endosomes at 6 hr APF prior to the onset of dendrite severing. Moreover, some of Nrg puncta were labelled by the late endosome/lysosome marker LAMP1-GFP while the others not at 6 hr APF (n=10; Figure 17H), which indicating a progressive process of Nrg trafficking via endocytic pathways towards lysosomal degradation.

Taken together, Nrg is downregulated though endocytic pathways prior to dendrite severing in ddaC neurons.

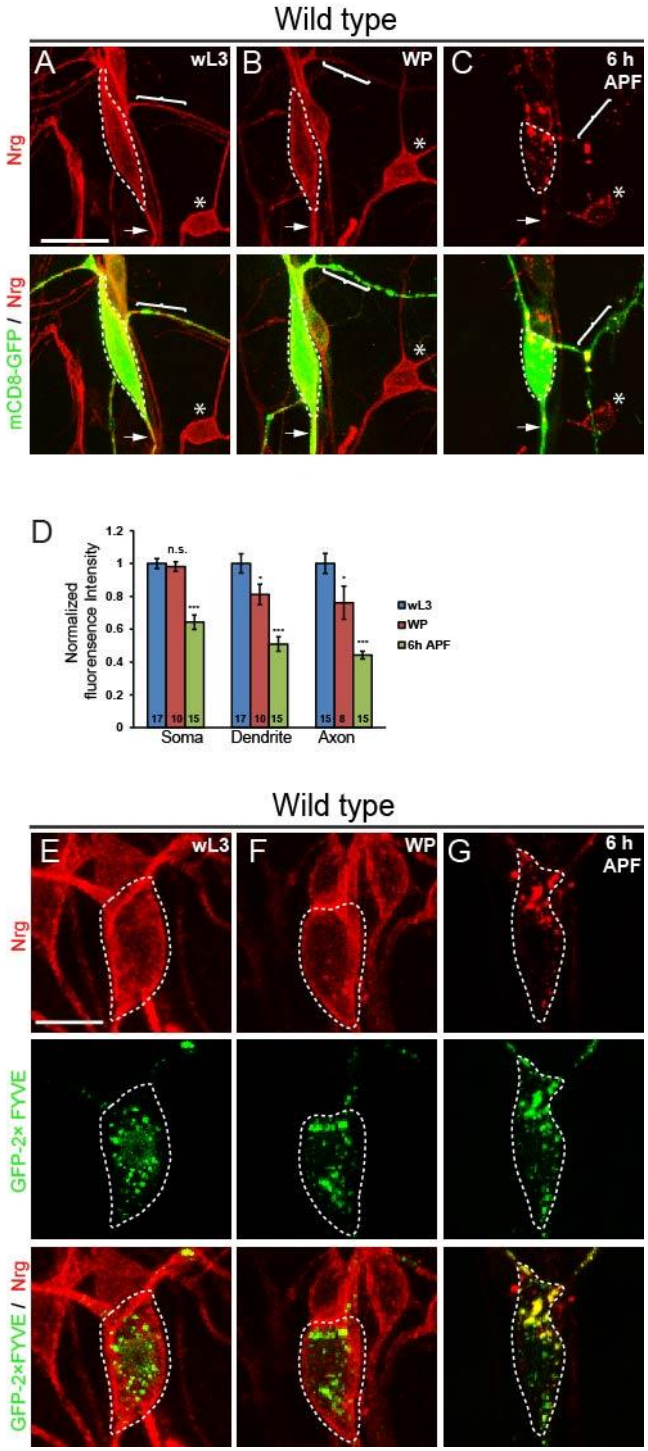

Figure 16. Nrg is actively endocytosed and degraded in wild-type ddaC neurons prior to dendrite pruning. (A-C, E-G) Confocal images of ddaC neurons expressing *UAS-mCD8-GFP* or *UAS-GFP-2×FYVE* driven by *ppk-Gal4* at wL3, WP and 6 h APF stages

immunostained for Nrg (in red). ddaC somas are marked by dashed lines, axons by arrows, proximal dendrites by curly brackets. ddaE somas are marked by asterisks. (A-C) The mCD8-GFP levels remained abundant in somas, axons and dendrites at wL3 (A), WP (B) and 6h APF (C) stages. In wild-type ddaC neurons, Nrg was primarily localized around the cortex of the somas, dendrites and axons at wL3 (A) and WP (B) stages. Nrg was redistributed to numerous intercellular punctate structures (C) with its greatly reduced intensity in ddaC somas, dendrites and axons at 6 h APF. (E, F) Nrg protein was primarily localized on the plasma membrane and exhibited little overlap with GFP-2xFYVE puncta in the cytoplasm of ddaC neurons at wL3 (E) and WP (F) stages. (G) Nrg-positive puncta were predominantly colocalized with GFP-2xFYVE signals at 6 h APF in ddaC neurons. (D) Quantification of Nrg immunostaining was performed as described in Experimental Procedures. The number of samples (n) in each group is shown on the bars. Error bars represent S.E.M.. *** $p<0.001$, * $p<0.05$. Dorsal is up in all images. Scale bars in A is 20 μm, and scale bar in E is 10 μm.

3.5.3.2 Endocytic pathways are required for the redistribution and downregulation of Nrg in ddaC neurons

Next, I examined the Nrg dynamics in endocytic pathways mutant background at 6 hr APF. Compared to wild-type ddaC neurons, $Rab5^{DN}$-expressing neurons exhibited drastic upregualtion of Nrg levels in different compartments (n=19; Fig 17B, D). Similar to w3L or WP stages, Nrg was accumulated on aberrant endosomes labelled by LAMP1-GFP in ddaC neurons at 6 hr APF (n=12; Fig 17I). In addition, Nrg was strongly upregulation on dendrites and axons (n=19; Fig 17B, D). Notably, Nrg appeared to enrich on plasma membrane on cell cortex (3.2-fold increase), dendrites and axons compared to wild-type neurons at 6 hr APF, which is much more striking than that at w3L stage (1.5-fold increase). Consistently, Nrg was accumulated in different cellular compartments including aberrant endosomes, cell cortex, dendrites and axons in $Vps4^{DN}$-expressing neurons at 6 hr APF (n=18; Fig 17C, D). Moreover, the upregulations of Nrg in $Rab5^{DN}$ (n=10; Fig 17F) or $Vps4^{DN}$-expressing (n=6; Fig 17G) ddaC neurons persisted at 16 hr APF, the

timepoint for observation of pruning defects. In addition, in order to avoid the defects at early larval stage, I used Gene-Switch system to express $Rab5^{DN}$ or $Vps4^{DN}$ at late larval stage to test the Nrg dynamics. With induction at late larval stage, only little Nrg accumulation was observed on the Avl-positive aberrant endosomes derived from $Rab5^{DN}$ (n=20; Fig 17P) or $Vps4^{DN}$-expressing (n=5; Figure 17R) ddaC neurons at WP stage. In contrast, at 6 hr APF, more drastic Nrg accumulations occur on aberrant endosomes of $Rab5^{DN}$ (62%; n=13; Fig 17Q) or $Vps4^{DN}$-expressing (79%; n=19; Figure 17S) ddaC neurons. These data suggest that a more active endocytosis of Nrg from WP stage to 6 hr APF, concomitant with onset of dendrite severing in ddaC neurons.

Collectively, Rab5/ESCRT endocytic pathways are required for Nrg redistribution and downregulation prior to onset of dendrite severing.

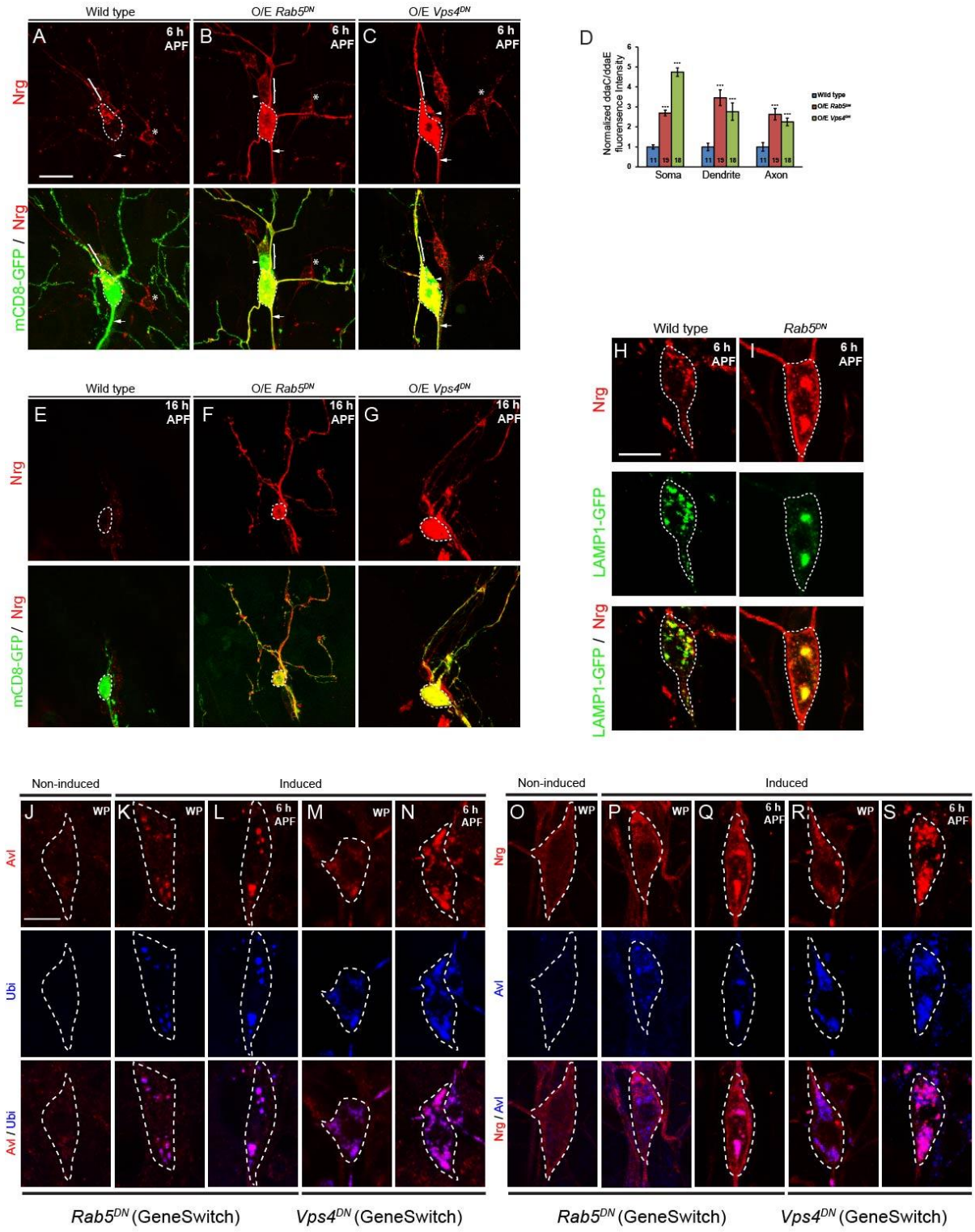

Figure 17. Nrg endocytosis and downregulation are disrupted in *Rab5*/*ESCRT* mutant ddaC neurons. (A-C, E-G) Confocal images of ddaC neurons expressing *UAS-mCD8-GFP* driven by *ppk-Gal4* at wL3, WP, 6 hr and 16 h APF stages immunostained for Nrg (in red). Compared to weak Nrg staining in wild-type ddaC neurons (A) at 6 h APF, Nrg levels were dramatically increased in the somas, dendrites and axons in ddaC neurons expressing $Rab5^{DN}$ (B) or $Vps4^{DN}$ (C). Please note that white arrowheads point to apoptotic ddaF neurons also

labeled by the stronger *ppk-Gal4* driver (Chr II). (D) Quantification of Nrg immunostaining was performed as described in Experimental Procedures. The number of samples (n) in each group is shown on the bars. Error bars represent S.E.M.. *** $p<0.001$. Compared to weak Nrg staining in wild-type ddaC neurons (E) at 16 h APF, Nrg levels were dramatically increased in the somas, dendrites and axons in ddaC neurons expressing $Rab5^{DN}$ (F) or $Vps4^{DN}$ (G). (E-G) at 16 h APF, Nrg upregulations in the somas, dendrites and axons in ddaC neurons expressing $Rab5^{DN}$ (F) or $Vps4^{DN}$ (G) persisted. (H-I) Confocal images of wild-type (H) and $Rab5^{DN}$–expressing (I) ddaC neurons expressing UAS-LAMP1-GFP at 6 h APF stages immunostained for Nrg (in red). Some of Nrg- puncta were colocalized with LAMP1-GFP signals in wild-type ddaC neurons at 6 h APF while Nrg completely co-localized with LAMP1-GFP positive aberrant endosomes at 6 h APF in $Rab5^{DN}$–expressing ddaC neurons. (J-S) Confocal images of ddaC neurons immunostained for Avl (A-N in red, O-S in blue), Ubiquitin (A-N in blue) or Nrg (O-S inred), In RU486-induced $Rab5^{DN}$ or $Vps4^{DN}$-expressing ddaC neurons, Nrg and Ub-positive deposits weakly accumulated on aberrant endosomes at WP (K, M, P, R), but strongly at 6 hr APF (L,N, Q, S), compared to those in non-induced controls (A-O). Dorsal is up in all images. Scale bars- in A is 20 μm and 10 μm in H, J.

3.6 Endocytic pathways restrain Nrg function to promote dendrite pruning in ddaC neurons

3.6.1 Nrg is downstream of Rab5/ESCRT-dependent endocytic pathways during dendrite pruning in ddaC neurons

3.6.1.1 Attenuation of Nrg is sufficient to rescue the dendrite pruning defects in endocytic pathways mutant ddaC neurons

Based on the Nrg dynamics via endocytic pathways, I further investigated whether Nrg is the downstream target of Rab5/ESCRT-dependent endocytic pathways in regulating dendrite pruning in ddaC neurons. To this end, I performed rescue experiments by attenuating Nrg levels in Rab5/ESCRT mutant ddaC neurons. Knockdowns of Nrg by two independent RNAi transgenes that eliminating the Nrg proteins (Fig 12D) strongly suppressed the

dendrite pruning defects caused by *Rab5*^{DN} overexpression with 0.6 and 0.6 primary and secondary dendrites attached to soma and 208±55 μm and 198±33 μm unpruned dendrites remained in ddaC neurons at 16 hr APF (28%, n=14, 38%, n=16; Fig 18B, C), compared to pruning defects with 4.5 primary and secondary dendrites attached to soma and 646±31 μm unpruned dendrites remained in *Rab5*^{DN}-expressing control ddaC neurons (93%, n=30; Fig 18A). Consistently, knockdown of Nrg via these two RNAi transgenes partially rescued the dendrite pruning defects resulting from *Vp4*^{DN} overexpression (72%, n=39; Fig 18F), compared to *Vps4*^{DN}-expressing controls (72%, n=39; Fig 18F). Moreover, I examined the proximal dendrite severing events, the hallmark of dendrite pruning. Interestingly, at 12.5 hr APF, knockdown of Nrg via two RNAi transgenes restored the proximal dendrite severing (67%, n=15, 70%, n=10; Fig 18L, M), compared to *Rab5*^{DN}-exrepssing controls (0%, n=10; Fig 18M), indicating the nrg attenuations restore the wild type pruning process instead of leading general dendrite instability.

In addition, knockdown of Robo or N-Cad via RNAi that eliminated the accumulations in *Rab5*^{DN}-expresing ddaC neurons (Fig 13J, L) was not able to rescue the dendrite pruning defects caused by *Rab5*^{DN} (Fig 19G-K), further suggesting the specificity of Nrg knockdown rescue. As control experiments, knockdown Nrg (n=10, Fig 19D), Robo (n=10, Fig 19E), or N-Cad (n=10, Fig 19F) via RNAi did not lead to obvious dendrite pruning phenotypes.

Next, I attempted to understand if Nrg is the sole downstream of endocytic pathways. Importantly, when *Rab5*^{DN} was overexpressed in *nrg*^{14} mutant ddaC neurons, no precocious pruning phenotype was observed (n=12; Fig 18Q), different from *nrg*^{14} mutants (Fig 15B), suggesting that Nrg is not the sole downstream of Rab5/ESCRT-dependent endocytic pathways during dendrite pruning.

Collectively, Nrg is downstream of Rab5/ESCRT-dependent endocytic pathways during dendrite pruning in ddaC neurons.

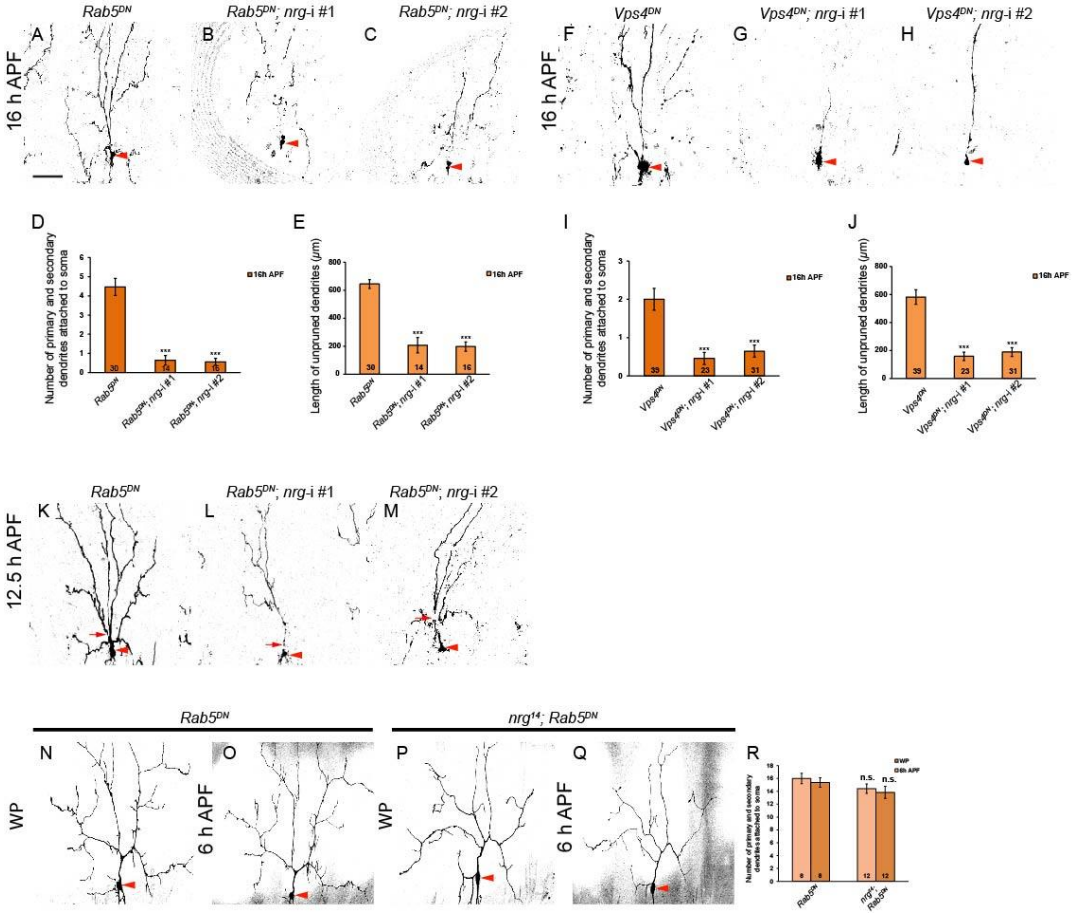

Figure 18. Attenuation of Nrg is sufficient to suppress the pruning defects in *Rab5/ESCRT* mutant ddaC neurons. (A-H, K-M, N-Q) Live confocal images of ddaC neurons expressing *UAS-mCD8-GFP* driven by *ppk-Gal4* at WP, 6 h, 12.5 h and 16 h APF. Red arrowheads point to the ddaC somas. (A-C) The control ddaC neurons co-expressing

Rab5^{DN} and the non-functional Mical$^{N\text{-}ter}$ fragment (A) exhibited strong severing defects at 16 h APF. The severing defects were drastically suppressed by knockdown of *nrg* using *nrg* RNAi #1 (B) or *nrg* RNAi #2 (C). (E-G) Consistently, *Vps4*^{DN}-expressing ddaC pruning defects were significantly suppressed by knockdown of *nrg* using *nrg* RNAi #1 (F) or *nrg* RNAi #2 (G), compared to the control ddaC neurons expressing *Vps4*^{DN} and *Mical*$^{N\text{-}ter}$ (E). (K-M) The defects of proximal dendrites serving (red arrows) in Rab5DN-expressing ddaC neurons (K) were rescued by knockdown of *nrg* using *nrg* RNAi #1 (L) or *nrg* RNAi #2 (M) at 12.5 h APF. (N-O) *Rab5*^{DN}-expressing *nrg*^{14} MARCM ddaC clones (Q) did not show precocious dendrite pruning at 6 h APF, similar to *Rab5*^{DN}-expressing ddaC clones (O). (D, I, R) Quantification of the average number of primary and secondary dendrites attached to the somas of wild-type and mutant ddaC neurons at WP stage, 6 h and 16 h APF. (E, J) Quantification of the average length of unpruned dendrites of ddaC neurons at 16 hr APF. The number of samples (n) in each group is shown on the bars. Error bars represent S.E.M. *** $p<0.001$. Dorsal is up in all images. Scale bar is 50 μm.

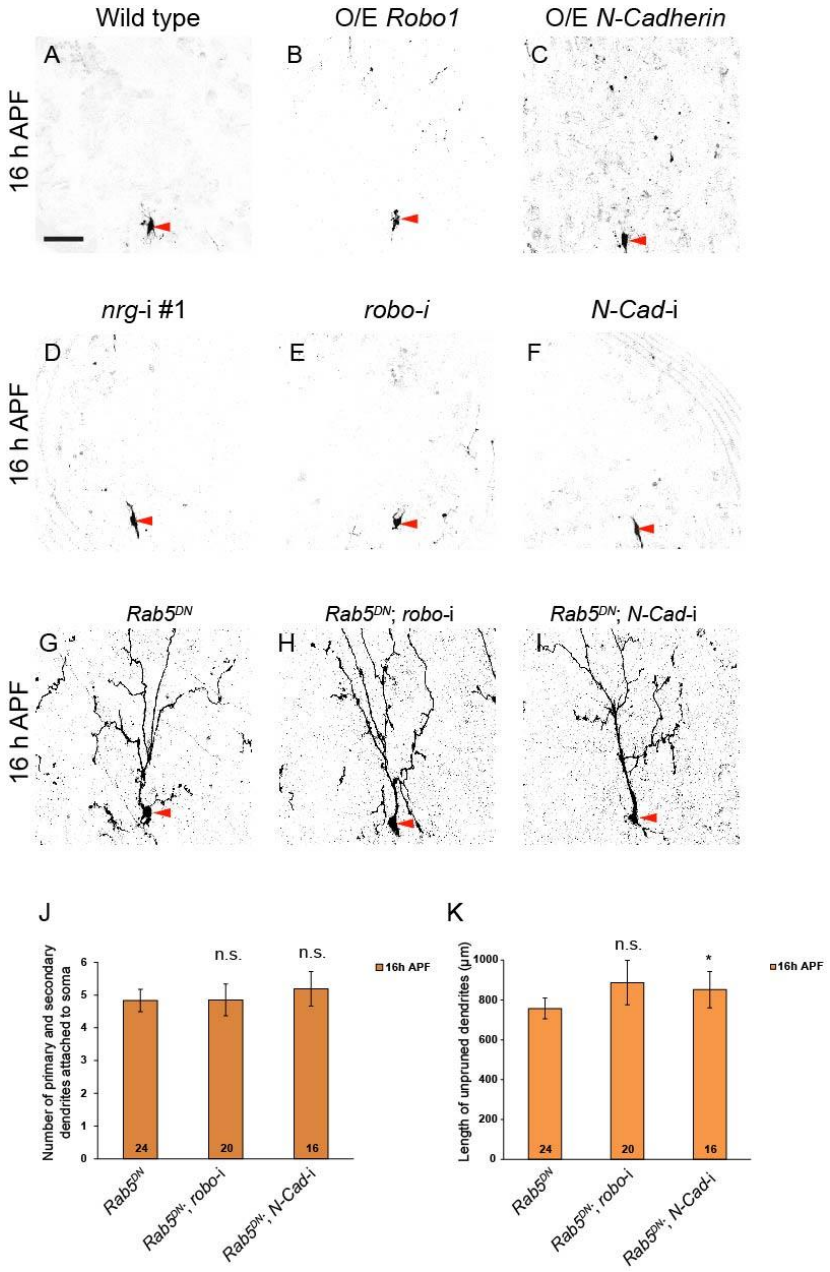

Figure 19. Robo and N-Cad are not required for dendrite pruning in ddaC neurons. (A-B) Live confocal images of ddaC neurons expressing *UAS-mCD8-GFP* driven by *ppk-Gal4* at 16 h APF. (A-C) Similar to wild-type ddaC neurons, ddaC neurons expressing Robo (B) or N-Cad (C) pruned their larval dendrites at 16 h APF. Dorsal is up in all images. Scale bar in A is 50 µm. See genotypes in Supplementary list of fly strains. (D-F) Knockdown by *nrg* RNAi #1 (D), *robo* RNAi (E) and *N-Cad* RNAi (F) in ddaC neurons did not lead to any severing defect at 16 h APF. (C-E) Compared to the control ddaC neurons co-expressing *Rab5^{DN}* and the non-functional *Mical$^{N\text{-}ter}$*(C), knockdown *robo* (D) or *N-Cad* (E) did not suppress the severing defect in *Rab5^{DN}*-expressing ddaC neurons at 16 h APF. (F) Quantification of the average number of primary and secondary dendrites attached to the somas of wild-type and mutant ddaC neurons at 16 h APF. (G) Quantification of the average length of unpruned dendrites of ddaC neurons at 16 hr APF. The number of samples (n) in

each group is shown on the bars. Error bars represent S.E.M. Dorsal is up in all images. Scale bar is 50 μm.

3.6.1.2Overexpression of Nrg lead to enhancement of dendrite pruning defects in endocytic pathways mutant ddaC neurons

Then, I tested the genetic interaction between Rab5/ESCRT mutant and Nrg overexpression. Consistently, overexpression of Nrg significantly enhanced the dendrite pruning defects caused by $Rab5^{DN}$ or $Vps4^{DN}$ overexpression in ddaC neurons. Overexpression of one copy of Nrg (n=24; Fig 20A) or Nrg-EGFP (24; Fig 20E) only led to mild pruning defects. However, co-overexpression of Nrg or Nrg-EGFP led to significant enhancement with 5.8±0.3 and 6.0±0.3 primary and secondary dendrites attached to soma and 858±24 μm and 942±42 μm unpruned dendrites remained in ddaC neurons at 16 hr APF (n=41, 38; Fig 20C, D), compared to the $Rab5^{DN}$-expressing controls with 4.2 primary and secondary dendrites attached to soma and 704±21 μm unpruned dendrites remained at 16 hr APF (n=47; Fig 20B). Consistently, overexpression of Nrg or Nrg-EGFP together with $Vps4^{DN}$ resulted in stronger pruning defects with 3.3±0.4 and 5.9±0.5 primary and secondary dendrites attached to soma and 594±41 μm and 821±66 μm unpruned dendrites remained in ddaC neurons at 16 hr APF (n=22, 20, Fig 20G, H), compared to the $Vps4^{DN}$-expressing controls with 1.3±0.2 primary and secondary dendrites attached to soma and 426±66 μm unpruned dendrites remained at 16 hr APF (n=16; Fig 20F). Indeed, overexpression of Nrg in endocytic pathways deficit background enhance the dendrite pruning defects,

further supports that Nrg and endocytic pathways function together to regulate dendrite pruning in ddaC neurons.

Taken together, the genetic interactions data suggests that Rab5/ESCRT-dependent endocytic pathways restrain the downstream target Nrg to promote dendrite pruning in ddaC neurons during early metamorphosis.

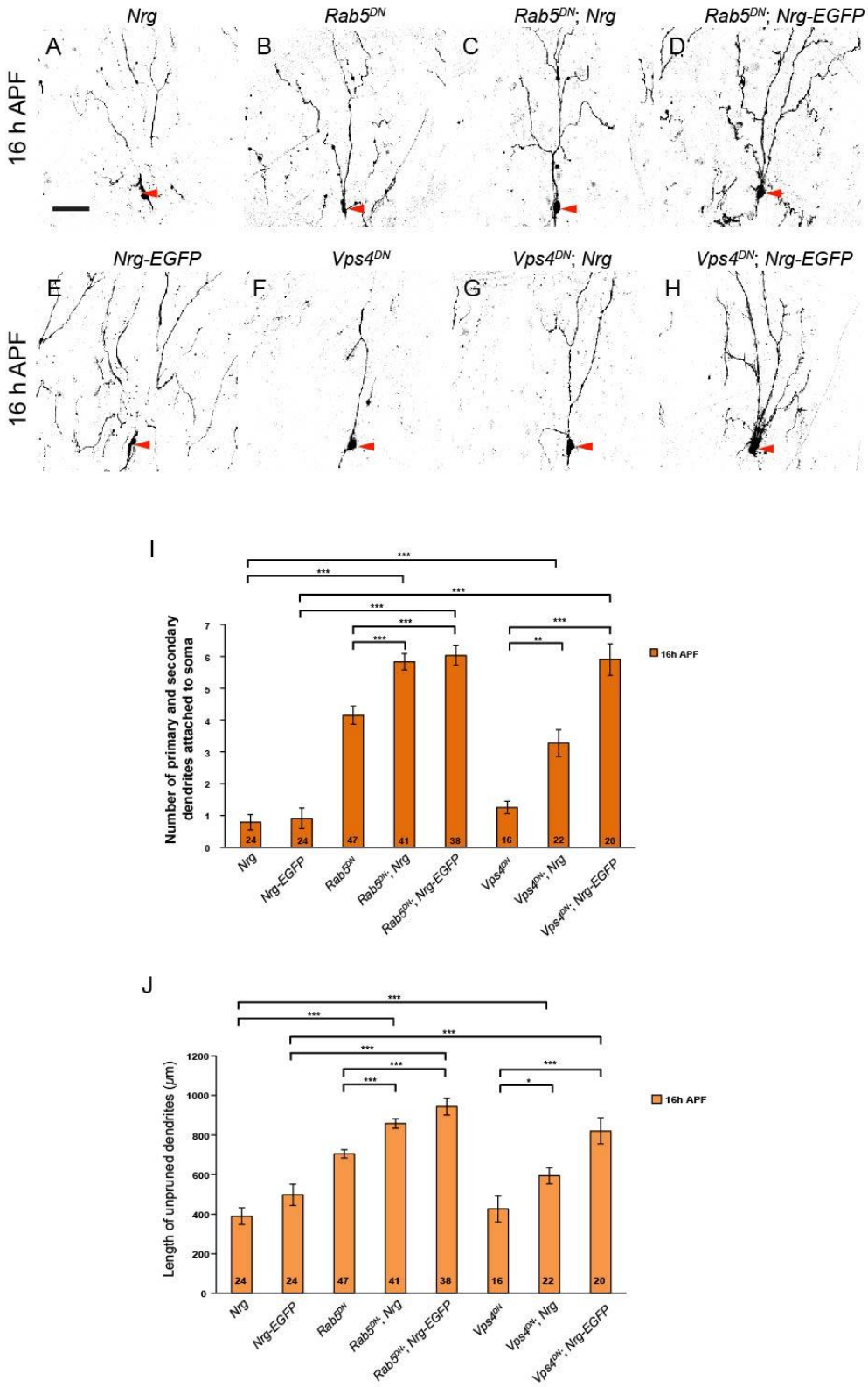

Figure 20. Overexpression of Nrg enhances the pruning defects in *Rab5/ESCRT* mutant ddaC neurons. (A-F) Live confocal images of ddaC neurons expressing *UAS-mCD8-GFP* driven by *ppk-Gal4* at 16 h APF. (A-C) The severing defects in *Rab5*^{DN}-expressing ddaC

neurons were significantly enhanced by co-overexpression of Nrg (B), Nrg-EGFP (C), compared to the control ddaC neurons co-expressing *Rab5*^{DN} and *Mical*$^{N\text{-}ter}$ (A). (D-F) Consistently, *Vps4*^{DN}-expressing ddaC neurons exhibited more severe severing defects with co-expressing Nrg (E), Nrg-EGFP (F), compared to the control ddaC neurons co-expressing *Vps4*^{DN} and *Mical*$^{N\text{-}ter}$ (D). (F) Quantification of the average number of primary and secondary dendrites attached to the somas of wild-type and mutant ddaC neurons at 16 h APF. (G) Quantification of the average length of unpruned dendrites of ddaC neurons at 16 hr APF. The number of samples (n) in each group is shown on the bars. Error bars represent S.E.M. *** $p<0.001$, ** $p<0.01$. Dorsal is up in all images. Scale bar in A is 50 μm.

3.6.2 Rab5/ESCRT-endocytic pathways is likely the downstream of Ecdysone signaling

It is well studied that ecdysone signaling are the trigger of dendrite pruning in ddaC neurons (Kirilly et al., 2009). Rab5/ESCRT-dependent endocytic pathways and Nrg appear to act as downstream of Ecdysone signaling. First, Rab5/ESCERT mutants do not affect the upregulation of EcR during early metamorphosis (Fig 6H, I), indicating endocytic pathways do not function upstream of ecdysone signaling. Second, Rab5/ESCRT mutants only affect dendrite pruning but not apoptosis (Fig 5G-I) while ecdysone signaling affects both. Third, Knockdown of Nrg via two independent RNAi partially rescued dendrite pruning defects in loss of ecdysone signaling backgrounds reported previously (Kirilly et al., 2009; Kirilly et al., 2011), such as overexpression of *EcR*^{DN} (Fig 21A-D), *Brm*^{DN} (Fig 21F-J) or *CBP RNAi* (Fig 21K-O), suggesting that Nrg downregulation via endo-lysosomal pathways might be downstream event of ecdysone signaling.

Thus, endocytic pathways are likely downstream of ecdysone signaling during dendrite pruning in ddaC neurons.

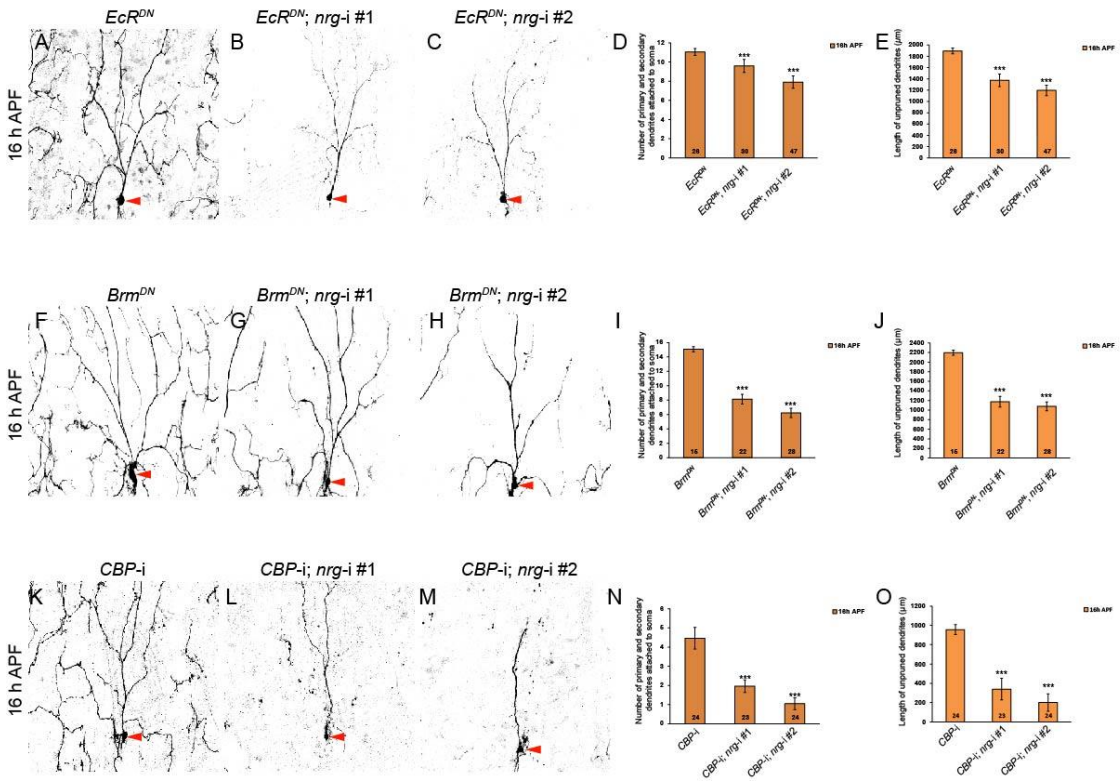

Figure 21. Attenuation of Nrg can partially suppress the pruning defects in ecdysone signaling mutant ddaC neurons. (A-C, F-H, K-M) Live confocal images of ddaC neurons expressing *UAS-mCD8-GFP* driven by *ppk-Gal4* at 16 h APF. Red arrowheads point to the ddaC somas. (A-C) The control ddaC neurons co-expressing EcR^{DN} and the non-functional $Mical^{N\text{-}ter}$ fragment (A) exhibited strong severing defects at 16 h APF. The severing defects were partially suppressed by knockdown of *nrg* using *nrg* RNAi #1 (B) or *nrg* RNAi #2 (C). (F-H) Similarly, knockdown of *nrg* using *nrg* RNAi #1 (G) or *nrg* RNAi #2 (H) partially rescued the pruning defects resulted from overexpression of $Brmn^{DN}$ (F) at 16 h APF. (K-M) knockdown of *nrg* using *nrg* RNAi #1 (L) or *nrg* RNAi #2 (M) also partially rescued the pruning defects of CBP RNAi-expressing ddaC neurons (K). (D, I, N) Quantification of the average number of primary and secondary dendrites attached to the somas of wild-type and mutant ddaC neurons at 16 h APF. (E, J, O) Quantification of the average length of unpruned dendrites of ddaC neurons at 16 hr APF. The number of samples (n) in each group is shown on the bars. Error bars represent S.E.M. *** $p<0.001$. Dorsal is up in all images. Scale bar in A is 50 µm.

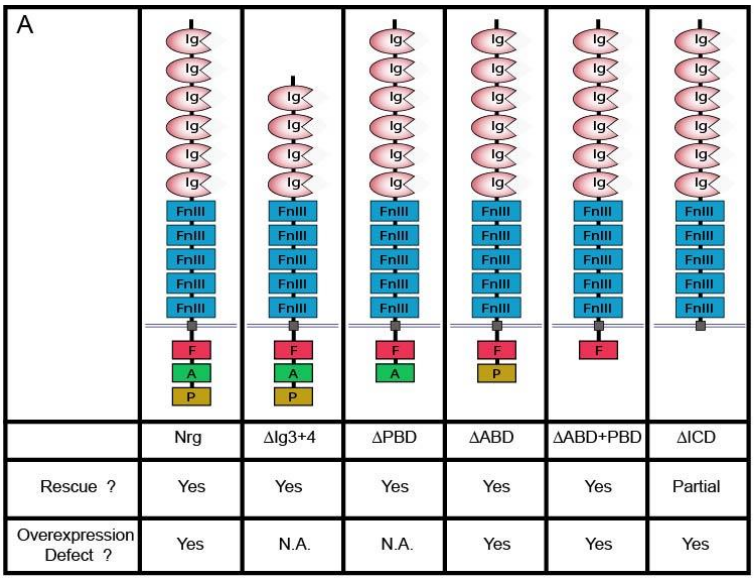

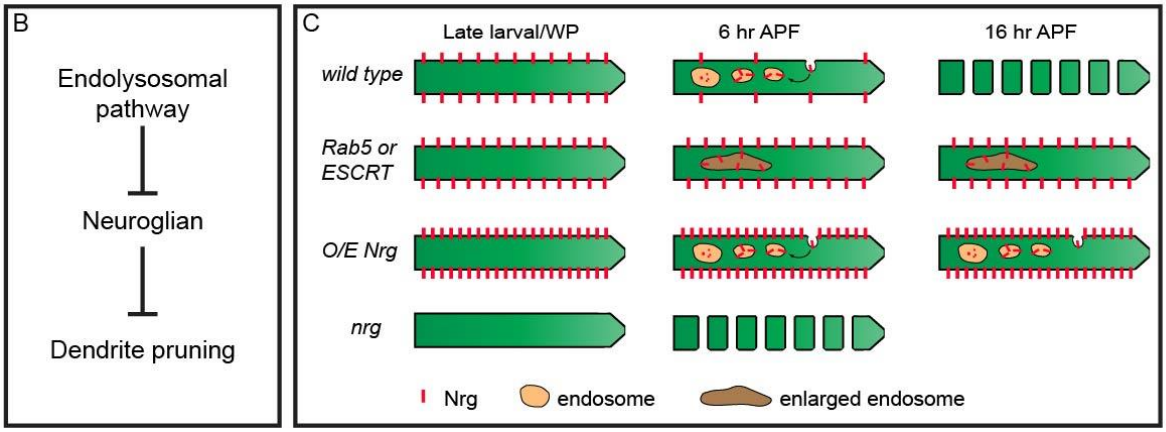

Figure 22. Endocytic pathways restrain the inhibitory function of Nrg to promote dendrite pruning in ddaC neurons. (A) Summary of the function of various Nrg truncations in ddaC dendrite pruning. Nrg is composed of six Immunoglobulin domains (Ig), five type III Fibonec9tin (FnIII), FERM binding domain (F), Ankyrin binding domain (A) and PDZ binding domain (P). (B) An illustration of endocytic pathways and Nrg functions in ddaC dendrite pruning. In wild-type situation, Nrg is removed by endocytic pathways during early metamorphosis to facilitate dendrite pruning. In *Rab5/ESCRT* mutants, Nrg degradation is blocked, which leads to inhibition of dendrite pruning. Nrg overexpression backgrounds resembles loss of *Rab5/ESCRT*, presumably due to overwhelming the endocytic machinery. In contrast, loss of Nrg accelerates dendrite pruning, which results in precocious dendrite pruning phenotypes in ddaC neurons.

Table 1. List of positive lines from RNAi screen in ddaC dendrite pruning.

Gene	Number	Penetrance
CG34376	V24084	50%
	V24085	54.50%
Arf1	V23082	80.00%
CG31302	V40235	91.70%
CG17737	V105763	31.60%
roadblock	V105760	33.30%
Rab5	V103945	68.75%
Caf1-180	V108240	50%
Rpt4	V52663	100%
unc-104	V23464	100%
Kibra	BL31755	66.70%
Hyd	BL32352	100%
eIF-2 β	V9416	100%
pp2A-29B	V23886	100%
CBP	V105115	100%

Table 2. List of receptors and Ligands fail to accumulate on enlarged endosomes in *Rab5^{DN}*, *Vps4^{DN}* or *Vps32^{G5}* mutant ddaC neurons.

Signaling Pathways	Receptors/Ligands	Mutant ddaCs
Dpp	Anti-Tkv	*Rab5^{DN}*, *Vps4^{DN}*
EGF	Anti-EGFR	*Rab5^{DN}*, *Vps4^{DN}*
PVR	Anti-PVR	*Rab5^{DN}*, *Vps4^{DN}*
Hedgehog	Anti-Smoothened	*Rab5^{DN}*, *Vps4^{DN}*
Hedgehog	Anti-Patched	*Rab5^{DN}*, *Vps4^{DN}*
Notch	Anti-Notch Intracellular	*Rab5^{DN}*, *Vps4^{DN}*, *Vps32^{G5}*
Notch	Anti-Notch Extracellular	*Rab5^{DN}*, *Vps4^{DN}*, *Vps32^{G5}*
Notch	Anti-Delta	*Rab5^{DN}*, *Vps4^{DN}*
Wingless	Anti-Wingless	*Rab5^{DN}*, *Vps4^{DN}*

Table 3. List of signaling reporters fail to upregulate in *Rab5^{DN}* or *Vps4^{DN}* mutant ddaC neurons.

Signaling Pathways	Effectors/LacZ reporters	Mutant ddaCs
EGF	Anti-p-ERK	*Rab5^{DN}*, *Vps4^{DN}*
Hedgehog	Anti-Ci, *patched-lacZ*	*Rab5^{DN}*, *Vps4^{DN}*
Wingless	Anti-Armadillo	*Rab5^{DN}*, *Vps4^{DN}*
Wingless	Anti-Senseless	*Rab5^{DN}*, *Vps4^{DN}*
Dpp	*dpp-lacZ*	*Rab5^{DN}*, *Vps4^{DN}*
Notch	*E(spl)m8-lacZ*	*Rab5^{DN}*, *Vps4^{DN}*

Table 4. List of signaling pathways with no effects on *Rab5^{DN}*-associated ddaC dendrite pruning defects.

Signaling Pathways	Dominant Negative (DN)	Mutant ddaCs
Hedgehog	*Ci^{Cell}*	*Rab5^{DN}*
EGF	*EGFR^{DN}*	*Rab5^{DN}*
PVR	*PVR^{DN}*	*Rab5^{DN}*
Dpp	*Tkv^{DN}*	*Rab5^{DN}*
Wingless	*Sgg^{S9A}*	*Rab5^{DN}*
Notch	*Notch^{DN}*	*Rab5^{DN}*

Table 5. List of antibodies from Developmental Studies Hybridoma Bank against cell-surface molecules.

Antibody name	Antigen
smoothened 20C6	smoothened
MAb83F6	TRP
Spitz	Spitz
sn 7C	fascin
4F3 discs large	discs large
DCAD2	cadherin, DE
N2 7A1 ARMADILLO	Armadillo
p1B2	p120 catenin
p4B2	p120 catenin

Cq4	Crumbs
F5H7	Fasciclin I
7G10	Fasciclin III
34b3	fasciclin II
8b4d2(MH2B)	glutamate receptor subunit, DGluR-IIA
19C2 Sema II	Sema II
C566.9	Coracle
BP 104	Neuroglian
DE Cad	shg DE-Cadherin
CF,6G11-S	integrin betaPS
DN-Ex # 8-S	N-cadherin
Ec11, anti-pericardin-S	anti-Pericardin
615.16-S	Coracle
10C9	atebloomer-S
Drosophila Ptc(Apa1)	Patched
15H2	Anti-Robo3 Cyto
14C9	Anti-Robo3 Extra
CF.2C7-S	integrin alphaPS2
anti-Robo-s 13C9	Robo
DK.1A4	integrin alphaPS1
10D3 anti-wrapper-s	wrapper
45E10-S	DPTP10D
9D82B3-S	Dlar
4C5-S	rhodopsin
12A7	Frizzled2
8B22F5	ptp receptor-linked, DPTP10D
24B10	chaoptin
3A6-S	ptp, DPTP99A
4C71B7	ptp,DPTP99A
C17.9C6-S	Notch, intracellular domain
F461.3B-S	Notch, extracellular domain
C458.2H-S	Notch, extracellular domain
Nrv5F7	Nervana protein
3F11	protein tyrosine phosphatase
1D4	Fasciclin
23C7	Wit-s

Chapter 4 Discussion

4.1 cell-autonomous function of endocytosis in Neuronal pruning

Endocytic pathways that mediate the homeostasis of plasma membrane lipid and proteins are crucial for various biological processes during neural development, such as neurtite outgrowth, axon guidance, neural migration, synapse formation ((Schwarz and Patrick, 2012; Villarroel-Campos et al., 2014; Yap and Winckler, 2012). Previously, it has been reported that the phagocytosis in phagocytes, such as glial cells, epithermal cells, hemocytes, is important for the removal of the debris after branches detachment (Han et al., 2014; Williams and Truman, 2005). However, little was known about the cell-autonomous role of endocytosis in neurons during pruning. Here, I first report that endocytic pathways are cell-autonomously required for neuronal pruning of sensory neurons in *Drosophila melanogaster*. Via genome-wide RNAi screen, I identified Rab5, a Rab family small GTPase that regulates early endosome formation, as a novel player in ddaC dendrite pruning. Genetic mutant clonal analysis and rescue experiments further confirm that Rab5 functions cell-autonomously in ddaC neuron during dendrite pruning. Importantly, two other early endosomal pathway components dynamin, a GTPase that regulates the fission of membrane budding, and Syntaxin 7, an endosomal SNARE protein that mediates endosomal membrane fusion, are

also required for ddaC dendrite pruning. Collectively, the early endosomal pathway is critical for dendrite pruning in ddaC neurons. This notion is also verified by parallel studies in ddaC neuron (Kanamori et al., 2015) or in MB γ gamma neurons (Issman-Zecharya and Schuldiner, 2014) recently, suggesting that early endosomal pathway might be generally involved in regulating neuronal pruning. The studies in *Drosophila* might also shed light on the mechanisms regulating neuronal pruning in vertebrates.

4.2. Endosomal degradation and recycling pathway in neuronal pruning

There are two main downstream routes for early endosomes and the contents, the recycling pathway back to plasma membrane and the degradation pathway to fuse with lysosomes. To test the potential involvement of endosomal recycling pathway, I and my colleagues tested Rab11, a Rab family small GTPase that regulates the recycling endosomes (Welz et al., 2014). Although we do not fully rule out the possible involvement of the recycling pathway in ddaC dendrite pruning, it is believed that the degradation pathway via endosomal maturation is a major route required for dendrite pruning in ddaC neurons. First, mutant of ESCRT complexes that are responsible for endosomal maturation showed comparable defects in ddaC dendrite pruning as Rab5 mutant. On the contrary, little pruning defect was observed in rab11 mutant ddaC neurons (Zhang and Wang, unpublished data). Second, both

Rab5 and ESCRT mutants exhibited similar blockade of endosomal trafficking and protein degradation, whereas Rab11 mutant did not (Zhang and Wang, unpublished data). Third, both Rab5 and ESCRT function through restraining CAM Nrg to facilitate ddaC dendrite pruning. Taken tighter, ESCRT-guided endosomal maturation and degradation is required for ddaC dendrite pruning, which also further supported by a recent report (Loncle et al., 2015).

After endosomal maturation, the final step of the degradation pathway is to fuse with lysosomes. It was shown that aberrant endosomes derived from Rab5/ESCRT mutant ddaC neurons were incapable to fuse with lysosomes, which explains the formation of ubiquitinated protein deposits. In order to examine the function of lysosomes, I tested Rab7, a small GTPase required for lysosome function (Bucci et al., 2000), a fab1, a FYVE domain protein that regulated endo-lysosomal fusion (Rusten et al., 2007), and spinster, a sugar transporter that regulates lysosome acidification(Sweeney and Davis, 2002). Surprisingly, neither pruning defects nor protein aggregates were observed in these mutant ddaC neurons (Zhang and Wang, unpublished data). I suspect that these mutants are not sufficient to induce cargo clog-up on plasma membrane or endocytic vesicles, which is responsible for causing pruning defects.

In summary, a cell-autonomous function of endocytic maturation and degradation is revealed in regulating neuronal pruning in *Dorosphila* sensory neurons.

4.3. Nrg degradation via endocytosis in neuronal pruning

The endocytic degradation pathway regulates the turnover of membrane proteins. Ubiquitination of membrane proteins is one of the important signals to trigger the endocytosis. Indeed, in the Rab5/ESCRT mutant ddaC neurons, enlarged aberrant endosomes and strong ubiquitinated protein aggregates were detected, suggesting the disruption of membrane protein trafficking and degradation. In order to search for the potential targets of endocytic pathways during ddaC dendrite pruning, some of the known endocytosed membrane proteins or ligands were tested through immunostaining or genetic interactions. However, it seems that none of the tested molecules (table 5) is involved in ddaC dendrite pruning. Then, making use of antibody collection of membrane proteins, Nrg, Robo and N-Cad have been isolated to enrich on aberrant endosomes. With further investigations, Nrg, a CAM, was found to be relocalized and downregulated via endocytic pathways prior to dendrite severing in ddaC neurons. More importantly, overexpression of Nrg is sufficient to inhibit ddaC dendrite pruning. Conversely, loss of Nrg results in precocious dendrite pruning phenotype. In addition, attenuation of Nrg in endocytic pathways mutant ddaC neuron leads to strong suppression of dendrite pruning defects. Collectively, a mechanism to downregulate CAM via endo-lysosomal degradation pathway is important to promote neuronal pruning. A following study in mushroom body γ neurons reveals a similar

mechanism that downregulating transmembrane receptor Patched via endo-lysosomal pathway is required for axon pruning (Issman-Zecharya and Schuldiner, 2014). However, Nrg should not be the sole downstream of endocytic pathways in ddaC dendrite pruning because Rab5/nrg double mutant ddaC neurons did not exhibit precocious pruning but dendrite pruning defects. Therefore, other targets of endocytic pathways might also contribute to dendrite pruning.

Recently, a follow-up study on endocytic pathways in ddaC dendrite pruning proposed an idea that Rab5/dynamin-dependent endocytosis might be important for local membrane thinning at the proximal dendrite regions during dendrite pruning (Kanamori et al., 2015). In the proximal dendrites around the severing site, a relative rapid membrane retrieval and endosome formation have been found to correlate with the dendrite thinning and compartmentalized calcium transients during dendrite pruning, suggesting the endocytic machinery appears to function locally to promote dendrite pruning. However, I believe that downregulation of Nrg via endocytic pathways plays a more important role during ddaC dendrite pruning. First, endocytosis of Nrg occurs in a global manner including dendrites, axons and soma, suggesting endocytic pathways function in the whole neuron. Second, overexpression of Nrg leads to much stronger pruning defects than the loss of calcium signaling. Third, attenuation of Nrg can strongly suppress the Rab5/ESCRT mutant pruning

defects. Therefore, regulating the turnover of membrane molecules seems to be the major function of endocytic machinery during dendrite pruning.

4.4. Inhibitory function of Nrg in neuronal pruning

Ig superfamily CAM Neuroglian, the only ortholog of mammalian L1 CAM family in Drosophila genome, has been widely studied in various aspects of neural development, such as outgrowth, synapse formation, pathfinding, etc. Here, a novel function of Nrg in inhibiting neuronal pruning is reported. Prior to dendrite severing, Nrg is downregulated by endocytic degradation pathways to facilitate dendrite pruning in ddaC neurons. This mechanism sheds light on the transition between stable and pruning stage. L1 CAMs consist of a large extra cellular domain, a single transmembrane region and a small intracellular domain that conserved between vertebrates and invertebrates. According to the genetic data, the ECD of Nrg is sufficient to induce dendrite pruning defects and partially rescue the precocious pruning in nrg mutant ddaC neurons, suggesting that the ECD of Nrg is required for the inhibitory function during dendrite pruning. The ECD contains 6 Ig domains and 5 FN3 domains, which functions in homophilic and heterophilc interactions with membrane proteins. It has been shown that Nrg homophilic interaction between ddaC and epithermal cells is important for the dendrite outgrowth (Yamamoto et al., 2006). However, the homophilic interaction seems to be dispensable for inhibitory function of Nrg during dendrite pruning in ddaC neurons. First, Ig 3

and 4, which is required for homophilic binding, do not required for the inhibitory function of Nrg in pruning. Second, co-overexpression of Nrg in both ddaC neurons and Glial/epithermal cells where ddaC neurons innervate does not enhance the pruning defects (Zhang and Wang, unpublished data). In addition to homophilic interactions, L1 CAMs can bind to other membrane molecules via ECD, such as EGFR (Islam et al., 2003), neuropilin/semaphoring to regulate axon outgrow (Chen et al., 2000). Besides, FGFR and also show genetic interaction with Nrg in during axon outgrowth (Forni et al., 2004). Recently, C. elegan L1 CAM ortholog Sax7 forms a tripartite complex with MNR-1 and DMA-1 as a ligand in regulating dendrite pattern via the FN domain (Dong et al., 2013). In order to further investigate the ECD of Nrg in regulating dendrite pruning, it is worthwhile to test these candidate molecules in Drosophila and search for other novel potential binding partners of ECD.

Although the genetic data suggest the importance of ECD, the involvement of ICD in ddaC dendrite pruning is not fully ruled out. It is well studied that the ICD of L1 CAMs interact with Ankrins via the conserved Ankrin-binding domain to link to spectrin/actin cytoskeleton (Enneking et al., 2013). However, the the ABD deletion does not affect the function of Nrg in regulating dendrite pruning. Consistently, loss of Ankrin2 that interacts with Nrg in regulating synapse formation does not lead to pruning phenotypes (Wang unpublished data). In addition, ICD contains FERM binding domain

that interacts with ezrin/meosin to link to actin cytoskeleton (Sakurai et al., 2008). It would be necessary to further test the function of ICD during dendrite pruning.

4.5. Trigger of Nrg endocytosis

Endocytosis of L1 CAMs has been shown to regulate outgrowth in both vertebrates and invertebrates (Kamiguchi, 2003; Yang et al., 2011). In mammalian studies, L1 together with Neuropilin-1 undergo endocytosis in response to semaphorin3A (Castellani et al., 2004). And the dynamics of Nrg is important for the proper stability and connections during synapse formation and axon targeting (Enneking et al., 2013). The active endocytosis of Nrg occurs prior to the onset of dendrite pruning specifically in ddaC neurons. It is an interesting question to understand the trigger of this temporal-spatial endocytosis. One of the most common mechanisms trigger endocytosis is the binding of ligand. As discussed above, the binding partners of ECD might function as ligands to trigger the endocytosis of Nrg during dendrite pruning. In addition, the modifications of membrane molecules have been shown to trigger endocytosis. Previous studies have shown that the dephosphorization of Y1176 of L1 and the conserved site Y1185 of Nrg is important for the endocytosis (Schaefer et al., 2002; Yang et al., 2011). Thus, it is possible that dephosphorylation of Nrg ICD via unknown signaling triggers the active endocytosis during dendrite pruning in ddaC neurons. Another common

modification served as endocytosis cue is ubiquitination. Our date suggest that Nrg is colocalized with ubiquitinated deposits on aberrant endosomes. It is interesting to test that if ubiquitination of Nrg triggers endocytosis.

4.6. Endocytic pathways and ecdysone signaling

Ecdysone signaling functions as a master regulator of neuronal remodeling in various cell types in Drosophila (Yamanaka et al., 2013). Our data suggests that Nrg downregulation via endocytic pathways is likely downstream of ecdysone signaling in ddaC neurons. First, neither endocytic pathways mutants nor Nrg overexpression (Zhang and Wang unpublished data) affect EcR upregulation, the hallmark of ecdysone signaling activation during early metamorphosis. Second, Knockdown of Nrg via RNAi partially rescued dendrite pruning defects in loss of Ecdysone signaling backgrounds, such as overexpression of EcR^{DN} (Fig 21A-D), Brm^{DN} (Fig 21F-J) or *CBP RNAi* (Fig 21K-O). However, the ecdysone signaling that is unregulated just before metamorphosis seems to be dispensable for general endocytic machinery because no aberrant endosomes observed in ecdysone signaling mutants ddaC neurons (Zhang and Wang, unpublished data). How the ecdysone signaling regulates endocytic pathways remains elusive. There are several hypotheses. First, ecdysone signaling might regulate the modification of Nrg during early metamorphosis that triggers the endocytosis. Previously, it is reported that ecdysone signaling activates ubiquitin ligase to promote dendrite pruning in

ddaC neurons (Wong et al., 2013). It is possible that Nrg is modified by ecdysone signaling. Second, ecdysone signaling might activate certain Nrg interactors to trigger the endocytosis, which might also involve auto-secretion. It would be interesting to test the involvement of secretion pathway in ddaC dendrite pruning. As discussed above, it is important to search for the binding partners of Nrg in the future.

Chapter 5 Conclusion

In order to understand the mechanisms of neuronal pruning, our lab has conducted a genome-wide reverse genetic screen in *Drosophila* ddaC neurons via *in vivo* RNAi knockdown technique. In the screen, I isolated Rab5, a core component in endocytic machinery, which is involved in dendrite pruning in ddaC neurons. In addition, I found that the entire endo-lysosomal pathways are important for dendrite pruning in ddaC neurons by examining various endocytic machinery components including dynamin, Syntaxy7 and ESCRT complexes. Collectively, the genetic and immunohistochemical data indicated that the endocytic pathways are required for dendrite pruning in ddaC neurons during early metamorphosis.

Endo-lysosomal pathways are important for the turnover of membrane associated proteins. Via immunohistochemistry and live imaging, aberrant endosomes with the ubiquitinated protein deposits were detected in endocytic mutant ddaC neurons. Interestingly, the aberrant endosomes were labeled by early and late endosomal markers but not lysosomal maker, which reflecting the failure of contents degradation via endosome/lysosome fusion. Thus, endocytic pathways are important in regulating protein trafficking and degradation in ddaC neurons.

In order to search for the potential targets of endocytic pathways, I conduct a candidature antibody-based immunostaining screen and identified Nrg, a conserved single-transmembrane cell adhesion molecule, as a cargo of

Endo-lysosomal pathways. Furthermore, the immunohistochemistry data suggested that Nrg undergoes active endocytosis prior to the onset of dendrite severing in ddaC neurons. Consistently, the genetic manipulations experiments revealed that, downstream of endocytic pathways, Nrg function in an inhibitory role specifically during dendrite pruning. Taken together, endo-lysosomal pathways actively downregulate Nrg during in a spatial-temporal manner to facilitate dendrite pruning in ddaC neurons during early metamorphosis.

In summary, this study uncovered a novel mechanism that downregulation of cell adhesion molecule via endo-lysosomal pathways to promote neuronal pruning (Fig 22B, C).

Reference

Aplin, A.E. (2003). Cell adhesion molecule regulation of nucleocytoplasmic trafficking. FEBS Lett *534*, 11-14.

Assaker, G., Ramel, D., Wculek, S.K., Gonzalez-Gaitan, M., and Emery, G. (2010). Spatial restriction of receptor tyrosine kinase activity through a polarized endocytic cycle controls border cell migration. Proc Natl Acad Sci U S A *107*, 22558-22563.

Awasaki, T., and Ito, K. (2004). Engulfing action of glial cells is required for programmed axon pruning during Drosophila metamorphosis. Curr Biol *14*, 668-677.

Bagri, A., Cheng, H.J., Yaron, A., Pleasure, S.J., and Tessier-Lavigne, M. (2003). Stereotyped pruning of long hippocampal axon branches triggered by retraction inducers of the semaphorin family. Cell *113*, 285-299.

Benson, D.L., Schnapp, L.M., Shapiro, L., and Huntley, G.W. (2000). Making memories stick: cell-adhesion molecules in synaptic plasticity. Trends Cell Biol *10*, 473-482.

Bodmer, R., Barbel, S., Sheperd, S., Jack, J.W., Jan, L.Y., and Jan, Y.N. (1987). Transformation of sensory organs by mutations of the cut locus of D. melanogaster. Cell *51*, 293-307.

Boulanger, A., Clouet-Redt, C., Farge, M., Flandre, A., Guignard, T., Fernando, C., Juge, F., and Dura, J.M. (2011). ftz-f1 and Hr39 opposing roles on EcR expression during Drosophila mushroom body neuron remodeling. Nat Neurosci *14*, 37-44.

Boulanger, A., and Dura, J.M. (2015). Nuclear receptors and Drosophila neuronal remodeling. Biochim Biophys Acta *1849*, 187-195.

Brand, A.H., and Perrimon, N. (1993). Targeted gene expression as a means of altering cell fates and generating dominant phenotypes. Development *118*, 401-415.

Bucci, C., Thomsen, P., Nicoziani, P., McCarthy, J., and van Deurs, B. (2000). Rab7: a key to lysosome biogenesis. Mol Biol Cell *11*, 467-480.

Buss, R.R., Sun, W., and Oppenheim, R.W. (2006). Adaptive roles of programmed cell death during nervous system development. Annu Rev Neurosci *29*, 1-35.

Campenot, R.B. (1982). Development of sympathetic neurons in compartmentalized cultures. II. Local control of neurite survival by nerve growth factor. Dev Biol *93*, 13-21.

Castellani, V., De Angelis, E., Kenwrick, S., and Rougon, G. (2002). Cis and trans interactions of L1 with neuropilin-1 control axonal responses to semaphorin 3A. EMBO J *21*, 6348-6357.

Castellani, V., Falk, J., and Rougon, G. (2004). Semaphorin3A-induced receptor endocytosis during axon guidance responses is mediated by L1 CAM. Mol Cell Neurosci *26*, 89-100.

Ceresa, B.P., and Schmid, S.L. (2000). Regulation of signal transduction by endocytosis. Curr Opin Cell Biol *12*, 204-210.

Chen, H., Bagri, A., Zupicich, J.A., Zou, Y., Stoeckli, E., Pleasure, S.J., Lowenstein, D.H., Skarnes, W.C., Chedotal, A., and Tessier-Lavigne, M. (2000). Neuropilin-2 regulates the development of selective cranial and sensory nerves and hippocampal mossy fiber projections. Neuron *25*, 43-56.

Cosker, K.E., Pazyra-Murphy, M.F., Fenstermacher, S.J., and Segal, R.A. (2013). Target-derived neurotrophins coordinate transcription and transport of bclw to prevent axonal degeneration. J Neurosci *33*, 5195-5207.

Cosker, K.E., and Segal, R.A. (2014). Neuronal signaling through endocytosis. Cold Spring Harb Perspect Biol *6*.

Cusack, C.L., Swahari, V., Hampton Henley, W., Michael Ramsey, J., and Deshmukh, M. (2013). Distinct pathways mediate axon degeneration during apoptosis and axon-specific pruning. Nat Commun *4*, 1876.

Dermaut, B., Norga, K.K., Kania, A., Verstreken, P., Pan, H., Zhou, Y., Callaerts, P., and Bellen, H.J. (2005). Aberrant lysosomal carbohydrate storage accompanies endocytic defects and neurodegeneration in Drosophila benchwarmer. J Cell Biol *170*, 127-139.

Dietzl, G., Chen, D., Schnorrer, F., Su, K.C., Barinova, Y., Fellner, M., Gasser, B., Kinsey, K., Oppel, S., Scheiblauer, S., *et al*. (2007). A genome-wide transgenic RNAi library for conditional gene inactivation in Drosophila. Nature *448*, 151-156.

Doherty, G.J., and McMahon, H.T. (2009). Mechanisms of endocytosis. Annu Rev Biochem *78*, 857-902.

Dong, X., Liu, O.W., Howell, A.S., and Shen, K. (2013). An extracellular adhesion molecule complex patterns dendritic branching and morphogenesis. Cell *155*, 296-307.

Dubois, L., Lecourtois, M., Alexandre, C., Hirst, E., and Vincent, J.P. (2001). Regulated endocytic routing modulates wingless signaling in Drosophila embryos. Cell *105*, 613-624.

Enneking, E.M., Kudumala, S.R., Moreno, E., Stephan, R., Boerner, J., Godenschwege, T.A., and Pielage, J. (2013). Transsynaptic coordination of synaptic growth, function, and stability by the L1-type CAM Neuroglian. PLoS Biol *11*, e1001537.

Entchev, E.V., Schwabedissen, A., and Gonzalez-Gaitan, M. (2000). Gradient formation of the TGF-beta homolog Dpp. Cell *103*, 981-991.

Fischer, J.A., Eun, S.H., and Doolan, B.T. (2006). Endocytosis, endosome trafficking, and the regulation of Drosophila development. Annu Rev Cell Dev Biol *22*, 181-206.

Forni, J.J., Romani, S., Doherty, P., and Tear, G. (2004). Neuroglian and FasciclinII can promote neurite outgrowth via the FGF receptor Heartless. Mol Cell Neurosci *26*, 282-291.

Garcia-Alonso, L., Romani, S., and Jimenez, F. (2000). The EGF and FGF receptors mediate neuroglian function to control growth cone decisions during sensory axon guidance in Drosophila. Neuron *28*, 741-752.

Godenschwege, T.A., Kristiansen, L.V., Uthaman, S.B., Hortsch, M., and Murphey, R.K. (2006). A conserved role for Drosophila Neuroglian and human L1-CAM in central-synapse formation. Curr Biol *16*, 12-23.

Godenschwege, T.A., and Murphey, R.K. (2009). Genetic interaction of Neuroglian and Semaphorin1a during guidance and synapse formation. J Neurogenet *23*, 147-155.

Goossens, T., Kang, Y.Y., Wuytens, G., Zimmermann, P., Callaerts-Vegh, Z., Pollarolo, G., Islam, R., Hortsch, M., and Callaerts, P. (2011). The Drosophila L1CAM homolog Neuroglian signals through distinct pathways to control different aspects of mushroom body axon development. Development *138*, 1595-1605.

Grueber, W.B., Jan, L.Y., and Jan, Y.N. (2002). Tiling of the Drosophila epidermis by multidendritic sensory neurons. Development *129*, 2867-2878.

Grueber, W.B., Ye, B., Moore, A.W., Jan, L.Y., and Jan, Y.N. (2003). Dendrites of distinct classes of Drosophila sensory neurons show different capacities for homotypic repulsion. Curr Biol *13*, 618-626.

Hall, S.G., and Bieber, A.J. (1997). Mutations in the Drosophila neuroglian cell adhesion molecule affect motor neuron pathfinding and peripheral nervous system patterning. J Neurobiol *32*, 325-340.

Han, C., Jan, L.Y., and Jan, Y.N. (2011). Enhancer-driven membrane markers for analysis of nonautonomous mechanisms reveal neuron-glia interactions in Drosophila. Proc Natl Acad Sci U S A *108*, 9673-9678.

Han, C., Song, Y., Xiao, H., Wang, D., Franc, N.C., Jan, L.Y., and Jan, Y.N. (2014). Epidermal cells are the primary phagocytes in the fragmentation and clearance of degenerating dendrites in Drosophila. Neuron *81*, 544-560.

Han, C., Wang, D., Soba, P., Zhu, S., Lin, X., Jan, L.Y., and Jan, Y.N. (2012). Integrins regulate repulsion-mediated dendritic patterning of drosophila sensory neurons by restricting dendrites in a 2D space. Neuron *73*, 64-78.

Hansen, C.G., and Nichols, B.J. (2009). Molecular mechanisms of clathrin-independent endocytosis. J Cell Sci *122*, 1713-1721.

Hashimoto, K., and Kano, M. (2013). Synapse elimination in the developing cerebellum. Cell Mol Life Sci *70*, 4667-4680.

Hayashi, Y., Hirotsu, T., Iwata, R., Kage-Nakadai, E., Kunitomo, H., Ishihara, T., Iino, Y., and Kubo, T. (2009). A trophic role for Wnt-Ror kinase signaling during developmental pruning in Caenorhabditis elegans. Nat Neurosci *12*, 981-987.

Hoopfer, E.D., Penton, A., Watts, R.J., and Luo, L. (2008). Genomic analysis of Drosophila neuronal remodeling: a role for the RNA-binding protein Boule as a negative regulator of axon pruning. J Neurosci *28*, 6092-6103.

Hortsch, M. (2000). Structural and functional evolution of the L1 family: are four adhesion molecules better than one? Mol Cell Neurosci *15*, 1-10.

Hortsch, M., Bieber, A.J., Patel, N.H., and Goodman, C.S. (1990). Differential splicing generates a nervous system-specific form of Drosophila neuroglian. Neuron *4*, 697-709.

Hung, R.J., Pak, C.W., and Terman, J.R. (2011). Direct redox regulation of F-actin assembly and disassembly by Mical. Science *334*, 1710-1713.

Huotari, J., and Helenius, A. (2011). Endosome maturation. EMBO J *30*, 3481-3500.

Hurley, J.H. (2010). The ESCRT complexes. Crit Rev Biochem Mol Biol *45*, 463-487.

Islam, R., Wei, S.Y., Chiu, W.H., Hortsch, M., and Hsu, J.C. (2003). Neuroglian activates Echinoid to antagonize the Drosophila EGF receptor signaling pathway. Development *130*, 2051-2059.

Issman-Zecharya, N., and Schuldiner, O. (2014). The PI3K class III complex promotes axon pruning by downregulating a Ptc-derived signal via endosome-lysosomal degradation. Dev Cell *31*, 461-473.

Jekely, G., and Rorth, P. (2003). Hrs mediates downregulation of multiple signalling receptors in Drosophila. EMBO Rep *4*, 1163-1168.

Jinushi-Nakao, S., Arvind, R., Amikura, R., Kinameri, E., Liu, A.W., and Moore, A.W. (2007). Knot/Collier and cut control different aspects of dendrite cytoskeleton and synergize to define final arbor shape. Neuron *56*, 963-978.

Jordens, I., Fernandez-Borja, M., Marsman, M., Dusseljee, S., Janssen, L., Calafat, J., Janssen, H., Wubbolts, R., and Neefjes, J. (2001). The Rab7 effector protein RILP controls lysosomal transport by inducing the recruitment of dynein-dynactin motors. Current Biology *11*, 1680-1685.

Kage, E., Hayashi, Y., Takeuchi, H., Hirotsu, T., Kunitomo, H., Inoue, T., Arai, H., Iino, Y., and Kubo, T. (2005). MBR-1, a novel helix-turn-helix transcription factor, is required for pruning excessive neurites in Caenorhabditis elegans. Curr Biol *15*, 1554-1559.

Kamiguchi, H. (2003). The mechanism of axon growth: what we have learned from the cell adhesion molecule L1. Mol Neurobiol *28*, 219-228.

Kanamori, T., Kanai, M.I., Dairyo, Y., Yasunaga, K., Morikawa, R.K., and Emoto, K. (2013). Compartmentalized calcium transients trigger dendrite pruning in Drosophila sensory neurons. Science *340*, 1475-1478.

Kanamori, T., Yoshino, J., Yasunaga, K., Dairyo, Y., and Emoto, K. (2015). Local endocytosis triggers dendritic thinning and pruning in Drosophila sensory neurons. Nat Commun *6*, 6515.

Karim, F.D., and Thummel, C.S. (1992). Temporal coordination of regulatory gene expression by the steroid hormone ecdysone. EMBO J *11*, 4083-4093.

Kawauchi, T., Sekine, K., Shikanai, M., Chihama, K., Tomita, K., Kubo, K., Nakajima, K., Nabeshima, Y., and Hoshino, M. (2010). Rab GTPases-dependent endocytic pathways regulate neuronal migration and maturation through N-cadherin trafficking. Neuron *67*, 588-602.

Kenwrick, S., and Doherty, P. (1998). Neural cell adhesion molecule L1: relating disease to function. Bioessays *20*, 668-675.

Kenwrick, S., Watkins, A., and De Angelis, E. (2000). Neural cell recognition molecule L1: relating biological complexity to human disease mutations. Hum Mol Genet *9*, 879-886.

Kidd, T., Bland, K.S., and Goodman, C.S. (1999). Slit is the midline repellent for the robo receptor in Drosophila. Cell *96*, 785-794.

Kirilly, D., Gu, Y., Huang, Y., Wu, Z., Bashirullah, A., Low, B.C., Kolodkin, A.L., Wang, H., and Yu, F. (2009). A genetic pathway composed of Sox14 and Mical governs severing of dendrites during pruning. Nat Neurosci *12*, 1497-1505.

Kirilly, D., Wong, J.J., Lim, E.K., Wang, Y., Zhang, H., Wang, C., Liao, Q., Wang, H., Liou, Y.C., and Yu, F. (2011). Intrinsic epigenetic factors cooperate with the steroid hormone ecdysone to govern dendrite pruning in Drosophila. Neuron *72*, 86-100.

Koelle, M.R., Talbot, W.S., Segraves, W.A., Bender, M.T., Cherbas, P., and Hogness, D.S. (1991). The Drosophila EcR gene encodes an ecdysone receptor, a new member of the steroid receptor superfamily. Cell *67*, 59-77.

Kristiansen, L.V., Velasquez, E., Romani, S., Baars, S., Berezin, V., Bock, E., Hortsch, M., and Garcia-Alonso, L. (2005). Genetic analysis of an overlapping functional requirement for L1- and NCAM-type proteins during sensory axon guidance in Drosophila. Mol Cell Neurosci *28*, 141-152.

Kudumala, S., Freund, J., Hortsch, M., and Godenschwege, T.A. (2013). Differential effects of human L1CAM mutations on complementing guidance and synaptic defects in Drosophila melanogaster. PLoS One *8*, e76974.

Kuo, C.T., Jan, L.Y., and Jan, Y.N. (2005). Dendrite-specific remodeling of Drosophila sensory neurons requires matrix metalloproteases, ubiquitin-proteasome, and ecdysone signaling. Proc Natl Acad Sci U S A *102*, 15230-15235.

Kuo, C.T., Zhu, S., Younger, S., Jan, L.Y., and Jan, Y.N. (2006). Identification of E2/E3 ubiquitinating enzymes and caspase activity regulating Drosophila sensory neuron dendrite pruning. Neuron *51*, 283-290.

Kurusu, M., Katsuki, T., Zinn, K., and Suzuki, E. (2012). Developmental changes in expression, subcellular distribution, and function of Drosophila N-cadherin, guided by a cell-intrinsic program during neuronal differentiation. Dev Biol *366*, 204-217.

Lee, H.H., Jan, L.Y., and Jan, Y.N. (2009). Drosophila IKK-related kinase Ik2 and Katanin p60-like 1 regulate dendrite pruning of sensory neuron during metamorphosis. Proc Natl Acad Sci U S A *106*, 6363-6368.

Lee, T., Lee, A., and Luo, L. (1999). Development of the Drosophila mushroom bodies: sequential generation of three distinct types of neurons from a neuroblast. Development *126*, 4065-4076.

Lee, T., Marticke, S., Sung, C., Robinow, S., and Luo, L. (2000). Cell-autonomous requirement of the USP/EcR-B ecdysone receptor for mushroom body neuronal remodeling in Drosophila. Neuron *28*, 807-818.

Lim, J.P., and Gleeson, P.A. (2011). Macropinocytosis: an endocytic pathway for internalising large gulps. Immunol Cell Biol *89*, 836-843.

Liu, Y., Rutlin, M., Huang, S., Barrick, C.A., Wang, F., Jones, K.R., Tessarollo, L., and Ginty, D.D. (2012). Sexually dimorphic BDNF signaling directs sensory innervation of the mammary gland. Science *338*, 1357-1360.

Lloyd, T.E., Atkinson, R., Wu, M.N., Zhou, Y., Pennetta, G., and Bellen, H.J. (2002). Hrs regulates endosome membrane invagination and tyrosine kinase receptor signaling in Drosophila. Cell *108*, 261-269.

Loncle, N., Agromayor, M., Martin-Serrano, J., and Williams, D.W. (2015). An ESCRT module is required for neuron pruning. Sci Rep *5*, 8461.

Loncle, N., and Williams, D.W. (2012). An interaction screen identifies headcase as a regulator of large-scale pruning. J Neurosci *32*, 17086-17096.

Lu, H., and Bilder, D. (2005). Endocytic control of epithelial polarity and proliferation in Drosophila. Nat Cell Biol *7*, 1232-1239.

Luo, L., and O'Leary, D.D. (2005). Axon retraction and degeneration in development and disease. Annu Rev Neurosci *28*, 127-156.

Martin, V., Mrkusich, E., Steinel, M.C., Rice, J., Merritt, D.J., and Whitington, P.M. (2008). The L1-type cell adhesion molecule Neuroglian is necessary for maintenance of sensory axon advance in the Drosophila embryo. Neural Dev *3*, 10.

Mori, Y., Matsui, T., and Fukuda, M. (2013). Rabex-5 protein regulates dendritic localization of small GTPase Rab17 and neurite morphogenesis in hippocampal neurons. J Biol Chem *288*, 9835-9847.

Mulcahy, L.A., Pink, R.C., and Carter, D.R. (2014). Routes and mechanisms of extracellular vesicle uptake. J Extracell Vesicles *3*.

Nagaraj, K., Kristiansen, L.V., Skrzynski, A., Castiella, C., Garcia-Alonso, L., and Hortsch, M. (2009). Pathogenic human L1-CAM mutations reduce the adhesion-dependent activation of EGFR. Hum Mol Genet *18*, 3822-3831.

Nikolaev, A., McLaughlin, T., O'Leary, D.D., and Tessier-Lavigne, M. (2009). APP binds DR6 to trigger axon pruning and neuron death via distinct caspases. Nature *457*, 981-989.

Oren-Suissa, M., Hall, D.H., Treinin, M., Shemer, G., and Podbilewicz, B. (2010). The fusogen EFF-1 controls sculpting of mechanosensory dendrites. Science *328*, 1285-1288.

Osterwalder, T., Yoon, K.S., White, B.H., and Keshishian, H. (2001). A conditional tissue-specific transgene expression system using inducible GAL4. Proc Natl Acad Sci U S A *98*, 12596-12601.

Paridaen, J.T., and Huttner, W.B. (2014). Neurogenesis during development of the vertebrate central nervous system. EMBO Rep *15*, 351-364.

Pulipparacharuvil, S., Akbar, M.A., Ray, S., Sevrioukov, E.A., Haberman, A.S., Rohrer, J., and Kramer, H. (2005). Drosophila Vps16A is required for trafficking to lysosomes and biogenesis of pigment granules. J Cell Sci *118*, 3663-3673.

Riccomagno, M.M., Hurtado, A., Wang, H., Macopson, J.G., Griner, E.M., Betz, A., Brose, N., Kazanietz, M.G., and Kolodkin, A.L. (2012). The RacGAP

beta2-Chimaerin selectively mediates axonal pruning in the hippocampus. Cell *149*, 1594-1606.

Rumpf, S., Lee, S.B., Jan, L.Y., and Jan, Y.N. (2011). Neuronal remodeling and apoptosis require VCP-dependent degradation of the apoptosis inhibitor DIAP1. Development *138*, 1153-1160.

Rusten, T.E., Vaccari, T., Lindmo, K., Rodahl, L.M., Nezis, I.P., Sem-Jacobsen, C., Wendler, F., Vincent, J.P., Brech, A., Bilder, D., *et al.* (2007). ESCRTs and Fab1 regulate distinct steps of autophagy. Curr Biol *17*, 1817-1825.

Sakurai, T., Gil, O.D., Whittard, J.D., Gazdoiu, M., Joseph, T., Wu, J., Waksman, A., Benson, D.L., Salton, S.R., and Felsenfeld, D.P. (2008). Interactions between the L1 cell adhesion molecule and ezrin support traction-force generation and can be regulated by tyrosine phosphorylation. J Neurosci Res *86*, 2602-2614.

Satoh, D., Sato, D., Tsuyama, T., Saito, M., Ohkura, H., Rolls, M.M., Ishikawa, F., and Uemura, T. (2008). Spatial control of branching within dendritic arbors by dynein-dependent transport of Rab5-endosomes. Nat Cell Biol *10*, 1164-1171.

Saugstad, L.F. (2011). Infantile autism: a chronic psychosis since infancy due to synaptic pruning of the supplementary motor area. Nutr Health *20*, 171-182.

Schaefer, A.W., Kamei, Y., Kamiguchi, H., Wong, E.V., Rapoport, I., Kirchhausen, T., Beach, C.M., Landreth, G., Lemmon, S.K., and Lemmon, V. (2002). L1 endocytosis is controlled by a phosphorylation-dephosphorylation cycle stimulated by outside-in signaling by L1. J Cell Biol *157*, 1223-1232.

Schafer, M.K., and Frotscher, M. (2012). Role of L1CAM for axon sprouting and branching. Cell Tissue Res *349*, 39-48.

Schindelin, J., Arganda-Carreras, I., Frise, E., Kaynig, V., Longair, M., Pietzsch, T., Preibisch, S., Rueden, C., Saalfeld, S., Schmid, B., *et al.* (2012). Fiji: an open-source platform for biological-image analysis. Nat Methods *9*, 676-682.

Schoenmann, Z., Assa-Kunik, E., Tiomny, S., Minis, A., Haklai-Topper, L., Arama, E., and Yaron, A. (2010). Axonal degeneration is regulated by the apoptotic machinery or a NAD+-sensitive pathway in insects and mammals. J Neurosci *30*, 6375-6386.

Schuldiner, O., Berdnik, D., Levy, J.M., Wu, J.S., Luginbuhl, D., Gontang, A.C., and Luo, L. (2008). piggyBac-based mosaic screen identifies a postmitotic function for cohesin in regulating developmental axon pruning. Dev Cell *14*, 227-238.

Schuldiner, O., and Yaron, A. (2015). Mechanisms of developmental neurite pruning. Cell Mol Life Sci *72*, 101-119.

Schwarz, L.A., and Patrick, G.N. (2012). Ubiquitin-dependent endocytosis, trafficking and turnover of neuronal membrane proteins. Mol Cell Neurosci *49*, 387-393.

Scott, C.C., Vacca, F., and Gruenberg, J. (2014). Endosome maturation, transport and functions. Semin Cell Dev Biol *31*, 2-10.

Selemon, L.D., and Zecevic, N. (2015). Schizophrenia: a tale of two critical periods for prefrontal cortical development. Transl Psychiatry *5*, e623.

Sheng, L., Leshchyns'ka, I., and Sytnyk, V. (2013). Cell adhesion and intracellular calcium signaling in neurons. Cell Commun Signal *11*, 94.

Siegenthaler, D., Enneking, E.M., Moreno, E., and Pielage, J. (2015). L1CAM/Neuroglian controls the axon-axon interactions establishing layered and lobular mushroom body architecture. J Cell Biol *208*, 1003-1018.

Silletti, S., Mei, F., Sheppard, D., and Montgomery, A.M. (2000). Plasmin-sensitive dibasic sequences in the third fibronectin-like domain of L1-cell adhesion molecule (CAM) facilitate homomultimerization and concomitant integrin recruitment. J Cell Biol *149*, 1485-1502.

Simon, D.J., Weimer, R.M., McLaughlin, T., Kallop, D., Stanger, K., Yang, J., O'Leary, D.D., Hannoush, R.N., and Tessier-Lavigne, M. (2012). A caspase cascade regulating developmental axon degeneration. J Neurosci *32*, 17540-17553.

Singh, K.K., Park, K.J., Hong, E.J., Kramer, B.M., Greenberg, M.E., Kaplan, D.R., and Miller, F.D. (2008). Developmental axon pruning mediated by BDNF-p75NTR-dependent axon degeneration. Nat Neurosci *11*, 649-658.

Song, Y., Ori-McKenney, K.M., Zheng, Y., Han, C., Jan, L.Y., and Jan, Y.N. (2012). Regeneration of Drosophila sensory neuron axons and dendrites is regulated by the Akt pathway involving Pten and microRNA bantam. Genes Dev *26*, 1612-1625.

Sousa, R., and Lafer, E.M. (2015). The role of molecular chaperones in clathrin mediated vesicular trafficking. Front Mol Biosci *2*, 26.

Sun, M., and Xie, W. (2012). Cell adhesion molecules in Drosophila synapse development and function. Sci China Life Sci *55*, 20-26.

Sundaresan, S., Kong, J.H., Fang, Q., Salles, F.T., Wangsawihardja, F., Ricci, A.J., and Mustapha, M. (2015). Thyroid hormone is required for pruning, functioning and long-term maintenance of afferent inner hair cell synapses. Eur J Neurosci.

Sweeney, N.T., Brenman, J.E., Jan, Y.N., and Gao, F.B. (2006). The coiled-coil protein shrub controls neuronal morphogenesis in Drosophila. Curr Biol *16*, 1006-1011.

Sweeney, S.T., and Davis, G.W. (2002). Unrestricted synaptic growth in spinster-a late endosomal protein implicated in TGF-beta-mediated synaptic growth regulation. Neuron *36*, 403-416.

Thelen, K., Kedar, V., Panicker, A.K., Schmid, R.S., Midkiff, B.R., and Maness, P.F. (2002). The neural cell adhesion molecule L1 potentiates integrin-dependent cell migration to extracellular matrix proteins. J Neurosci *22*, 4918-4931.

Thompson, B.J., Mathieu, J., Sung, H.H., Loeser, E., Rorth, P., and Cohen, S.M. (2005). Tumor suppressor properties of the ESCRT-II complex component Vps25 in Drosophila. Dev Cell *9*, 711-720.

Thummel, C.S. (1996). Flies on steroids--Drosophila metamorphosis and the mechanisms of steroid hormone action. Trends Genet *12*, 306-310.

Tojima, T., and Kamiguchi, H. (2015). Exocytic and endocytic membrane trafficking in axon development. Dev Growth Differ *57*, 291-304.

Tsubouchi, A., Caldwell, J.C., and Tracey, W.D. (2012). Dendritic filopodia, Ripped Pocket, NOMPC, and NMDARs contribute to the sense of touch in Drosophila larvae. Curr Biol *22*, 2124-2134.

Unsain, N., Higgins, J.M., Parker, K.N., Johnstone, A.D., and Barker, P.A. (2013). XIAP regulates caspase activity in degenerating axons. Cell Rep *4*, 751-763.

Vaccari, T., and Bilder, D. (2005). The Drosophila tumor suppressor vps25 prevents nonautonomous overproliferation by regulating notch trafficking. Dev Cell *9*, 687-698.

Vaccari, T., Rusten, T.E., Menut, L., Nezis, I.P., Brech, A., Stenmark, H., and Bilder, D. (2009). Comparative analysis of ESCRT-I, ESCRT-II and ESCRT-III function in Drosophila by efficient isolation of ESCRT mutants. J Cell Sci *122*, 2413-2423.

Van Battum, E.Y., Brignani, S., and Pasterkamp, R.J. (2015). Axon guidance proteins in neurological disorders. Lancet Neurol *14*, 532-546.

Vanderhaeghen, P., and Cheng, H.J. (2010). Guidance molecules in axon pruning and cell death. Cold Spring Harb Perspect Biol *2*, a001859.

Villarroel-Campos, D., Gastaldi, L., Conde, C., Caceres, A., and Gonzalez-Billault, C. (2014). Rab-mediated trafficking role in neurite formation. J Neurochem *129*, 240-248.

Vohra, B.P., Sasaki, Y., Miller, B.R., Chang, J., DiAntonio, A., and Milbrandt, J. (2010). Amyloid precursor protein cleavage-dependent and -independent axonal degeneration programs share a common nicotinamide mononucleotide adenylyltransferase 1-sensitive pathway. J Neurosci *30*, 13729-13738.

Waddell, S., Armstrong, J.D., Kitamoto, T., Kaiser, K., and Quinn, W.G. (2000). The amnesiac gene product is expressed in two neurons in the Drosophila brain that are critical for memory. Cell *103*, 805-813.

Waites, C.L., Craig, A.M., and Garner, C.C. (2005). Mechanisms of vertebrate synaptogenesis. Annu Rev Neurosci *28*, 251-274.

Watts, R.J., Hoopfer, E.D., and Luo, L. (2003). Axon pruning during Drosophila metamorphosis: evidence for local degeneration and requirement of the ubiquitin-proteasome system. Neuron *38*, 871-885.

Watts, R.J., Schuldiner, O., Perrino, J., Larsen, C., and Luo, L. (2004). Glia engulf degenerating axons during developmental axon pruning. Curr Biol *14*, 678-684.

Wei, C.H., and Ryu, S.E. (2012). Homophilic interaction of the L1 family of cell adhesion molecules. Exp Mol Med *44*, 413-423.

Welz, T., Wellbourne-Wood, J., and Kerkhoff, E. (2014). Orchestration of cell surface proteins by Rab11. Trends Cell Biol *24*, 407-415.

Williams, D.W., Kondo, S., Krzyzanowska, A., Hiromi, Y., and Truman, J.W. (2006). Local caspase activity directs engulfment of dendrites during pruning. Nat Neurosci *9*, 1234-1236.

Williams, D.W., and Truman, J.W. (2005). Cellular mechanisms of dendrite pruning in Drosophila: insights from in vivo time-lapse of remodeling dendritic arborizing sensory neurons. Development *132*, 3631-3642.

Wong, J.J., Li, S., Lim, E.K., Wang, Y., Wang, C., Zhang, H., Kirilly, D., Wu, C., Liou, Y.C., Wang, H., *et al.* (2013). A Cullin1-based SCF E3 ubiquitin ligase targets the InR/PI3K/TOR pathway to regulate neuronal pruning. PLoS Biol *11*, e1001657.

Wucherpfennig, T., Wilsch-Brauninger, M., and Gonzalez-Gaitan, M. (2003). Role of Drosophila Rab5 during endosomal trafficking at the synapse and evoked neurotransmitter release. J Cell Biol *161*, 609-624.

Xiang, Y., Yuan, Q., Vogt, N., Looger, L.L., Jan, L.Y., and Jan, Y.N. (2010). Light-avoidance-mediating photoreceptors tile the Drosophila larval body wall. Nature *468*, 921-926.

Xu, N.J., and Henkemeyer, M. (2009). Ephrin-B3 reverse signaling through Grb4 and cytoskeletal regulators mediates axon pruning. Nat Neurosci *12*, 268-276.

Yamamoto, M., Ueda, R., Takahashi, K., Saigo, K., and Uemura, T. (2006). Control of axonal sprouting and dendrite branching by the Nrg-Ank complex at the neuron-glia interface. Curr Biol *16*, 1678-1683.

Yamanaka, N., Rewitz, K.F., and O'Connor, M.B. (2013). Ecdysone control of developmental transitions: lessons from Drosophila research. Annu Rev Entomol *58*, 497-516.

Yang, W.K., Peng, Y.H., Li, H., Lin, H.C., Lin, Y.C., Lai, T.T., Suo, H., Wang, C.H., Lin, W.H., Ou, C.Y., *et al.* (2011). Nak regulates localization of clathrin sites in higher-order dendrites to promote local dendrite growth. Neuron *72*, 285-299.

Yap, C.C., and Winckler, B. (2012). Harnessing the power of the endosome to regulate neural development. Neuron *74*, 440-451.

Yu, F., and Schuldiner, O. (2014). Axon and dendrite pruning in Drosophila. Curr Opin Neurobiol *27*, 192-198.

Yu, X.M., Gutman, I., Mosca, T.J., Iram, T., Ozkan, E., Garcia, K.C., Luo, L., and Schuldiner, O. (2013). Plum, an immunoglobulin superfamily protein, regulates axon pruning by facilitating TGF-beta signaling. Neuron *78*, 456-468.

Zhang, Y., Yeh, J., Richardson, P.M., and Bo, X. (2008). Cell adhesion molecules of the immunoglobulin superfamily in axonal regeneration and neural repair. Restor Neurol Neurosci *26*, 81-96.

Zheng, X., Wang, J., Haerry, T.E., Wu, A.Y., Martin, J., O'Connor, M.B., Lee, C.H., and Lee, T. (2003). TGF-beta signaling activates steroid hormone receptor expression during neuronal remodeling in the Drosophila brain. Cell *112*, 303-315.